This is to certify that the
dissertation entitled

FLOW ANALYSIS AND MODELING OF CENTRIFUGAL COMPRESSOR IMPELLERS

presented by

ZEYAD A. AL-SUHAIBANI

has been accepted towards fulfillment
of the requirements for the

Ph.D degree in Mechanical Engineering

Major Professor's Signature

05/23/05

Date

FLOW ANALYSIS AND MODELING OF CENTRIFUGAL COMPRESSOR IMPELLERS

By

Zeyad A. Al-Suhaibani

A DISSERTATION

Submitted to
Michigan State University
in partial fulfillment of requirements
for the degree of

DOCTOR OF PHILOSOPHY

Department of Mechanical Engineering
2005

ABSTRACT

FLOW ANALYSIS AND MODELING OF CENTRIFUGAL COMPRESSOR IMPELLERS

By

Zeyad A. Al-Suhaibani

Centrifugal compressors performance is heavily affected by impeller design because of the nature of the flow in the impeller. Improvement and modification of a centrifugal impeller is a major task for designers in the turbomachinery field.

A series of impellers' experimental test data was used for the comparison of different configurations and rotational speeds. Four different centrifugal impellers and their modified versions were tested at Solar Turbines. These impellers cover a wide area of specific speeds from 58 to about 135. The comparative study of these test results indicated noticeable compressor stage and impeller performance differences between the original and the modified impellers' configurations. Details are discussed to give a broader understanding for the effect cutting an impeller on its performance as well as the compressor performance.

Comparing the compressor stage and impeller performance of four different rotational speeds has been also done. Since the impellers cover a wide range of the specific speeds, the effect of specific speed on the impeller and stage performance was also another task of this study.

CFX TASCflow, which is a CFD package, was used to simulate the flow. The primary grid generation was done using a FORTRAN code. The CFD and 1-D code results were used to compare with the experimental result. More details will be given throughout this dissertation to help understand the flow in such device in order to improve it.

With Love to My Mother and Father

ACKNOWLEDGEMENTS

At first I thank ALLAH (SWT) my Lord who enabled me to complete this work and I ask him to always help me in participating to make the future of humanity much better. Then I want to express my thanks to the people and organization that have helped me throughout my study. The first person whom I thank is Professor Abraham Engeda who was always guiding me in my course work as well as my research. He was always helping, supporting, guiding, and encouraging me throughout my study in the Department of Mechanical Engineering at Michigan State University. I am also proud of the other members of my guidance committee, Professor Chichia Chiu, Professor Tom Shih, and Professor Craig Somerton for their help and effort. Special thanks go to Dr. Somerton whom I bothered the most with my questions and he was always doing his best to help and give valuable advices.

I want also to thank Mike Cave and Tim David from Solar Turbines (a leading company in compressor and Turbine industry) who showed a great help during this study. I would also like to specially acknowledge Mr. Craig Gunn at Michigan State University for his help in preparing this dissertation. Another close friend who helped me so much in preparing this dissertation is Mahmoodul Haq. I also appreciate the assistance and great friendship from Dr. Faisal Mahroogi, Dr. Yinghui Dai, Dr. Donghui Zhang, and all other students in Turbomachinery lab during my Ph.D. program at Michigan State University. Doug Neal is another student at the Department of Mechanical Engineering who should be acknowledged for his help in dealing with CFX installation. I should also not forget to thank the other faculty and staff at my beloved Department (the Department of

Mechanical Engineering at Michigan State University) which I hope I will keep a good contact with in the future.

After thanking the people who showed a great help academically I want to thank who was behind all the financial support that is the Saudi Arabia government. A great portion of that thanks goes to the Department of Mechanical Engineering at King Saud University in Riyadh. They took care of all financial issues helping me to concentrate on my study.

The last but most important for me is thanking my family members whom I gave hard time during my study because of the effort that I have to put to finish my studies. My mother Aishah Abraham Al-Suhaibani and My father AbdulRahman Muhammad Al-Suhaibani are the ones who have kept me patient all the time and have encouraged me to finish this journey of learning. I also appreciate their way of educating me which has helped me a great deal throughout my academic life. I must not forget my strong supporter, my wife, Reem Abdullah Al-Suhaibani who was patient helping me in every way she could. She stood by me and was a very trusted and compassionate friend in all my life. Her family was also supportive to me to enable us completing this degree. Last but not least I am grateful to my children AbdulRahman, Abdullah, Abeer, Ghadeer, and Tariq for the joy they have brought into our life and their love that has been a great source that has motivated me.

TABLE OF CONTENTS

LIST OF FIGURES

LIST OF TABLES

NOMENCLATURE USED

A	Area
AR	Area ratio
AS	Aspect ratio
a	Speed of sound
BK	Blockage
b	Passage width from hub to shroud
C	Absolute velocity
C_p	Specific heat at constant pressure or Pressure recovery coefficient
C_v	Specific heat at constant volume
c	Constant or speed of sound or chord length
D	Diameter or Dean number
d	Diameter
H	Head
h	enthalpy
i	Incidence angle
k_s	Equivalent roughness
L	Flow passage length or blade loading
M	Mach number
M_u	Impeller tip Mach number at Impeller exit
M_{1s}	Impeller tip Mach number at Impeller inlet (shroud)
$\dot{m}$	Mass flow rate
N	Impeller rotating speed [rpm]

P	Pressure
PS	Pressure side
Q	Volume flow rate
R	Radius of cross-section
Re	Reynolds number ($=u_{ave}d/\nu$)
r	Radial location or radius of curvature of curved section
SS	Suction side
s	Space or pitch
T	Temperature
th	Throat
U_1	Blade peripheral speed at impeller inlet
U_2	Blade peripheral speed at impeller tip
u_{ave}	Average velocity of flow regime
V	Speed ($=\sqrt{u^2+v^2+w^2}$)
V_n	Normal velocity to cross-section
W	Relative velocity or width
Y	Total pressure loss coefficient
Z	Vane number
z	Axial coordinate

GREEK

α	Flow angle with reference to radial or axial direction
β	Relative flow angle with reference to radial direction
Φ	Flow coefficient

γ	Specific heat ratio
η	Efficiency
μ	Work coefficient or dynamic viscosity
υ	Kinematic viscosity
π_s	Static pressure ratio
π_t	Total pressure ratio
θ	Angle
ρ	Density
σ	Slip factor
τ_t	Total temperature ratio
ω	rotating speed [rad/s]
Ψ	Head coefficient

SUBSCRIPT

0	Station at upstream or the Total value
1	Station at pipe exit or impeller inlet
2	Station at impeller exit
3	Station at diffuser leading edge
4	Station at diffuser trailing edge
5	Station at volute inlet
6	Station at compressor discharge
a	Actual
ave	Averaged quantity

DP	Design point.
f	Friction
i	ideal
m	Meridional direction
n	Number of vanes or normal direction
r	Radial component
ref	Reference
s	Static or isentropic
t	Total
tip	Station 2 (impeller tip)
t-t	Total-to-total
t-s	Total-to-static
u	Tangential component
z	Axial component
θ	Tangential component

Chapter 1 INTRODUCTION

1.1 Turbomachinery

Turbomachinery is the term that refers to rotating machinery that either extracts or adds energy to fluids by the dynamic action of one or more moving blade rows, called stages. The rotor changes the kinetic energy, stagnation enthalpy, and stagnation pressure of the fluid. This definition covers everything from classic fans to turbopumps of the space shuttle main engines. Turbines, Pumps, Compressors and Fans are major categories of turbomachinery. Turbomachines are major components in many applications such as aerospace and marine vehicle applications; energy applications; land propulsion systems; hydraulic; gas and steam turbines; industrial pipeline; and processing equipment applications such as gas, petroleum, and water pumping plants. Moreover, turbomachinery has a wide variety of other applications such as heart-assist pumps, industrial compressors, and refrigeration plants.

1.2 Compressor

A compressor is a machine that compresses air (or a gas) from a lower intake pressure to a higher exhaust pressure through reduction in volume. A compressor needs a driving unit that provides power to operate it and that may be a gasoline engine, diesel engine, electric motor, or a turbine. The major fluid mechanics problem in turbomachinery shows up in the design of compressors because the flow is going from lower to higher pressure. The design of a turbine, with its flow going from higher to lower pressure, always works and with fair care it would have a high efficiency.

Compressors are found in one stage to multi stages when it is needed. The compression ratio varies depending on the type and application of the compressor. Since most turbines need a compressor to provide a compressed gas, the compressor development is then more demanding.

1.2.1 Background

The major fluid-mechanics problem in turbomachinery encountered during the design of compressors. The design of a turbine almost always works because it operates from a high to a low pressure. Actually, if the design of a turbine is given reasonable care it works at high efficiency. On the other hand a compressor, particularly the axial-flow type, may not build a pressure at all. Until almost the beginning of the twentieth century, the isentropic efficiencies of the compressors did not exceed 50 percent.

After Papin's centrifugal blowers, which were invented in 1705, there seems to be not much development until 1884, when Charles Parsons patented an axial-flow compressor. In 1887 he constructed and sold a three-stage centrifugal compressor that was used for ship ventilation. Ten years later he returned to experiments on axial-flow compressors and made an eighty-one-stage machine in 1899 that reached about 70 percent efficiency. This number of stages was very high and could be an all-time record. At the beginning of the twentieth century around 1907 his company had made or had on order forty-one stage, axial-flow compressors, but they were plagued by poor aerodynamics, and consequently he stopped production in 1908. Based on some of their publications, Parsons seems to use far too high a spacing/chord ratio for the rotor-blade settings, and all blade rows would likely be stalled over much of the operating range. Some years later, Parsons returned to making radial-flow compressors.

Auguste Rateau is another major pioneer who was working on compressors at same time. In 1892 he published a major paper on turboblowers. About ten years later he designed a turbocompressor to give a pressure ratio of 1.5 at 12,000 rpm; but when tested, it gave a low isentropic efficiency of only 56 percent. He did not stop there but kept designing and building compressors of increasing pressure ratio and mass flow, and gradually their efficiencies increased.

The development of compressor design did not stop there but rather kept going because there is still need for it.

1.2.2 Compressor Classification

A compressor uses the driving power to increase the pressure of a fluid. The gas enters a compressor at relatively low pressure and exits at a higher pressure. In the industry there is a very wide range of service requirements so, there are many different types of compressors that are used. Before selecting a compressor type for an application, some basic information related to its performance requirements should be at hand. This includes some parameters (such as pressure ratio, flow rate and cost consideration) and could include other special characteristics like space limitation and nose. One can then consider the type of machine needed from a range of types of compressors that are available.

In general, there are two basic compressor types: positive displacement compressors and continuous flow compressors. Each type is then classified further as shown in the following (Figure 1-1).

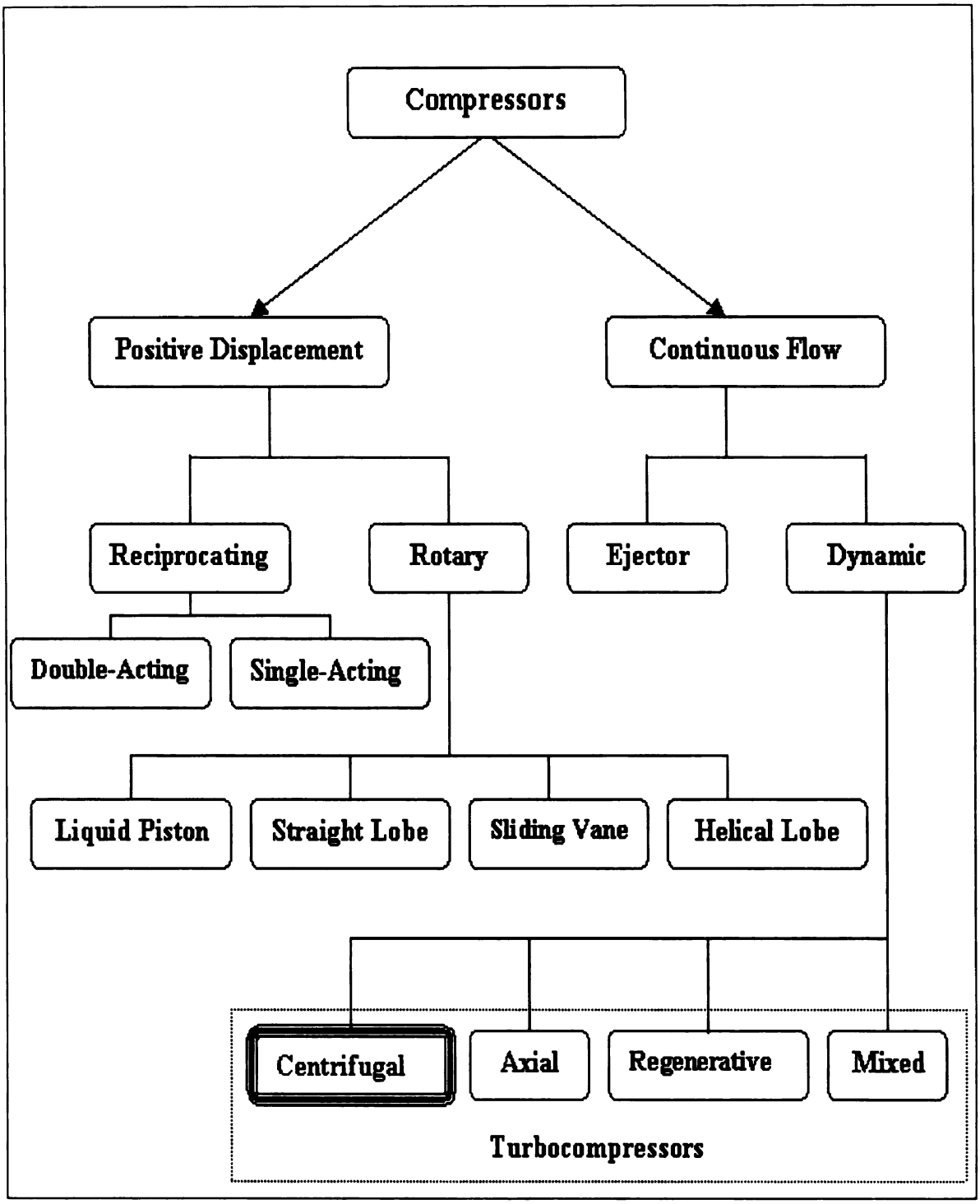

Figure 1-1 Classification of Compressors

In the positive displacement type, a given quantity of gas is trapped in a compression chamber and the occupied volume is mechanically reduced, causing a corresponding rise in the gas pressure before it is discharged. At constant speed, the air flow remains basically constant while the discharge pressure varies. These compressors are available in two types: reciprocating and rotary. A reciprocating compressor can be thought of like a bicycle pump. A piston reduces the volume in the cylinder occupied by the gas, which results in compressing it to a higher pressure. This piston is driven through a crankshaft and connecting rod by an electric motor. In single-acting compressors a compression stroke is in one direction only, while the double-acting ones allow a compression stroke as the piston moves in both directions. Large industrial reciprocating air compressors are double-acting and they use water for cooling. Multi-stage double-acting compressors are very efficient compressors compared to rotary units and are typically larger, noisier, and more costly. The size of reciprocating compressors varies from less than 1 hp to more than 600 hp.

The other type of the positive displacement compressors is the rotary compressor. Recently, rotary compressors have gained more popularity in American industry. The compression process in rotary compressors is caused by the positive action of rotating elements. Normally, they are used in sizes from 30 up to 200 hp. The helical lobe, also known as rotary screw, is the most popular type of rotary compressor. Male and female screw-rotors mesh, trap air, and reduce the volume of the air along the rotors, causing a pressure rise of the air at the discharge point. Rotary screw compressors have the advantage of low initial cost, compact size, and low weight and are easy to maintain. The other types of rotary compressors are less popular, including sliding vane, liquid piston,

and straight lobe. Both reciprocating and rotary compressors will not be further discussed in this study.

The continuous flow compressors are classified into ejector and dynamic type compressors. Ejectors are designed to convert the pressure energy of a moving fluid to velocity energy to entrain the suction fluid. The mixed fluids will then be recompressed by converting velocity energy back to pressure energy. This is based on the theory that a properly designed nozzle followed by a properly designed throat will economically make use of the high pressure fluid to compress from a low pressure region to a higher pressure. This change from pressure head to velocity head is the basis of the jet vacuum principle. Ejectors are reliable and economical to produce vacuum. Some advantages of the ejector design are its low initial cost, lack of moving parts, and simplicity of operation.

The dynamic compressor is the second type of continuous flow compressors in which air or gas is compressed by the mechanical action of rotating vanes or impellers imparting velocity and pressure to the flowing medium. In other words they raise the pressure of the air by accelerating the fluid to a high velocity then convert the energy from the velocity of the air to pressure. The dynamic compressors are subdivided into regenerative, axial, mixed, and centrifugal (or called radial) type compressors. These four categories are also called "Turbocompressors".

In a regenerative type compressor the gas moves helically in the casing and reenters the impeller many times in its peripheral path from inlet to discharge. The main advantage of regenerative turbomachines is the ability to generate high head but at low flow rates. At certain tip speed the regenerative compressors have the ability to develop

much higher heads than any other type of compressors. Other advantage of these types of compressors is the advantage of no surge or stall instability. (Moffat 1987)

In axial compressors the flow comes and leaves the rotor axially. This type of compressor is made up from rows of airfoil cascades. One half of these rows are called rotors that are connected to the central shaft of the compressor. The other rows are called stators, which are fixed to the outer casing and do not rotate. Stators are meant to increase pressure while keeping the flow from spiraling around the axis by bringing the flow back parallel to the axis. For many aircraft applications it is preferred to have axial compressors. In an average single-stage centrifugal compressor the pressure ratio is about 4. In a similar single-stage axial compressor the pressure ratio is 1.2. Axial compressors are preferred over others is some cases because it is easier and more efficient to link several stages together and produce a multistage axial compressor. For a typical multistage axial compressor of 8 stages the pressure ratio is about 4. In a multistage centrifugal compressor the flow needs to be ducted back to the axis at each stage, which is less efficient for aircraft because greater cross-sectional area is needed. [NASA web]

In centrifugal compressors the flow comes axially and leaves radially (perpendicular to the axis of rotation). The centrifugal compressors give a high pressure ratio per stage compared to the axial compressors. This type will be discussed in more details in the next section.

In the mixed flow compressors the axial and radial components of the velocity are considerably present at the rotor outlet. They are designed to have an advantage of both axial and centrifugal compressors.

Even though fans and blowers create a pressure difference like compressors, they normally are not called compressors. For fans, a typical Pressure Ratio (π is between 1.0 and 1.1. For blowers it is slightly higher, which is between 1.1 and 2.0. When the pressure ratio is higher than 2.0, it is normally called a compressor. (Engeda 2004)

1.3 Demands on this Study

A centrifugal compressor is a commonly used machine in petroleum and gas industry. Due to the limitations of the operating range of many centrifugal compressors, in many cases the compressor needs to be shutdown to prevent damage. Shutting down a compressor even for a short time will cost millions of dollars and may cause the whole plant to be shutdown. Due to the current oil prices, the loss will be even more. Therefore, the importance of having wide operating range centrifugal compressors for such applications can not be ignored. The centrifugal compressor manufacturers attempt to offer a standard line of compressors, which would provide a large flow range for a variety of inlet conditions and process gases. Modifying an existing design is another common practice that is preferred by the centrifugal compressor manufacturers rather than a new design. The operating range of centrifugal compressors depends heavily on their impeller design. Due to these reasons the study of the effect of centrifugal impeller design on the flow range is essential for the development of these machines to meet the current gas industry requirement.

1.4 Objective and Organization of this Study

The objective of this study is to analyze and model the flow of centrifugal compressor impellers. The compressor industry makes money by one of three ways: producing new machines, solving a current problem, or modifying a previous design to meet customer satisfaction. This work is related to the third reason where centrifugal compressor impellers are modified so the compressor could have a better performance or wider operating range. The following steps explain how the goals of this work were systematically achieved.

1. Experimental testing of the compressor with four original and four modified impellers has been done at SOLAR TURBINES Laboratories. The impellers' geometries drawings and experimental data were provided to the Turbomachinery Lab at MSU to be analyzed and studied.
2. The experimental data for all the eight impellers, which cover a wide area of specific speeds, were analyzed and studied as part of this work.
3. The experimental data were also compared with results obtained from a One-dimensional (1-D) code done at the Turbomachinery Lab at MSU.
4. A CFD study was added to model four extreme impellers that have the lowest and highest specific speed for both the original and the modified.
    i. The grid from the available drawings for the four impellers was generated.
    ii. Then the numerical simulation was done using CFX-TASCFlow and results were obtained.

iii. The results were then compared with the experimental data and one-dimensional results and then discussed.

Based on the previous steps, this work was carried out and presented in this dissertation. It consists of six chapters starting with the general introduction to turbomachinery and compressors in Chapter 1. Chapter 2 presents a general and theoretical discussion of a centrifugal compressor, its components, and the centrifugal impeller in particular. This Chapter, also, includes some of the previous research work related with the current study. Chapter 3 deals with CFD analysis in general and gives more details about the CFX-TASCFlow package used in this work. It also discusses the major steps in CFD analysis, which are the pre-processing, the solver, and the post-processing. Grid generation, boundary conditions, and the turbulence modeling are discussed in more details in this chapter. Chapters 4 mainly presents and discusses the experimental data for all the impellers and compares them with the results obtained from the 1-D analyses. Chapter 5 shows the CFD results and compare it with the experimental data. Chapter 6 draws the conclusions focusing mainly on the effect of the specific speed, the rotational speed and the cut the impeller on the compressor stage performance and the operating range.

Chapter 2 CENTRIFUGAL COMPRESSOR AND IMPELLER DESIGN CONSIDERATIONS

2.1 Centrifugal Compressor

2.1.1 Development Need and Applications

Centrifugal Compressors have a very wide area of applications. Because of the advantages of the higher-single stage pressure ratio and the wider stable operating range over axial compressors, the centrifugal compressor has been widely used. Centrifugal compressors are found in small gas turbine engines, turbochargers, and refrigeration systems and are used extensively in the petrochemical and process industry. Although they are not used in high-thrust devices most low-to-moderate thrust turboshaft, turboprop, and turbojet engines have centrifugal compressors. Sometimes in aircraft engines the centrifugal compressor is combined with an axial one to achieve better performance. Industrial facilities use compressed air for too many operations. Almost every industrial facility has at least a centrifugal compressor. Their applications go even beyond that use, like health applications and much more. Although all the previous applications are important, the driving force for centrifugal compressors development is their involvement in airspace and power generation applications. Therefore, the demand on efficient and reliable centrifugal compressors is increasing because of their association with many industries, which are on demand today.

In the previous applications and much more compressors can be found in small scale as well as large ones. They also differ in the pressure ratio that they built and the driving device. So, it is clear that for a certain application there will be a certain

centrifugal compressor that will be preferred over others. Looking at the application type carefully the centrifugal compressor type can then be selected.

Compared to the other types of compressors, centrifugal compressors are reliable, compact, and robust; they have better resistance to foreign object damage and are less affected by performance degradation due to fouling. Centrifugal compressors are mainly used in areas where the requirements are high pressure ratio and low to moderate mass flow (Figure 2-1). They also have the advantage of a wide stable operating range compared to some other types of compressors. In centrifugal compressors the gas flows in a radial direction perpendicular to the axis of rotation, which makes them more compact.

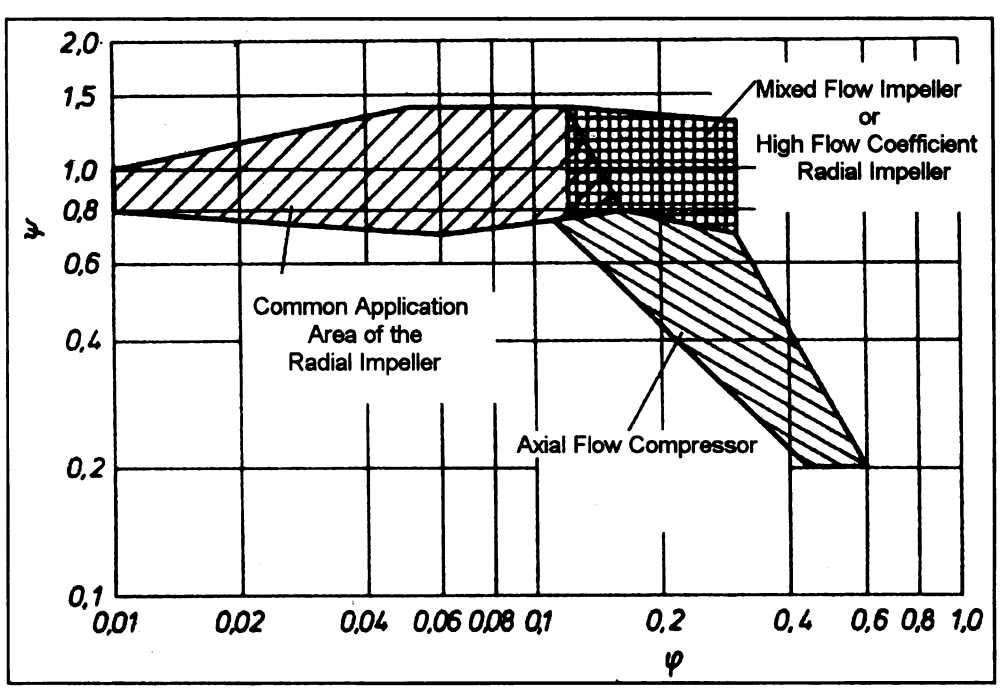

Figure 2-1 Application areas of turbocompressors

Since the centrifugal compressor finds a wide variety of application each application places its own demands on the design of the compressor. For these reasons it is a common practice by the centrifugal compressor manufacturers to offer a standard line of compressors that would provide large flow range for a variety of inlet conditions and process gases.

The main four components in centrifugal compressors are shown in Figure 2-2, as follows: (1) a stationary inlet casing, (2) a rotating impeller, (3) a stationary diffuser of the vaneless or vaned type, and (4) the collector or volute. In a multistage centrifugal compressor the return channel is another essential component.

The fluid is drawn in through the inlet casing into the eye of the impeller of the first stage (in multistage compressor) parallel to the axis of rotation. In order to add angular momentum, the impeller whirls the fluid outwards and turns it into a direction perpendicular to the rotation axis. As a result, the energy level is increased, resulting in both higher pressure and velocity. The gas then proceeds through a vaned or a vaneless diffuser, which convert some of the kinetic energy of the fluid into static pressure. In a single stage centrifugal compressor the diffuser is followed by the volute whose function is to collect the flow from the diffuser and deliver it to the discharge pipe. It is possible for the fluid to gain a further deceleration in the volute and thereby an additional pressure rise. In a multistage centrifugal compressor the diffuser is followed by a return channel and the volute is placed after the last stage (Figure 2-3). Multistaging some times is needed for centrifugal compressor to achieve higher pressure ratio. The contribution of each component of the compressor is shown in Figure 2-7.

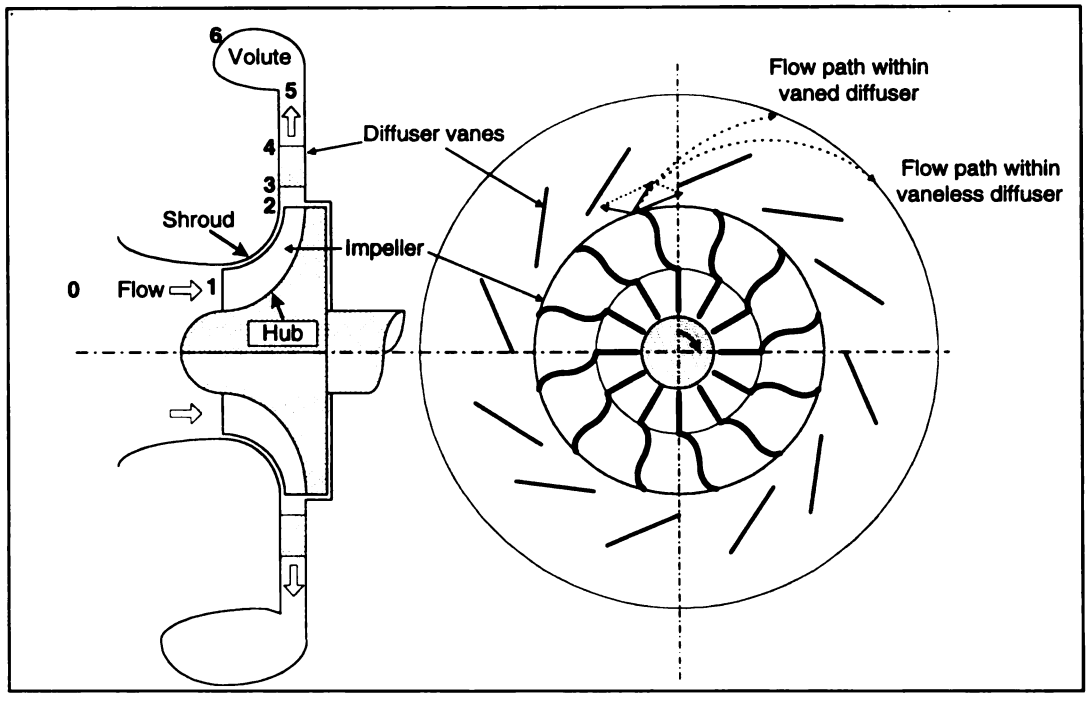

Figure 2-2 A Single Stage Centrifugal Compressor

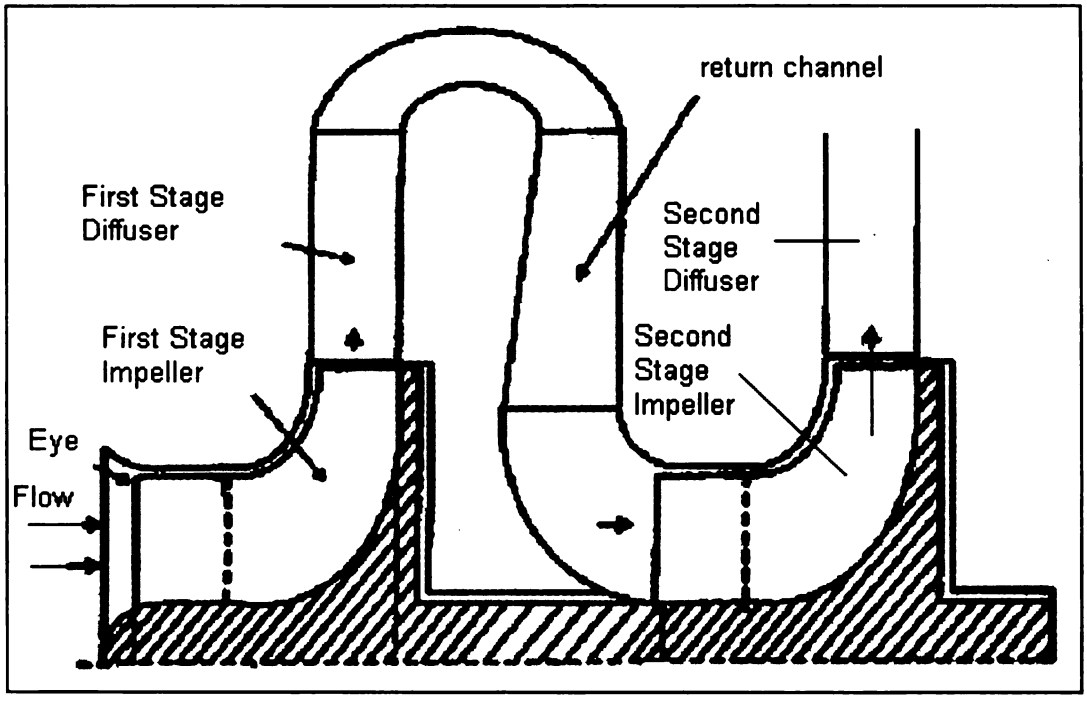

Figure 2-3 A Multistage Centrifugal Compressor

2.1.2 Centrifugal Compressor Design

The flow in a centrifugal machine is highly complex and not easy to explain. It is three dimensional, highly turbulent, viscous, and unsteady in many cases. This makes the design of the centrifugal compressor more difficult than other machines. Dimensional analysis and similarity principles are very useful in designing centrifugal compressors like designing many other machines. The dimensionless parameters state that the machines, which are geometrically similar, have similar velocity triangles. Some of the dimensionless parameters, which are commonly used in designing centrifugal compressors, are the head coefficient, the work factor, the flow coefficient, the efficiency, the specific speed, the specific diameter, and Mach number. The specific speed and specific diameter are a group of dimensionless parameters that are used for stage selection applications. The other group of dimensionless parameters (the head coefficient and the flow coefficient) are generally used to predict the off-design characteristics of the machine. Dimensionless parameters will be discussed more in the impeller section.

Common Approach:

A widespread method that a designer would follow to design a simple centrifugal stage starts from the non-dimensional specific speed verses the specific diameter chart. This chart was presented by Balje (1981) and was calculated at the design point of different geometrically of different machines. He then produced what is termed the Cordier line, which has a single operating point for each machine type. Balje (1981) made a good use of these $n_s - d_s$ charts (Figure 2-4).

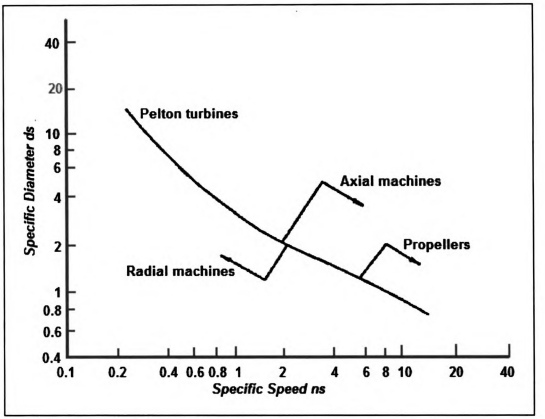

Figure 2-4 Cordier Line (Adapted from Balje 1981)

To design a centrifugal stage some data should be available. These data include the mass flow rate, the inlet total pressure and temperature, the pressure ratio, and rotational speed, which depend on the driving device. Based on having these data, the designer can use the relation of the non-dimensional $n_s - d_s$ charts. The designer knows that n_s and d_s have different definitions but all are dimensionless and need to be consistent. Balje chart can be used to estimate d_2 and other parameters. A quick estimation of the size of the tip impeller diameter can be found from the following equation:

$$d_s = \frac{d_2 \Delta h_{0s}^{1/4}}{\sqrt{Q}} \tag{2-1}$$

where: d_2 is the impeller tip diameter (at the impeller outlet)

Δh_{0s} is the total isentropic enthalpy given as:

$$\Delta h_{0s} = c_P T_{01} \left(\left(\frac{P_{03}}{P_{01}} \right)^{\frac{\gamma-1}{\gamma}} - 1 \right) \tag{2-2}$$

Q is the volume flow rate which can be found from continuity equation:

$$\dot{m} = \rho A c = \rho Q \tag{2-3}$$

where:

A is the cross sectional area

$\dot{m}$ is the mass flow rate

C is the axial velocity

ρ is the gas density

For Balje chart to be used, either n_s or d_s need to be known. The equation of the specific speed is given as

$$n_s = \frac{\omega\sqrt{Q}}{\Delta h_{0s}{}^{3/4}} \tag{2-4}$$

The specific speed above is a non-dimensional quantity, when the rotational speed ω, is given in rad/s, and Q and Δh_{0s} are in a consistent set of units such as: m^3/s and J/kg respectively.

Balje (1981), also, presented another graph that relates the specific speed to the machine efficiency for radial, axial, and mixed machines (Figure 2-4). Therefore, for a

certain machine type the design point will be near the peak efficiency, which gives estimation for the specific speed. Then from the known data Q can be found from the specific speed equation. After that the Specific diameter equation can be used to find d_2. The other parameters at inlet and exit of each component at every stage can be found using ideal gas relations and general thermo-fluid formulas. Balje (1981) gave a systematic way to fine the other parameters of the centrifugal compressor. Throughout the design, some suitable assumption need to be done and iterations may also be required to get a reasonable design.

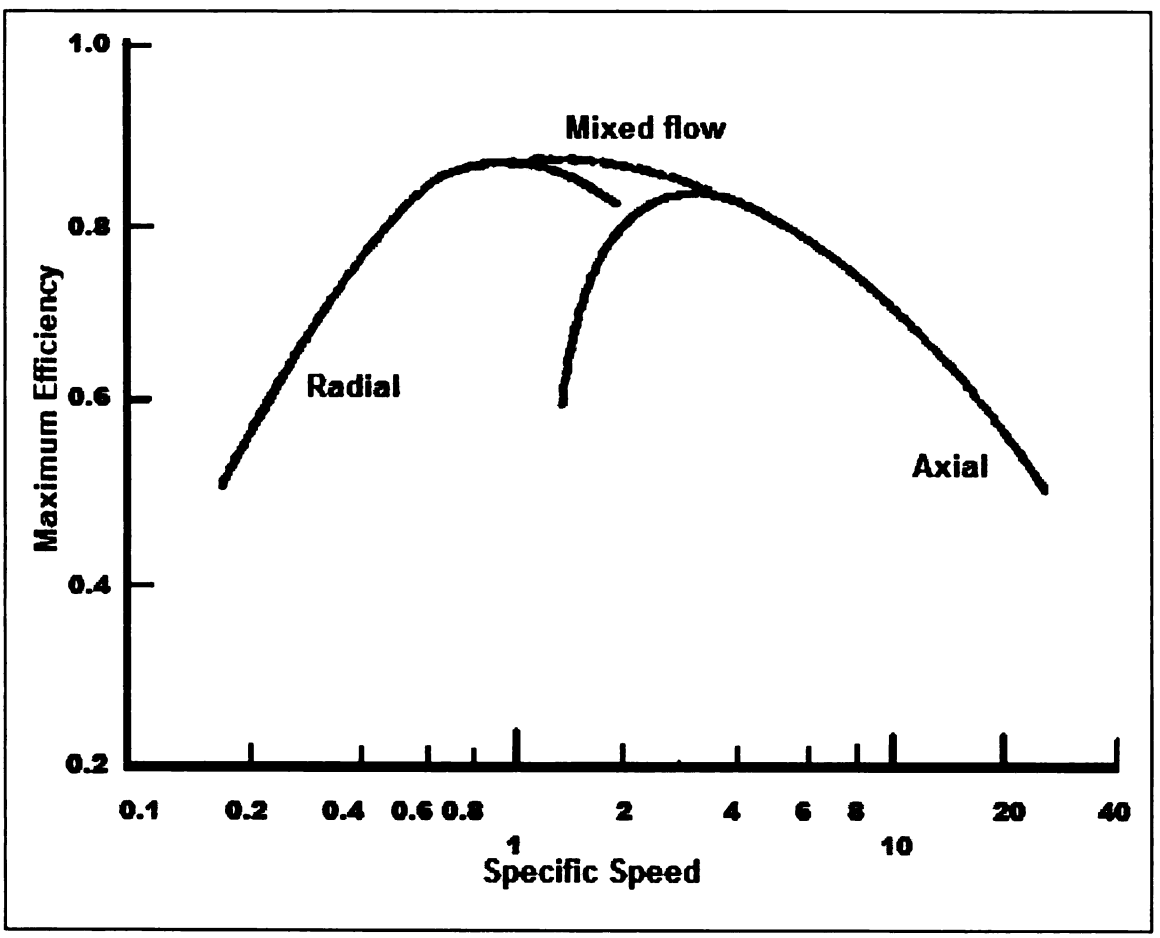

Figure 2-5 Selection of Compressor Type with Specific Speed (Adapted from Balje 1981)

Japikse (1996) gave a more detailed design procedure including some solved examples and some computer codes as well. In addition Rogers (1974), Dean (1976), Whitefield (1990), and Aungier (2000) discussed the design of the centrifugal compressor. Additional people discussed a specific component design as it can be seen in the following section.

Current Centrifugal Compressor Design Trends:

- The design of bladed components typically begins in simplified codes such as one-dimensional and streamline-curvature codes.
- This one-dimensional flow design calculations use empirical data from the literature and test results from a previous design to give preliminary results about the compressor performance, as well as impeller and diffuser geometrical parameters. The calculation routine is sequential, iterative and quick with modern personal computers.
- For the one-D calculations, input data includes the compressor pressure ratio, inlet temperature, inlet pressure, fluid properties, rotational speed and mass flow. Simple one-D codes includes variables that can be altered later: specific speed, different geometrical ratios, number of blades in the impeller and diffuser, loss constants, inlet flow angles, volute pressure recovery factor, etc.
- One-D calculation of compressor efficiency is mostly based on measured data. The radial, vaneless diffuser is calculated analytically, including viscous effects and also the volute is calculated analytically. Between the diffuser and the volute there is a semi-empirical loss coefficient model, based measurements in the

literature. Reynolds number correction for efficiency is done by referring to literature.

- One-D calculation results include:
    1. Pressure, temperature, enthalpy, density at inlet and outlet of the impeller, and inlet and outlet of the diffuser and volute.
    2. Pressure, temperature and enthalpy must be given both in static and total/stagnation values.
    3. The main geometry parameters for the impeller, diffuser, and volute, as well as compressor specific speed and power consumption.
    4. Isentropic efficiency and pressure ratio in each point and pressure recovery in the diffuser and volute.
    5. Velocity triangles, deviation angle, and relative Mach number in the impeller wheel inlet and outlet
    6. Advanced one-D codes also estimate off-design performance and surge point and produce the compressor performance map.
- Next follows, the generation of the impeller blade geometry. The main geometry data of the impeller, such as the main dimensions and the blade angles obtained from one-D flow design are used as input data for three-dimensional modeling. The blade design is started with defining the camber lines for the hub and shroud of an impeller blade. A three-D modeling software provides a graphical blade design environment for modifying the camber line geometry. Such a program is exclusively used for geometrical design, No flow calculation is done at this stage.

- Geometry specification usually takes place in special-purpose codes, as opposed to full CAD packages.
- The next stage is to define the thickness distributions for the hub and shroud of the blade, and they can be modified graphically, as well. Based on the camber lines and the thickness distributions, the suction and pressure side co-ordinates for the hub and shroud are finally calculated. The blade can be displayed using various projections, and enlargements of blade details can be displayed, as well. When the blade designer accepts the blade geometry, the numerical geometry data can then be generated for compressor flow CFD analysis: finite element method (FEM) based stress and vibration analysis (FEM) and computer aided manufacturing (CAM). If any non-conformity is found in the blade geometry, or the results from either the CFD or FEM analysis do not meet the requirements, the design procedure must be repeated partially or totally, even starting from one-dimensional flow design.
- Specialized grid generators are now available which take data directly from the geometry generation codes and provide automated templates for rapidly building grids.
- Non-axisymmetric components such as inlets and volutes are often developed in CAD packages or specialized codes. The CAD packages can export the data in IGES or in native CAD format, which can now be read into some CFD pre-processors and grid generators.
- On the post-processing side, customized automated tools are now available. Post-processors contain post-processing "macros" (a sequence of post-processor

commands), which can provide both quantitative information and graphical images. Performance predictions for individual components or for the entire model can be obtained.

- Available information includes averaged total and static temperature and pressures, loss coefficients, efficiency, flow distortion etc. In addition, useful circumferentially-averaged meridional profiles of a variety of quantities can be obtained.
- Qualitative plotting of fully 3-D, blade-to-blade and circumferentially-averaged quantities can be automated, providing the analyst a detailed view of the flow field, enabling visual assessment of its quality.
- The high complexity of the flow, especially in the rotating impeller, makes the CFD modeling very difficult. Much research has been done in analyzing the flow and the different viscous phenomena. The selection of the turbulence model has a great influence on simulation accuracy, particularly if there is instability in the real flow. When time-dependent calculation of the whole compressor becomes a routine practice (at the moment it requires a lot of computation time), the accuracy of modeling obviously increases.
- The performance of the final compressor geometry is tested in the test facility.
- Industrial designers and analysts require CFD software to provide accurate solutions to their applications of interest in a cost-effective and timely manner. With the widespread availability of affordable workstation class computing, the main issues are therefore accuracy and productivity (productivity also being directly related to cost). The information provided by the CFD must be of

sufficient accuracy to allow the designer to make appropriate decisions based on the available information, and it must be available rapidly enough to fit within the time scales of the design cycle

- Productivity in the usage of CFD has improved significantly over the past five years, for several reasons, including:
    1. More powerful computing, including PC's.
    2. The development of parallel processing.
    3. Links between CFD codes and other design tools and with CAD.
    4. Customized and semi-automated grid generation tools.
    5. Specialized pre- and post-processing tools and environments.

The more powerful computing now available enables the analysis of larger grids and more components together in a shorter period of time. The recent availability of parallel computing further expands the size of model that can be analyzed, and reduces turnaround time. The results are not only of higher quality but obtainable sufficiently quickly to be useful within the design cycle.

The centrifugal compressor is not an easy device to be designed. Its design combines many design considerations, which are mainly based on three major fields: stress, rotordynamics, and aerodynamics. Stress problems are clearer on impeller blades and diffuser vanes. They are caused by the material strength limitations that are limited by the aerodynamic performance requirement and the manufacturing cost. Rotordynamics is another field of design considerations. These include the purely mechanical vibration of the machine caused by the impeller rotation as well as the flow induced vibratory

effect. They give some restrictions on the design of compressor components to prevent the entire machine from significance vibrations.

2.1.3 Compression Process

Compression of gasses tends to behave according to the following equation $P.v^n = \text{Constant}$, where P is the pressure and v is the specific volume (Volume/unit mass).

Compressing a gas from P_1 to P_2 is shown in the T-s (h-s) and P-v diagrams depending on the value of n (Figure 2-6):

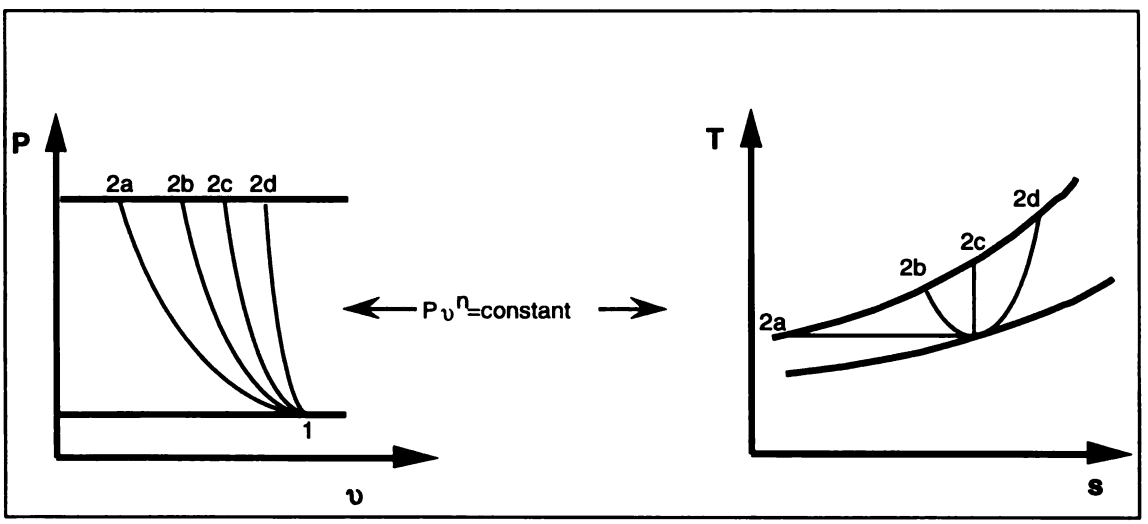

Figure 2-6 P-v and T-s for a compression process

where:

1-2a: Isothermal compression, with highest cooling n=1

1-2b: Polytropic compression with cooling, n<k

1-2c: Reversible, adiabatic compression, n=k

1-2d: Polytropic compression, with friction effect and heat, rejection, n>k

Figure 2-7 shows a typical example of h-s diagram for a centrifugal compressor stage. The numbers shown correspond to the locations shown in Figure 2-2. The upper line in

Figure 2-7 represent the stagnation (Total) pressure values (the dashed line) while the other one is representing the static values (the solid line).

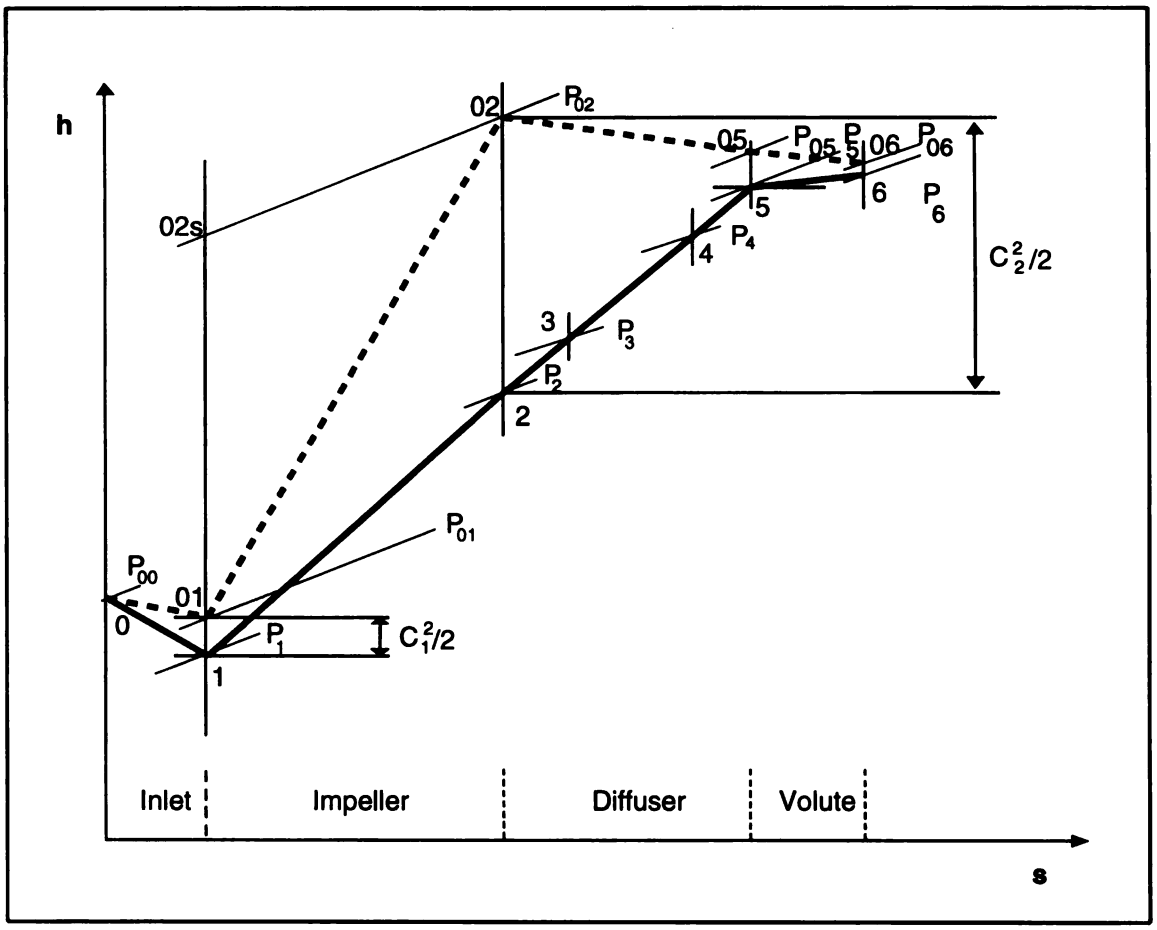

Figure 2-7 Atypical Example of h-s diagram for a centrifugal compressor stage

The change of the stagnation (total) properties for the flow inside the centrifugal compressor components with no cooling are given in Figure 2-8.

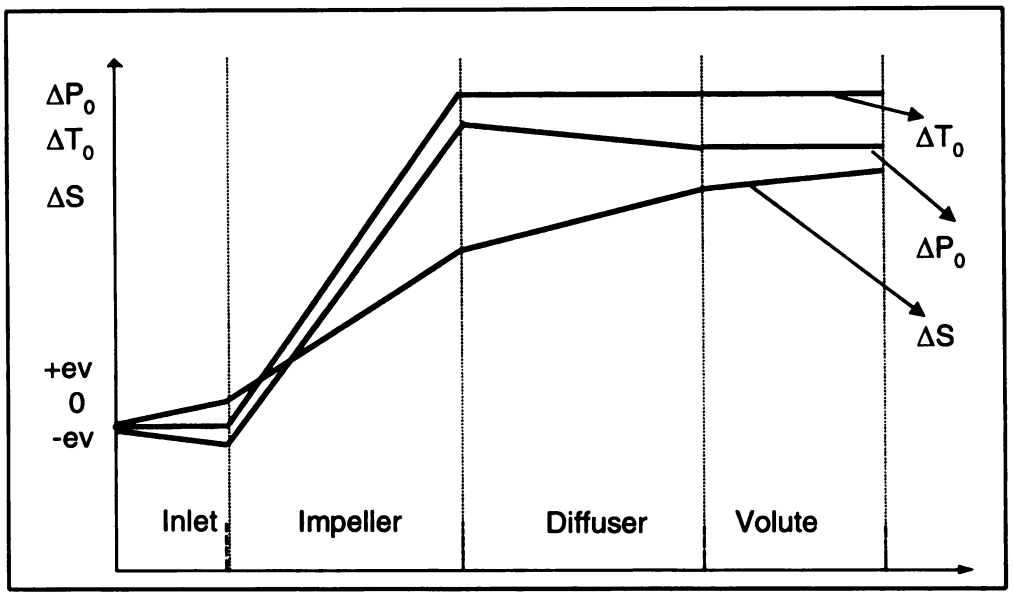

Figure 2-8 Total pressure, temperature change and Entropy rise (loss) in centrifugal compressors

2.1.4 Centrifugal Compressor Components

The wide range of demands on centrifugal compressors brings many design considerations. Most of the design requirements need solutions to two major problems: stress and aerodynamics. The stress problems are caused by the material strength limitations and the capability to accurately predict blade and impeller steady state and vibrational stress for complex impeller shapes at high rotational speeds. The aerodynamic problem is to efficiently accomplish large air deflections and diffusion at high flow velocity, with the added difficulty of very small passage flow areas required to get good efficiency and high pressure ratio. Even though the individual components of the compressor are capable of achieving high efficiency, it is the efficiency of the whole stage that is of great importance. Thus, component matching is an essential aspect of design. It is often required to redesign one or more components of the compressor due to improper matching and sometimes the efficiency of a component is sacrificed to achieve good matching.

The actual and ideal head characteristic are different due to the internal losses in the compressor (Figure 2-9). These losses include mainly the incidence loss as well as the friction loss. If the inlet flow is highly distorted or swirling, it affects the incidence losses. On the other hand, the friction loss is a function of the square of the flow velocity and the passage length which the fluid particles follow.

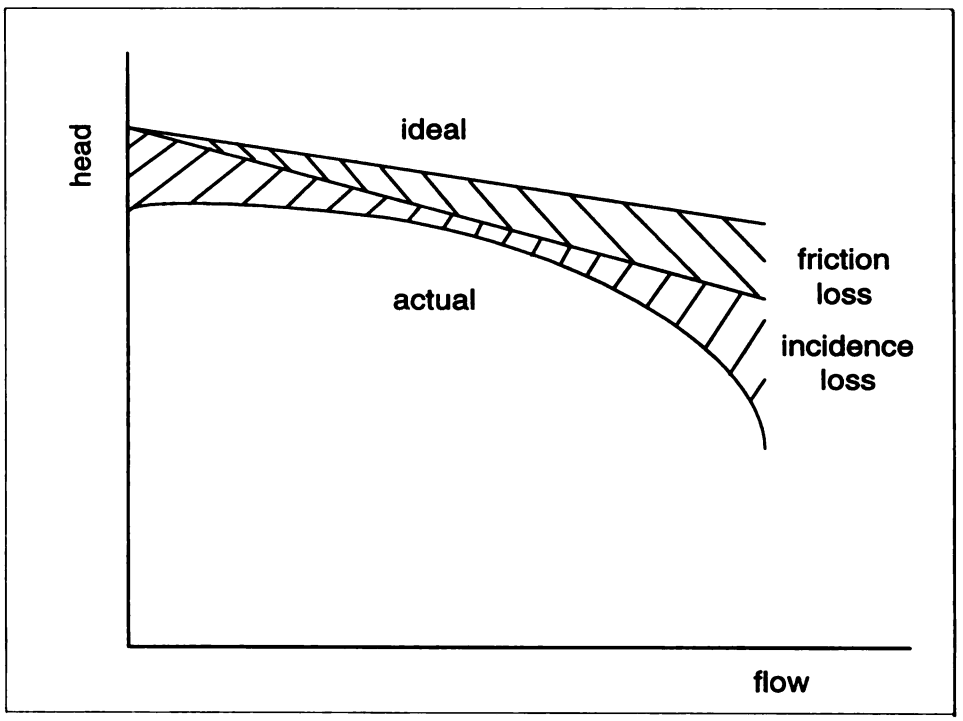

Figure 2-9 Ideal and actual head characteristic of a compressor

2.1.4.1 Inlet:

In centrifugal compressors, like many other machines the inlet plays an important role. There are more than one type of inlet that are in used. These include a straight inlet and a curved inlet. The objective of the inlet device is to bring the flow as uniform as possible to the impeller's eye with or without a preferred level of inlet swirl. A good design for the inlet would give a better efficiency as well as a better operating range for

the compressor. This can be achieved when the design parameters are matched between the inlet and the impeller. Therefore, the flow properties after an inlet component have a great affect on the impeller performance and then on the entire compressor.

2.1.4.2 Impeller (General):

Figure 2-7 shows that the major rise in static enthalpy is in the impeller as well as the diffuser. But, looking at Figure 2-8 we can see clearly the importance of designing an efficient impeller. This figure show that the impeller is the only component in the compressor where a significant rise in the stagnation (total) temperature and pressure occurs. In other words the impeller is the heart of the compressor where the energy is transferred from the shaft to the fluid by increasing the velocity and pressure of the fluid. The impeller is an essential element of the centrifugal stage because of the pressure it builds (Figure 2-7) In centrifugal compressors it is the only major rotating part, which makes the flow more complex than other compressor components. Two main types of impellers are available: unshrouded (open), which does not have a front cover, and shrouded (closed), which has a front cover. When a shrouded impeller is used, the secondary flow arising, because of the tip clearance, can be avoided. On the other hand when the unshrouded impeller is used, the cover friction losses can be avoided so, clearly a trade-off must be made. Another disadvantage of shrouded impeller is the high stress generated by the front cover, which limits the use of this type of impeller to relatively low rotational speed machines. A detailed discussion of the centrifugal impeller will be done later in this chapter.

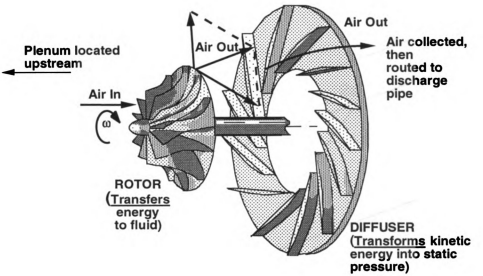

Figure 2-10 Key Components of centrifugal compressors

2.1.4.3 Diffuser:

The diffuser is used to convert (transform) the kinetic energy available in the gas after it exits the impeller into static pressure by decelerating the fluid (Figure 2-6). The process of diffusion or the decrease of velocity to gain static pressure is another essential process of a centrifugal compressor. Diffusers may be found as vaned or vaneless. Since there is a possibility of separation, the rate of diffusion must be limited and the process is inevitably accompanied by a loss of energy. For compressible flow, the diffuser effectiveness is defined by the ratio of the isentropic enthalpy change corresponding to the actual rise of pressure to the enthalpy change corresponding to the isentropic rise of pressure caused decelerating the gas. Figure 2-11 shows that the actual rise of static pressure is less than that of the isentropic change of velocity, which makes it less than unity.

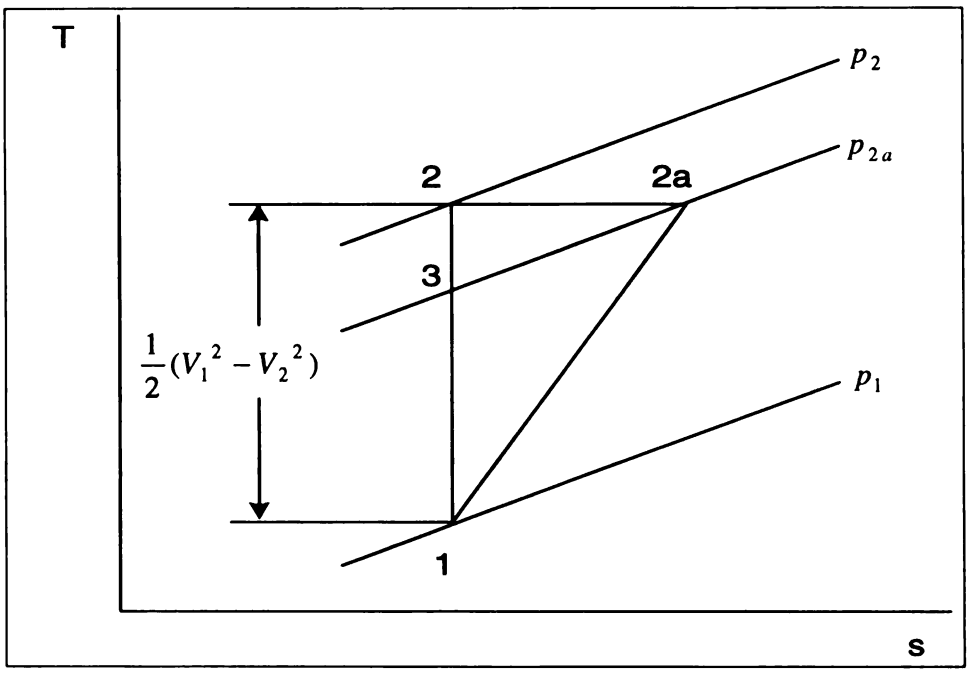

Figure 2-11 T-s diagram of diffusion process

So the diffuser effectiveness of compressible flow can be defined as

$$\eta_d = \frac{h_3 - h_1}{h_2 - h_1} \tag{2-5}$$

where $h_3 - h_1$ is the isentropic enthalpy change from p_1 to p_{2a}

$$h_3 - h_1 = C_p(T_3 - T_1) = C_p T_1(\frac{T_3}{T_1} - 1) = C_p T_1[(\frac{p_{2a}}{p_1})^{\frac{\gamma-1}{\gamma}} - 1] \tag{2-6}$$

and

$$h_2 - h_1 = \frac{1}{2}(V_1^2 - V_2^2) \tag{2-7}$$

which eventually gives

$$\eta_d = \frac{C_p T_1[(\frac{p_{2a}}{p_1})^{\frac{\gamma-1}{\gamma}} - 1]}{\frac{1}{2}(V_1^2 - V_2^2)} \tag{2-8}$$

Vaneless diffusers are easy to design and manufacture. They are used in process compressors, turbocharger compressors, and refrigeration compressors. A vaneless diffuser gave a reasonable static pressure recovery compared to their prices. This type of diffuser is simple to design and manufacture because it consists of two parallel walls forming an open radial annular passage from the impeller exit to the diffuser outer radius. Another advantage of the vaneless diffuser is that it does not have a throat, which makes choking not likely to happen. This leads to a possibility of a wide operation range. Figure 2-12 shows the flow path and velocity triangle in a vaneless diffuser.

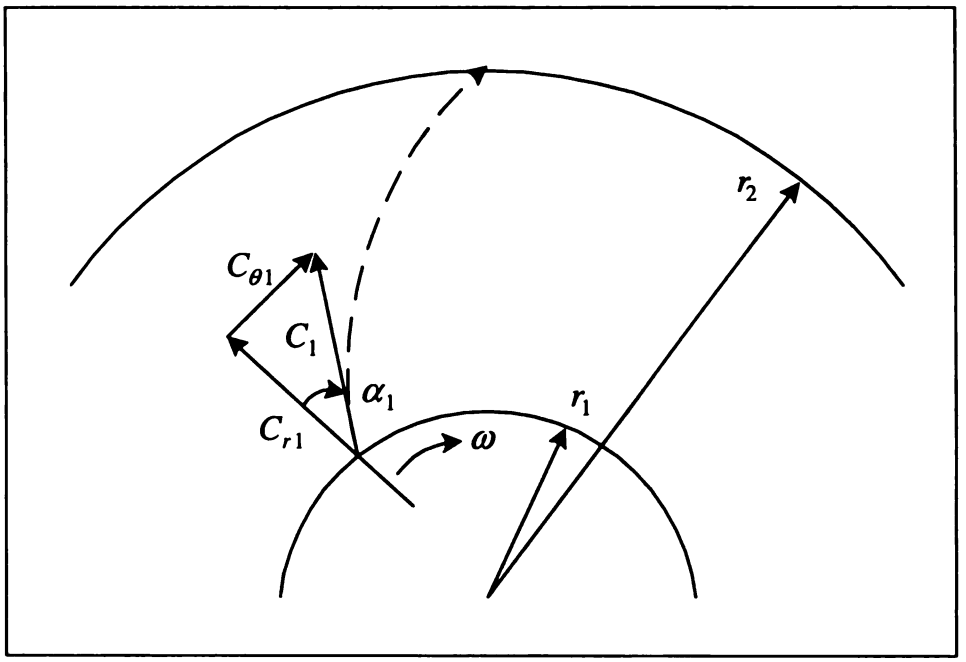

Figure 2-12 Flow path and Velocity triangle in a vaneless diffuser

The vaned diffuser is the other type of diffuser. It consists of diffusing channels that are between vanes, in order to have more diffusion compared to a vaneless diffuser with the same radial space. Even though, the losses are quite high in a vaned diffuser, high efficiency may still be reached with a vaned diffuser because of the increased diffusion that increases the efficiency for the next component such as a volute. The vaned diffuser

throat is the smallest area between the leading edge of one vane and the other side of the next vane. Depending on the throat area of the impeller blade passage, the vaned diffuser may control the compressor maximum flow ("choke") or the minimum flow ("surge"). A critical part of the aerodynamic design is matching the vaned diffuser to the impeller, which is dependent on the vaned diffuser area and the vane setting angle. This will affect the overall efficiency as well as the flow range of the compressor. Locating the vanes at certain distances from the impeller exit (impeller tip) will reduce the vibration, the noise, and the value of Mach number before reaching the diffuser vane leading edge.

Because of their importance and wide range of applications, vaned diffusers vary from the simple to design and manufacture to the 3-D diffuser, which are used in advanced applications.

2.1.4.4 Return Channel:

For a multistage machine, as the flow exits the diffuser, a bend for the flow path is required to turn the flow to the next stage. The return channel connects each stage to the next one and carries the flow from radial back to the axial direction in multistage centrifugal compressors.

2.1.4.5 Volute:

In a single stage centrifugal compressor, the diffuser discharges into a volute that leads the fluid to the exit to the piping system. For a multistage centrifugal compressor this happens in the last stage. It consists of a circular channel that is located circumferentially around the diffuser exit, with a gradually increasing area to get hold of the increasing mass flow rate as the flow collection process goes on. The full-collection plane is the location where all the mass flow from the diffuser has been collected by the volute to be

discharged to the piping system. What divides the collected and uncollected flow is called the volute tongue. An exit cone may be connected to the volute exit to deliver the compressed gas to the piping system. Having a circumferential uniform static pressure over the impeller outlet, is the major objective in designing a good volute. If this goal is not accomplished, the fluid flow in the impeller circulate with every rotation of the shaft leading to a development of vortexes, which results in vane vibration and lower compressor efficiency or even damages the compressor.

2.2 Centrifugal Impeller

As was mentioned earlier, the impeller is the most important part in the centrifugal compressor and actually it is the part that makes the compressor centrifugal. Since it is mostly the only rotating part in the compressor, the energy transfer takes place there.

As a result of the impeller rotation, the energy level of the fluid increases giving more pressure and higher velocity, which is the main objective of the centrifugal impeller. Depending on the throat area of the impeller blade passage, the impeller could control the compressor maximum flow (choke) or the minimum flow (surge). So, matching the design of the impeller inlet to the compressor inlet as well as impeller exit to the diffuser inlet is needed to get rid of some aerodynamic problems. It is now clear how important to design an efficient impeller, which is a wide area of study.

2.2.1 Inducer

The fluid enters the centrifugal impeller through the inducer, which is the inlet section of the impeller, in which the relative flow is turned from the inlet direction which is parallel to the machine axis to almost radial. So, the objective of the inducer is to guide the flow from axial to radial direction, while increasing its angular momentum. The

designer tries to keep the flow subsonic by minimizing the inlet relative Mach number. The design of the inducer has a very obvious effect on the impeller performance and hence on the overall compressor efficiency.

A number of design considerations should be taking care of to determine the eye-hub diameter ($\mathbf{dh_1}$) of the inducer. It can be dictated by the minimum shaft and retaining nut diameter if inboard bearings are used. The size of the shaft and bearing diameter dictate the eye-hub diameter to be large for compressors with outboard bearings. Other factors that affect the choice of the eye-hub diameter and the inducer stress/vibration considerations, the impeller manufacturing techniques, and the number of blades selected. The inducer, eye-tip diameter ($\mathbf{ds_1}$) at the shroud is another parameter that the designer would take care of because of its importance. Normally, the highest inlet relative Mach number occurs in that area; and, therefore, a special attention should be taken to choose that parameter. Assuming no pre-whirl and a uniform axial velocity the relative velocity at the inducer eye can be driven from the velocity triangle as

$$W_{s1}^{\ 2} = C_{x1}^{\ 2} + U_{s1}^{\ 2} \tag{2.10a}$$

$$W_{s1} = \sqrt{C_{x1}^{\ 2} + (\pi N d_{s1})^2} \tag{2.10b}$$

where: **N** is rotational speed of the impeller.

The relative Mach number at the eye tip ($\mathbf{M_{ws1}}$) can then be written as

$$M_{ws1} = \frac{W_{s1}}{a_1} = \frac{W_{s1}}{\sqrt{\gamma R T_1}} = \frac{\sqrt{C_{x1}^{\ 2} + (\pi N d_{s1})^2}}{\sqrt{\gamma R T_1}} \tag{2.10c}$$

Ignoring the width of the blades we can approximate the mass flow rate to be

$$\dot{m} = \frac{\pi(d_{s1}^{\,2} - d_{h1}^{\,2})C_{x1}\rho_1}{4} \tag{2.10d}$$

This gives

$$C_{x1} = \frac{4\dot{m}}{\pi(d_{s1}^{\,2} - d_{h1}^{\,2})\rho_1} \tag{2.10e}$$

Substituting for C_{x1} in eq.2.10c the relative Mach number at the inducer becomes

$$M_{ws1} = \sqrt{\frac{\left(\frac{4\dot{m}}{\pi(d_{s1}^{\,2} - d_{h1}^{\,2})\rho_1}\right)^2 + (\pi N d_{s1})^2}{\gamma RT_1}} \tag{2.10f}$$

For a certain mass flow rate and impeller speed, N, $\mathbf{d_{s1}}$ should be chosen to give the minimum relative Mach number according to eq 2.10f. Plotting $\mathbf{M_{ws1}}$ versus $\mathbf{d_{s1}}$ would give a figure similar to the following.

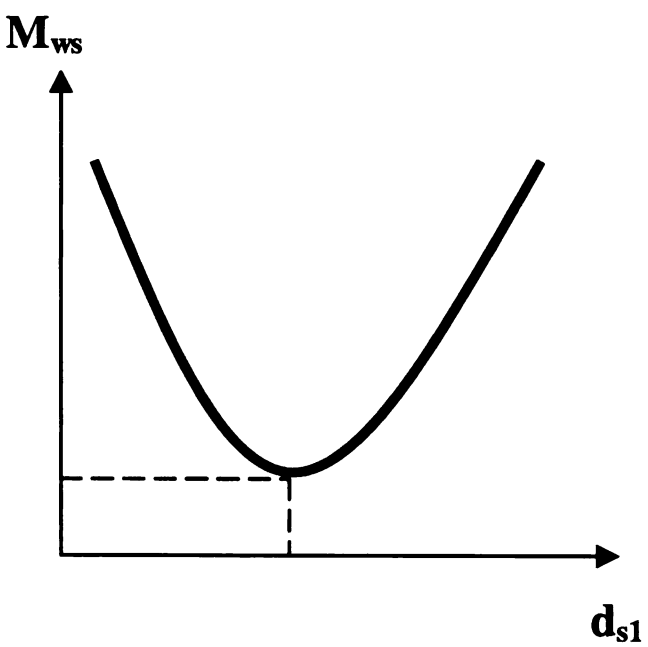

Figure 2-13 Change of the relative Mach number with the inducer eye tip diameter

The relative Mach number (M_{ws1}) may be reduced more if a pre-while is provided for the flow (inlet guide vanes). Doing so will reduce the energy transfer in the impeller. The designer may add inlet guide vanes when designing high-pressure ratio compressors because the inlet Mach number exceeds unity, which allows shock waves to form reducing the impeller efficiency. A trade-off should be made between improving the stage performance from the impeller and a reduction in the stage performance from the diffuser. So, a careful evaluation for each application needs to be taking care of when using inlet guide vanes. Thus, a variable inlet guide vanes may a valid choice to be enable to change the compressor flow characteristic as needed.

2.2.2 Dimensionless Parameters

When designing a centrifugal impeller, the designer needs to use dimensional analysis and similarity roles. For a long time, dimensionless parameters were used to describe the flow and they are still in use. They are used in comparing data from a certain machines or to predict the performance of a different machine. They are, also, used to predict the performance at different rotating speed or operating flow point (different operating point). In testing a scale-model, dimensional analyses are carried out. Some important dimensionless parameters like flow coefficient, isentropic head coefficient, work coefficient, slip factor, and efficiency will be discussed in next few paragraphs.

The flow coefficient based on inlet volume flow rate can be defined as

$$\phi = \frac{Q}{\frac{\pi}{4} D_2^{\,2} U_2} \tag{2.12}$$

The isentropic head coefficient is given as

$$\psi = \frac{\Delta h_{ois}}{\frac{1}{2}U_2{}^2} = \frac{C_p T_{01}\left[\left(\frac{P_{02}}{P_{01}}\right)^{\frac{\gamma-1}{\gamma}} - 1\right]}{\frac{1}{2}U_2{}^2} \tag{2.13}$$

Work coefficient or some time called the actual head coefficient is another dimensionless parameter given by

$$\mu = \frac{\Delta h_o}{\frac{1}{2}U_2{}^2} = \frac{C_p(T_{02} - T_{01})}{\frac{1}{2}U_2{}^2} = \frac{U_2 C_{u2} - U_1 C_{u1}}{\frac{1}{2}U_2{}^2} \tag{2.14}$$

Efficiency can then be defied as

$$\eta = \frac{\psi}{\mu} \tag{2.15}$$

Machine Mach number or called the impeller tip Mach number is another important dimensionless parameter defined as

$$M_u = \frac{U_2}{a_1} = \frac{U_2}{\sqrt{\gamma R T_1}} = \frac{\pi}{60}\frac{D_2 N}{\sqrt{\gamma R T_1}} \tag{2.16}$$

2.2.3 Incidence

The angle of attack of the flow at the impeller blade leading edges causes the incidence loss for the impeller. If the relative flow angle does not match the blade angle, there will be a tangential component of relative velocity that is not used and appears as a head (pressure) loss. If the incidence is high, additional losses takes place due to the boundary layer separation (Figure 2-14). For the impeller blade-leading edge, the incidence is defined to be the difference between the relative flow angle (the angle

between the relative velocity and the axial direction) at impeller inlet and the actual blade angle (the angle that the blade leading edge make with the axial direction) (Figure 2-15)

$$i = \beta_1 - \beta_{1b} \tag{2-17}$$

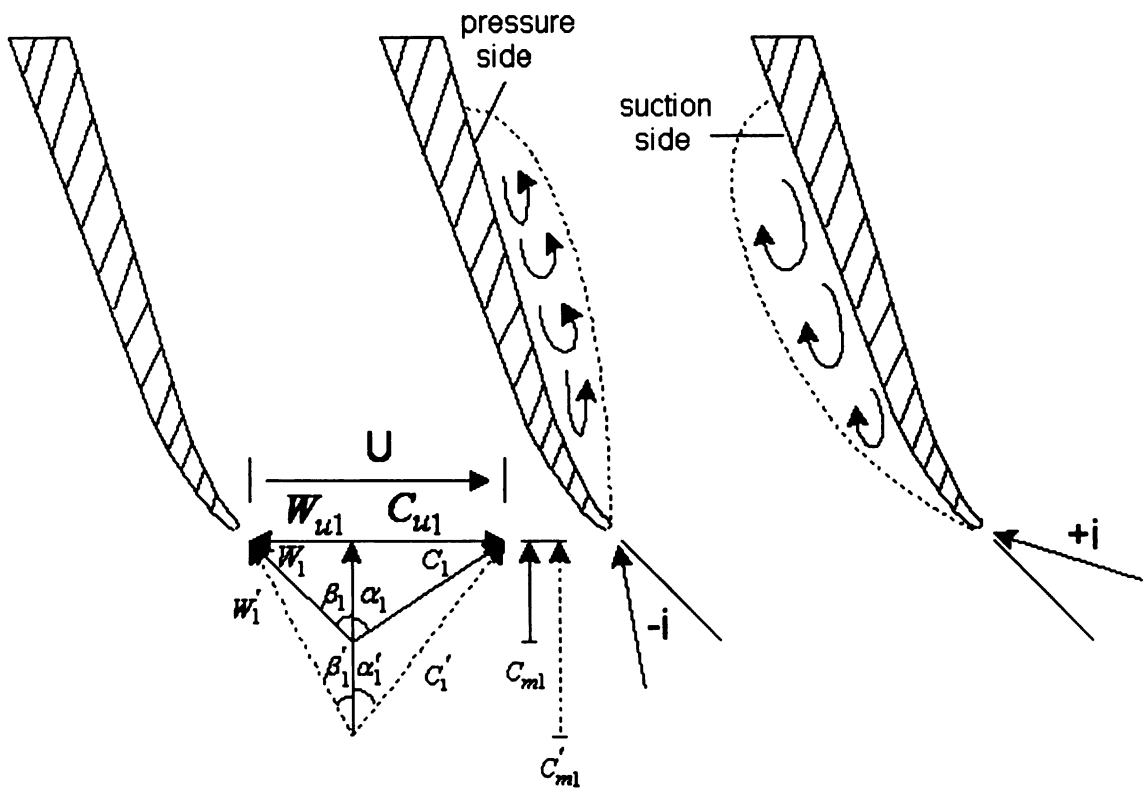

Figure 2-14 Incidence Variations Upon Mass Flow Change and Boundary Layer Separation

Getting a little positive incidence at the design point in addition to a suitable choice of the throat area would improve the design. On the other hand, a bad choice for the throat area affects the mass flow rate and may damage the compressor. The impeller rotates the fluid and turns it into a direction perpendicular to the axis of rotation, which consequently adds a momentum to the fluid.

Positive incidence (angle) corresponds to the incidence that causes the flow to acts on the pressure side of the blade, which is the side pushing the flow in the direction

of rotation. On other hand, negative incidence acts on the suction side of the blade as shown in Figure 2.14. At the design point, the incidence should be kept close to zero and the efficiency is the maximum provided that the inlet system of the compressor has uniform flow condition before entering the impeller inducer.

In case of off-design points the high positive and negative incidence will cause separation in the boundary layer (Figure 2-14). Prescribed swirl at impeller inlet is another cause of such a problem which would be solved by having inlet guide vanes. From the velocity triangle at impeller inlet, the relative flow angle decreases with the increased mass flow rate, which causes negative incidence and the boundary layer separation on the pressure side of the impeller blade at the extreme condition. However, the decreased mass flow rate increases the relative flow angle and, hence, causes positive incidence and boundary layer separation on the suction side of the impeller at the extreme condition. Because, flow in the impeller has less momentum on the suction side than on the pressure side, it is beneficial to have a small negative incidence. This increases the impeller performance since the flow with the small negative incidence makes up for the momentum deficit on the suction side.

Typical velocity triangles at inlet and exit of impeller are shown in Figure 2-17 for a case of prewhirl at the impeller inlet.

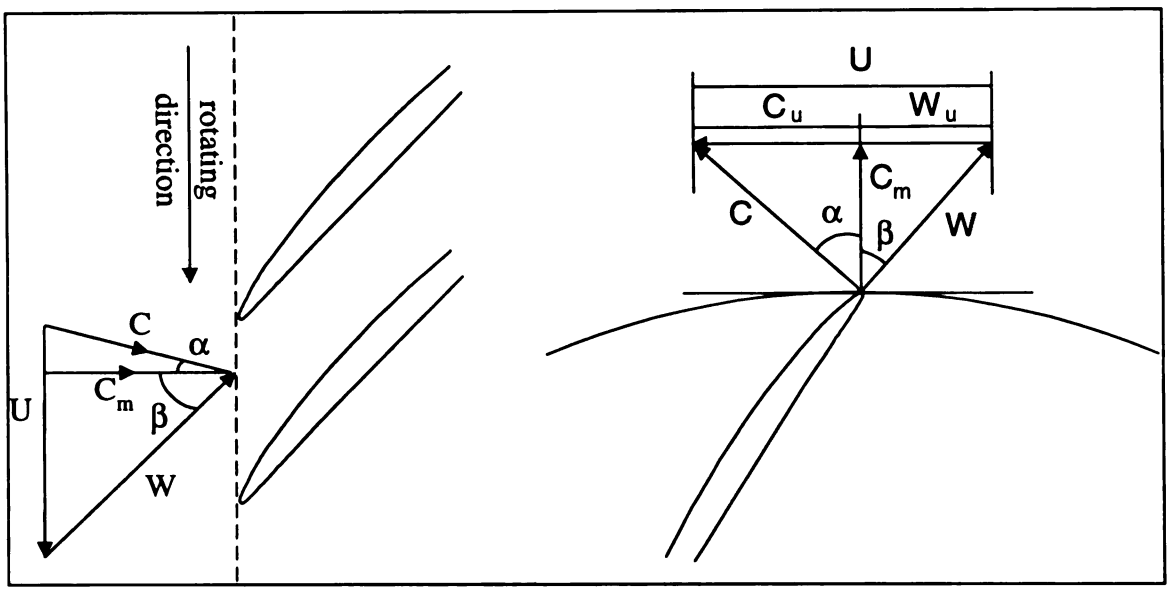

Figure 2-15 Inlet and Exit Velocity Triangles of Impeller

2.2.4 Impeller Thermofluids Relations and Blade Geometry

The head change in a compressor can be related to the impeller inlet and exit velocities using Euler equation. The Euler equation is derived from the conservation of linear momentum, which is the rate of change in linear momentum of a volume moving with the fluid is equal to the surface forces and body forces acting on the fluid. By the conservation of momentum principle, the change of angular momentum can be obtained by equating the change in the tangential velocities to the summation of all forces acting on the rotor (i.e. the net torque of the rotor), that can be written between inlet and exit as

$$\tau = \dot{m}(r_2 C_{u2} - r_1 C_{u1}) \tag{2-18}$$

where C_{u1} and C_{u2} are the tangential velocity at inlet and exit of the impeller respectively. The rate of change of energy transfer is the product of the torque and the angular velocity, which gives the total energy transferred to be

$$E = \tau\omega = \dot{m}(r_2 \omega C_{u2} - r_1 \omega C_{u1}) = \dot{m}(U_2 C_{u2} - U_1 C_{u1}) \tag{2-19}$$

where U_1 and U_2 are the tip velocity at r_1 and r_2 respectively.

The energy transferred per unit mass flow is equal to the change in total (stagnation) enthalpy h_0 and hence

$$\Delta h_0 = U_2 C_{u2} - U_1 C_{u1} = h_{02} - h_{01} = C_p (T_{02} - T_{01}) \quad (2\text{-}20)$$

Then, it is also possible to relate the enthalpy change to the exit blade angle. Using the velocity triangle at the impeller exit and assuming no prewhirl (C_{u1}=0), the enthalpy rise is given by

$$C_{u2} = U_2 + C_{m2} \tan \beta_2 \quad (2\text{-}21)$$

with the convention that β_2<0 for a backward swept impeller which means that the blades of an impeller are inclined backward at outlet.

Introducing the theoretical head rise

$$\psi = \frac{\Delta h_o}{U_2^{\,2}} \quad (2\text{-}22)$$

and the flow coefficient

$$\varphi = \frac{C_{m2}}{U_2} \quad (2\text{-}23)$$

to make a non-dimensional representation of the enthalpy rise versus mass flow rate, the following relation is obtained.

$$\psi = 1 + \varphi \tan \beta_2 \quad (2\text{-}24)$$

Figure 2-16shows the velocity triangles and flow angle change upon the increased mass flow rate for three different impeller blade shapes.

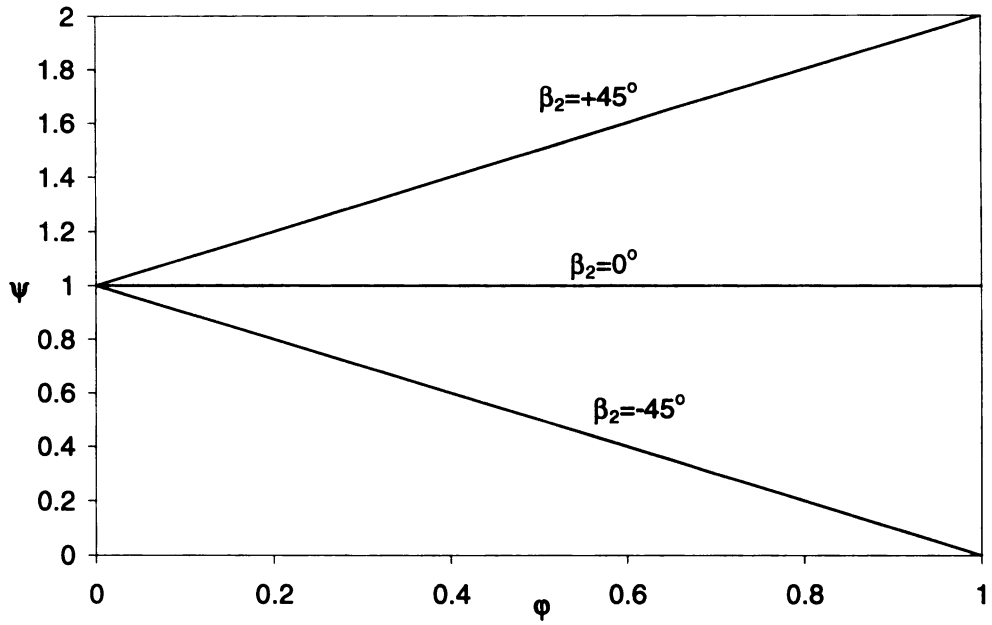

Figure 2-16 Effect of Exit Blade Angle on the Head Rise and the Flow Range

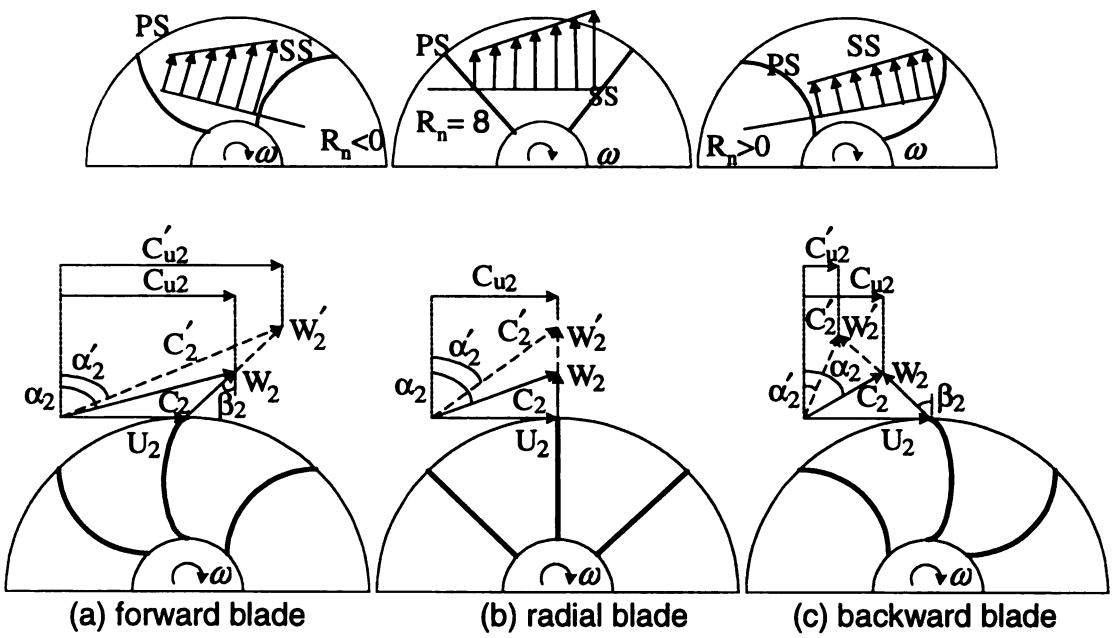

Figure 2-17 Velocity Triangles Velocity Profile for Different Blade Shapes

By studying equation (2-24), if mass flow rate is increased, the actual head is increased for a forward-leaned blade impeller, is independent for a radially-ending impeller, and is decreased for a backward-swept impeller which can be seen clearly in Figure 2-16. For backward-swept impeller, the increasing head with decreasing mass-flow rate gives more stable compressor stage characteristics and consequently a greater operating range.

The enthalpy change in the machine can also be expressed in the following way.

$$\Delta h_0 = \frac{1}{2}\left[\left(U_2^2 - U_1^2\right) + \left(W_1^2 - W_2^2\right) + \left(C_2^2 - C_1^2\right)\right] \qquad (2\text{-}25)$$

and

$$W^2 = C^2 + U^2 - 2UC_u \qquad (2\text{-}26)$$

Equation (2.25) shows that the enthalpy rise in a centrifugal compressor is due to three different contributions. The first term in that equation represents the change of energy of a particle as it moves from one radius to another. Casey and Marty, 1986, presented that the effect of these centrifugal forces are about one-half of the work input and can be accomplished without loss. The rise in enthalpy due to the diffusion of the relative flow is represented by the second term. This term is approximately one-fifth of the total work input. The last term in that equation represents the diffusion of the absolute velocity, assuming that the velocity at the inlet and exit of the stage is equal; and it is approximately about one-third of the work input.

2.2.5 Efficiency, head Coefficient and Flow Coefficient

Centrifugal compressors, as in any type of turbomachinery, there exist an optimum efficiency over a certain range of flow. The flow coefficient Φ of a centrifugal stage can be correlated to the efficiency, and is most commonly defined by Equation 2-

12. The optimum flow coefficient range has been well established to be between 0.06 and 0.11, as shown in figures 1.1 and 1.18. Even though low flow coefficient stages, $\Phi <$ 0.02, tend to have very poor efficiency, there are strong demands from current applications to extend the application area to as low as Φ=0.004. In a multistage machine, the volume-flow rate decreases as the pressure of the flow is increased through the stages. As the last stages are reached, the flow coefficient Φ is, therefore, smaller than at the inlet of the machine. The impeller and diffuser channel are narrower to handle the smaller volume flow rate. The friction losses are thereby increased, and a smaller efficiency is to be expected. Also, the disk friction losses and the leakage losses are known to be inversely proportional to the volume flow rate. Hence, low-flow coefficient compressors are inherently inclined to have lower efficiency than the earlier stage.

If efficiency is directly related to flow coefficient, one would think that the only way to improve the performance of such compressors is to increase their flow coefficient. Looking back at the above equation, this would imply decreasing D_2 or reducing U_2. In both cases, that would lead to a decrease in the work input of the machine, which is not desirable. Centrifugal impeller design is often based on a series of compromises to obtain an optimum configuration for a particular application. Currently, industrial centrifugal compressors are designed in the flow coefficient range Φ = 0.01 to 0.16. But often the need arises, as opposed to the low flow coefficient, to design high flow coefficient centrifugal stages; but the aerodynamic challenges are not easy to satisfy, therefore, a designer usually decides on a mixed flow impeller stage.

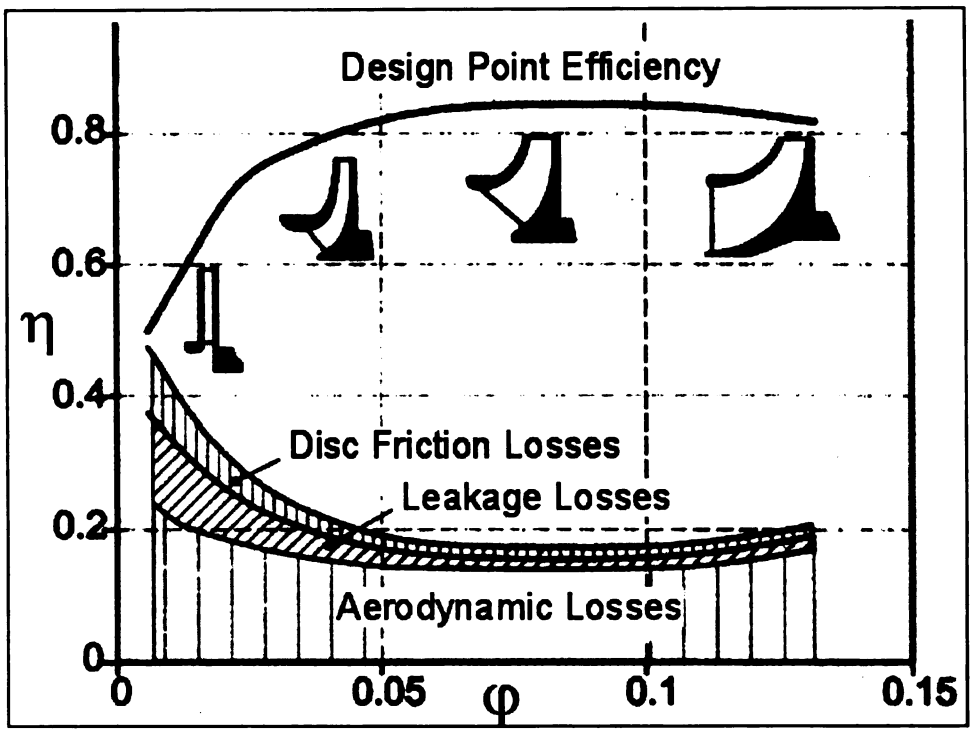

Figure 2-18 Application Areas of Typical Industrial Centrifugal Compressors

In the cylindrical coordinate system, the energy transfer through turbomachinery is governed by the rate of change of the angular momentum (UCu). The function of turbomachinery involves the exchange of significant levels of kinetic energy. In turbomachinery, a pump uses liquids for a working fluid, while a compressor uses gases. For a compressor, three different terms (a fan, a blower, and a compressor) may be used depending on the pressure ratio or the pressure rise achieved. Furthermore, depending on the discharge flow direction, a compressor can be classified as axial, centrifugal (or radial), or mixed flow.

For a steady flow the work input and exchanged heat can be related to the change in total enthalpy and elevation by using the first law of thermodynamics as follows:

$$\frac{\dot{Q}+\dot{W}}{\dot{m}} = (h_2 - h_1) + \frac{1}{2}\left(C_2^{\,2} - C_1^{\,2}\right) + g(z_2 - z_1) \qquad (2\text{-}30)$$

Assuming ideal gas behavior, no change in altitude, and adiabatic (no heat exchange with surrounding) the change in energy is directly related to the change in total temperature as

$$\frac{\dot{W}}{\dot{m}} = \dot{w} = (h_2 - h_1) + \frac{1}{2}\left(C_2^{\,2} - C_1^{\,2}\right) = (h_{02} - h_{01}) = C_p.(T_{02} - T_{01}) \qquad (2\text{-}31)$$

As was mentioned earlier the compression process can be represented in a T-s (h-s) diagram. A typical compression process is shown in Figure 2.19. The isentropic efficiency compares the actual enthalpy change during the compression process to the one that would have taken place for an isentropic process. It is defined by

$$\eta_{is} = \frac{h_{02s} - h_{01}}{h_{02} - h_{01}} = \frac{T_{02s} - T_{01}}{T_{02} - T_{01}} \qquad (2\text{-}32)$$

State 1, here, refers to the total (stagnation) conditions at the inlet. State 2 corresponds to the exit conditions. Using the total conditions at state 2 gives the total-to-total isentropic efficiency definition, while using the static conditions at the exit gives the total-to-static isentropic efficiency. From equation (2-31), if stages having a large exit velocity then the difference between these two efficiencies will be large. Either one of these definitions are used depending on the type of application. Normally, the total-to-total efficiency is used if the exit velocity is used. On other hand the total-to-static efficiency is used if the exit velocity is not used. For a perfect gas with constant specific heat, the above equation becomes

$$\eta_{is} = \frac{C_p(T_{02is} - T_{01})}{C_p(T_{02} - T_{01})} = \frac{\left(\frac{P_{02}}{P_{01}}\right)^{\frac{\gamma-1}{\gamma}} - 1}{\frac{T_{02}}{T_{01}} - 1} \tag{2-33}$$

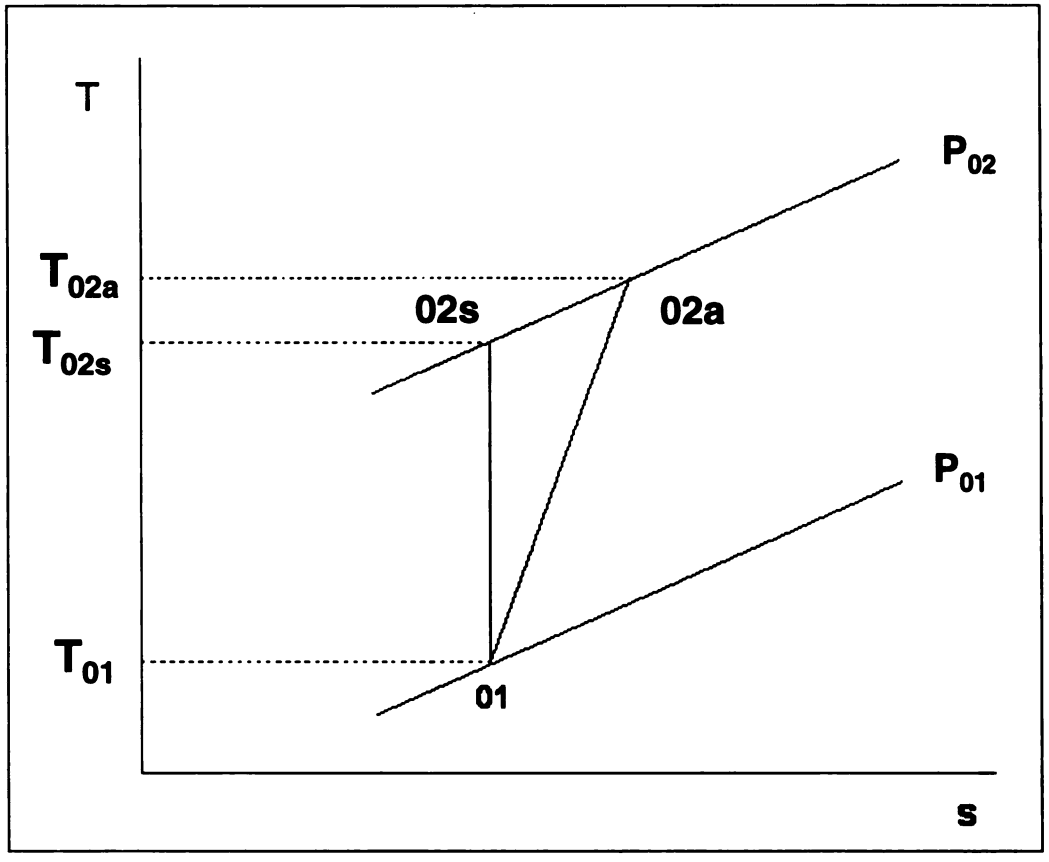

Figure 2-19 Representation of a compression process in a T-S diagram

2.2.6 Head Rise

The head rise (enthalpy) is an essential need in the centrifugal compressor design. The isentropic head can be defined as the energy transferred through a compressor per unit mass of fluid. For example, If a compressor produces 1 m of head, it means that one

kg-force is needed to elevate one kg of gas mass to a height of one meter. The head cannot be measured directly but for a compressible ideal gas flow it is given by

$$\Delta h_{ois} = C_p \Delta T_{ois} \tag{2-27}$$

where

$$C_p = \frac{\gamma R}{\gamma - 1} \tag{2-28}$$

and for an isentropic compression process

$$\Delta T_{ois} = T_{01}\left[\left(\frac{p_{02}}{p_{01}}\right)^{\frac{\gamma-1}{\gamma}} - 1\right] \tag{2-29}$$

The head rise as well as the total pressure ratio are used to express the energy exchange into the impeller and can be used interchangeably.

2.2.7 Operating Range between Surge and Choke

The performance of the compressor can be represented with a curve(s) that shows the pressure ratio (on the y-axis) versus the mass-flow rate (on the x-axis) for different rotational speeds, or the head versus the volume-flow rate. In a dimensionless form it is represented by the head coefficient versus the flow coefficient. Figure 2.20 shows a sample performance curve for a centrifugal compressor stage.

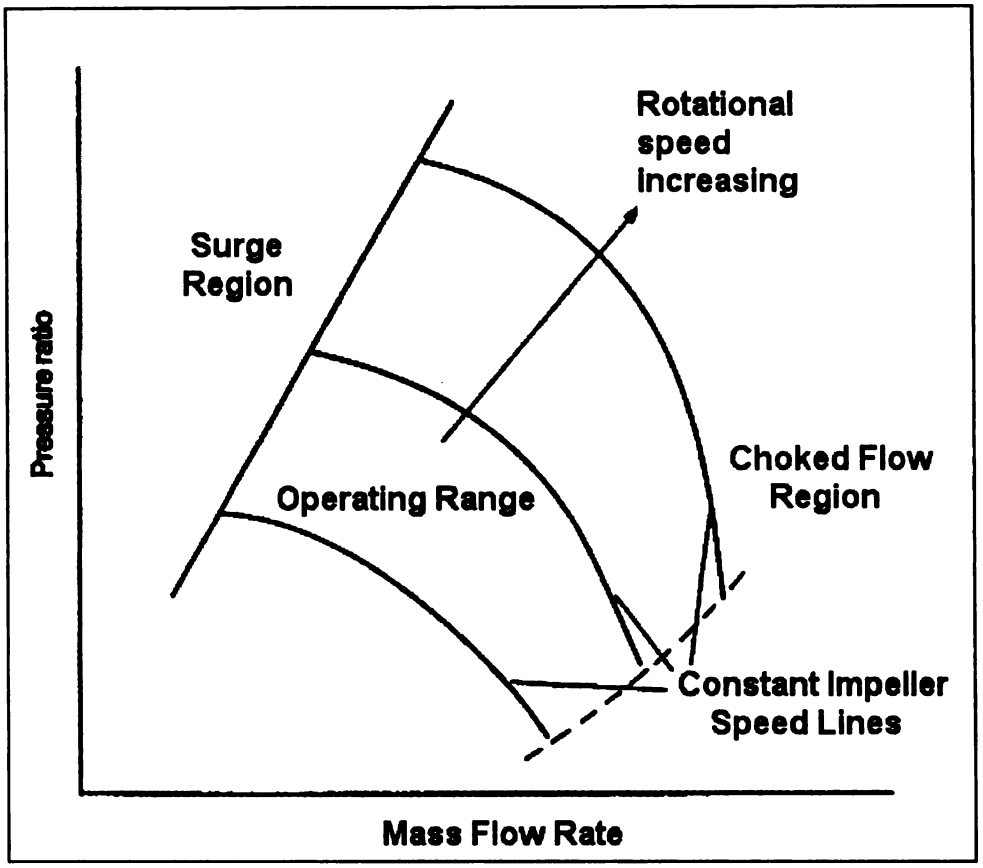

Figure 2-20 A sample performance curve of a centrifugal compressor

Looking at the above figure, there are three different regions that exist. On the right side is the choke limit line, which is obtained when sonic conditions are reached in the minimum section of the compressor. This could happen in the impeller throat or diffuser throat, whichever is more critical. In the compressor map, the choke limit appears as a vertical line because the efficiency and the pressure ratio drop significantly. On the other side is the stall (or surge) region and line. This region is unstable. Rotating stall is an unstable phenomenon, often prior to surge. It may happen in the impeller or the diffuser. Rotating stall is a local instability in which the separated flow rotates in one component of the compressor. These regions of separated flow are called cells. If the

compressor runs at high pressure, the pressure change caused by the rotating stall generates noticeable mechanical vibration that can cause a big damage to the machine. Therefore, the compressor should not operate in this region. For a vaneless diffuser, the diffuser inlet flow angle has been linked to the occurrence of this phenomenon (Senoo 1978).

Throughout the compressor surge, oscillations of the mass flow rate occur between the exit and inlet which may damage the machine. For high density gas, this has more effect on the compressor. Van den Braembussche (1984) related the value of $d\Psi/d\Phi$ to the occurrence of this phenomenon. He explain that for a negative value of $d\Psi/d\Phi$ (i.e. increasing pressure for decreasing mass flow) any disturbance in the flow will be damped out, resulting in a stable operating point. But when $d\Psi/d\Phi$ becomes positive, the flow would likely become unstable. This, on the global system, will affect the compressor as well as the inlet and the discharge pipe. So operating the compressor in this region should be avoided. It should be operated at a medium flow coefficient, called the operating range between the choke and the surge regions, in which a high efficiency can be obtained that is normally close to the design point.

Because of the importance of this topic many other studies have been made to prevent surge. Sorokes from Dresser-Rand Company combined a good summery of literature review plus Dresser-Rand experience. Surge control sensors are also devolving to help in this area. The development in this area will allow compressors to have wider operating ranges and will avoid costly and unnecessary recycling of flow (McKee 2003). There is active work in this area to develop a dependable surge control to operate centrifugal compressors reliably and safely, closer to the surge limit. (McKee 2000).

2.2.8 Slip Factor

Slip occurs in centrifugal compressor because the relative flow leaving the impeller is not totally guided by a finite number of blades. This leads to a modified velocity triangle (Figure 2.21). As a result, the magnitude of the tangential component of velocity will be reduced, which cause a reduction of the pressure ratio and more power consumption. So, with slip, more rotating speed is needed to get the same pressure ratio as if there was no slip (ideal).

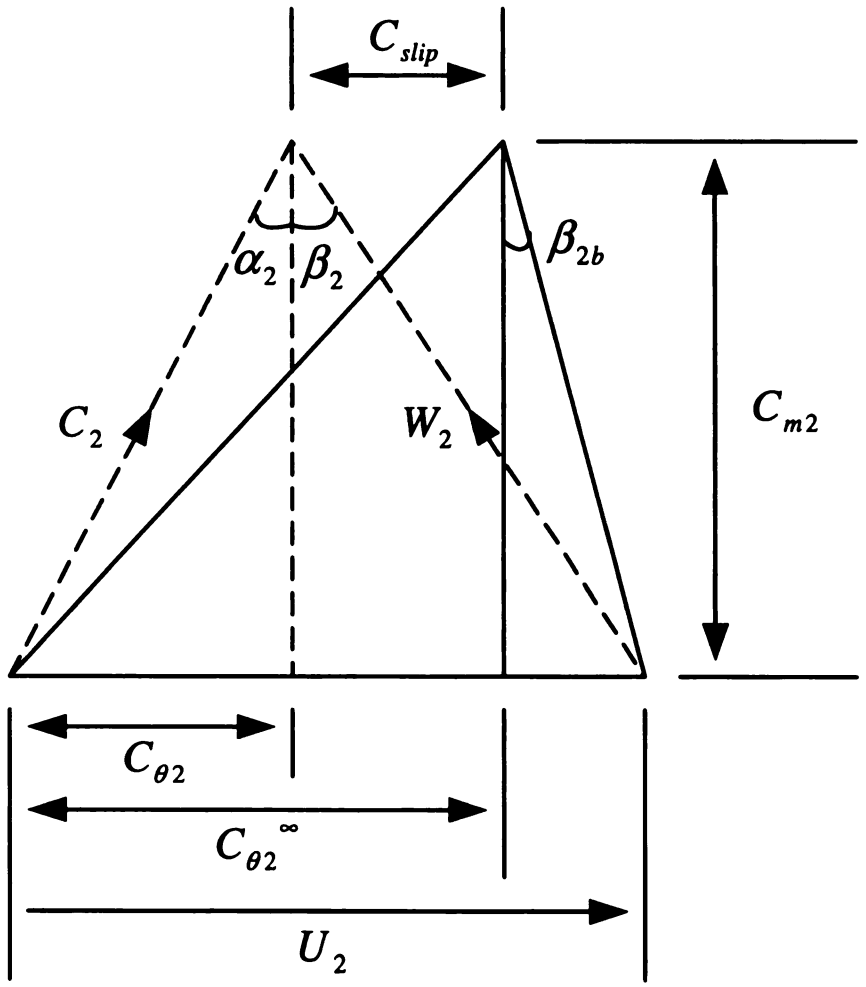

Figure 2-21 Slip effect on velocity triangle at impeller exit for back-swept blade

As a result of the increase in the rotational speed of the impeller, it will experience more stress and higher velocities that cause an increase in friction losses and a reduction in efficiency. A common definition for the slip factor is

$$\sigma = 1 - \frac{C_{slip}}{U_2} = 1 - \frac{C_{\theta 2}^{\infty} - C_{\theta 2}}{U_2} \tag{2-34}$$

From the velocity triangle shown in Figure 2.8, the tangential component of velocity is, now, rewritten as

$$C_{\theta 2} = \sigma U_2 + C_{m2} \tan \beta_{2b} \tag{2-35}$$

Because of the need to account for the losses due to slip in design many correlations became available in the literature to predict the value of the slip factor.

Wiesner (1967) gave a correlation that is one of the most commonly used correlations as

$$\sigma = 1 - \frac{\sqrt{\cos \beta_{2b}}}{Z^{0.7}} \tag{2-36}$$

This equation where obtained by fitting data of the some theoretical curves that was found by Buseman (1928) for inviscid flow. This correlation was validated by over 60 compressor and pumps with various blade angles and blade numbers and compared to other correlations, by Wiesner. This shows a good agreement with exception of some machinesthat was off by few percent.

The effect of both the blade number and blade angle on the slip factor is shown in the following figure. It can be seen that slip factor increases with an increase in the blade

number. In addition, the slip factor is less for a radial impeller compared to a back-swept impeller.

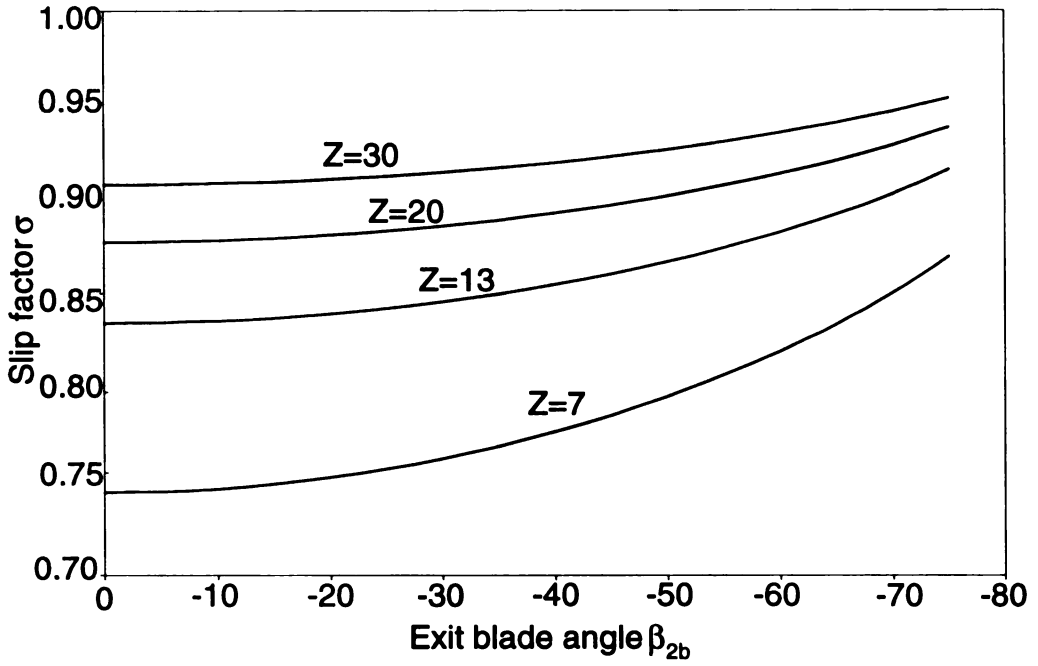

Figure 2-22 Influence of the blade number and the exit blade angle on the slip factor

The concept of a relative eddy was used by Stodola (1927) to derive the slip velocity and the slip factor. The flow into the impeller inlet has no rotary motion; but after passing through the impeller passage, the relative flow will have an angular velocity, that is equal in magnitude and the opposite in direction, to the impeller rotating speed. The actual relative velocity is then formed by the vector summation of the eddy and the radial component of velocities.

$$C_{slip} = \frac{\pi U_2 \cos \beta_{2b}}{Z} \tag{2-37}$$

$$\sigma = 1 - \frac{\pi \cos \beta_{2b}}{Z} \tag{2-38}$$

where β_{2b} is the impeller blade exit angle and Z is the number of blades.

Another slip-factor correlation was also provided by Stanitz (1952). For blade angles in the range of -45° to $+45^{\circ}$, this correlation is considered to be acceptable.

$$\sigma = 1 - \frac{0.63\pi}{Z} \tag{2-39}$$

Chapter 3 CFD ANALYSIS

3.1 Need and Development of CFD

Computational Fluid Dynamics (CFD) is a computer based tool that is used to simulate the behavior of fluid flow and heat transfer. Simulating such processes needs to be done by solving the governing equations of fluid flow and heat transfer (in a particular form) over the region of interest, with known boundary conditions of that region. (CFX-5 manual)

For many years, computers have been used to solve many fluid flow problems. It is believed that the automatic digital computer was built by Atanasoff in the late 1930s and was used from the beginning to solve some problems in fluid dynamics; but the explosion in computational activity did not begin until a third ingredient, the general availability of high-speed digital computers, that occurred in the 1960s(TB). Too many programs have been written to solve either a particular problems or particular type of problem. About 30 years ago general purpose CFD solvers were developed based on the understanding of some complex mathematics required to generalize some key algorithms. In the early 1980s powerful computing machines, as well as more understanding of the fluid dynamics came together to help the development of CFD. (CFX-5) The availability of previously unthinkable computing power has motivated many changes. The need for such changes was more visible in industry and research laboratories, where the need to solve complex problems was urgent and critical. Recently, changes brought about by the computer have become noticeable in many of our daily lives. In the educational process, computers are found to be used widely at all levels. (Tannehill and others 1997)

CFD was used as a tool almost exclusively in research. Recently, development in computing power, together with the advanced graphics and the interactive 3-D management of models, allowed the process of making a CFD model and analyzing the results to be done in much less time and therefore saving money. Nowadays, as a consequence of this development, Computational Fluid Dynamics has become a dependable design tool helping to reduce design time and cost. Improving the design processes throughout the engineering world is the overall result of such development. Comparing CFD with scale model testing, it gives an accurate alternative as well as cost-effective. Being able to vary the parameters on the simulation very quickly is another clear advantage of CFD. (CFX-5)

Engineers and scientists are using CFD more often in a wide range of fields. In the process industry, for example, CFD is used in turbines, compressors, pumps, mixing vessels, and chemical reactors. It is also used in building construction and in design for air conditioning and ventilation. Health and safety is another area where CFD is used to investigate the effects of fire and smoke. CFD plays a large role in the development of the motor industry where modeling of combustion and car aerodynamics is an issue. In the filed of electronics CFD is used to simulate the heat transfer within and around circuit boards. For environmental applications CFD is use to solve many problems such as the dispersion of pollutants in air or water. In medicine simulating a blood flow through grafted blood vessels is another area where CFD can be used. Power, energy and airplanes industry is a very wide area of application for CFD. All these application drive the development of CFD. (CFX-5)

3.1.1 CFD and Industry

Even though the development of CFD mostly takes place in an educational environment, industry is the major motivation of it. The industrial manufacturers are doing their best to reduce the design time and cost. So, they are putting more efforts on developing numerical models that physically describe the behavior of their hardware as accurately as possible. This is even truer for manufacture is producing large machinery. First, the excessive high construction costs for one-of-a-kind hardware. Second, the long time that is required for constructing the environment of the experiment. Third, the high risk of some machines that deals with human lives. Under these circumstances, design engineers are no longer able to rely only on past experience and the use of the traditional 1-D empirical based tools. Getting the design correct from the first time would save time and money. This requirement also applies for diagnosing aerodynamic problems that occur in machines that are already installed. If there is a problem with a running machine, the shut-down time is often very limited in order to minimize the customer's production loss. So, there is normally little opportunity for testing that may take time. (Tannehill and others 1997)

Experimental in addition to theoretical methods were the traditional methods used to develop designs for equipment and vehicles involving fluid flow and heat transfer. After the exploration of the digital computer, a third method (the numerical approach) was found. Even though the experimental method continues to be important (especially when the flows are complicated) the demand is clearly toward greater dependence on computer-based predictions in design. (Tannehill and others 1997)

The use of CFD provides a cost-effective and time saving way to design and investigate fluid flow hardware. The success of this method, CFD, depends strongly on the user as well as the models in the code. Even though CFD are used for the initial design to solve current problems, it may also be used to minimize experimental work or to validate the results that were found using other techniques. (Tannehill and others 1997)

Applying CFD to turbomachinery has its own benefits as well as challenges. The experimental setup cost much money and time to get results. A single problem, for example, could cost a shut down for a whole plant for weeks because a turbine or a compressor needs to be disassembled and taken somewhere for testing. These problems are common in industrial plants and may cost hundreds of thousands or even millions of dollars.

In CFD, the turbulence models, the grid density, quality of the model, and the numerical schemes are traditional topics that need to be taken care of when solving problems. In addition to these, for modeling turbomachinery cases, more problems would arise such as handling the rotation of the flow and the interface between the rotating and stationary components. For example, for a centrifugal compressor stage, a CFD model typically needs two interfaces. The first one is to couple the stationary inlet region to the rotating impeller. The second one is to couple the rotating impeller to the downstream stationary components such as diffuser, return bend, and return channel or volute.

3.2 CFD Mathematics

Navier-Stokes equations are the set of equations that describe the processes of momentum, heat, and mass transfer. These equations are partial differential equations that were derived by two scientists in the nineteenth century. Up to this date, there is no

known general analytical solution for those equations. As an alternative, they can be discretised and numerically solved. In addition to Navier-Stokes equations, other equations that describe more processes, such as combustion, may also be solved in conjunction. Mostly, these additional equations may be driven using an approximating model. Turbulence models as an example of particular importance. (CFX-5 manual)

There are three major numerical discretisation techniques that are used to discretise partial differential equations: the finite difference method, the finite element method, and the finite volume method. All of these methods are used to transform a partial differential equation into its numerical analogue. (Shaw 1992)

The finite difference method is based upon the use of the Taylor series to construct the equations that describe the derivatives of a variable as the differences between two values of the variable at two points in space or time. Smith (1985) wrote a comprehensive reference for this method. The second method is the finite element method. It is named so because the domain over which the partial differential equation applies is divided into a finite number of smaller domains that are known as elements. The Zienkiewicz and Taylor book (1989) is assumed to be standard reference for this method. The most common method used in CFD is the third method, which is known as the finite volume method. In some ways this method is similar to the finite difference method, but some implementations of it also come from the finite element method. This method is very popular in CFD because it was developed specifically for solving the equations of heat transfer and fluid flow. Patankar (1980) gave a well detailed description for this method.

Since all of these methods are used to discretise partial differential equations they have some similarities. They produce equations for the values of the variable at a finite number

of points in the domain. They also require that we know a set of initial conditions as well as boundary conditions of the problem so that we can solve the equations. Explicit or implicit forms may be produced from these techniques. (Shaw 1992)

Even though the above methods are similar in some ways they have differences as well. Both the finite difference method and the finite volume method generate the numerical equations for a certain point based on the values at the adjacent points. However, the finite element method generates the equations for each element independently of the other elements. In this method the interaction between elements is taken into consideration when forming the global matrices. Another difference between these methods is that in the finite element method the derivative boundary conditions is taken care of when forming the element equations then the fixed values of variables must be applied to the global matrices. The other two methods, however, can apply the fixed-value boundary conditions easily by inserting the values into the solution while the derivative boundary conditions require modification of the equations. (Shaw 1992)

The development of these methods may help to overcome their disadvantages and make them more efficient.

The method of particular importance to us here is the finite volume method because it is the one that is mostly used in CFD codes. The main idea in this method is to divide the region of interest into small subregions, called control volumes. Then for each control volume the equations are discretised and solved iteratively. A solution can then be obtained by approximating the value of each variable at specific points throughout the domain. This will drive a complete full picture of the behavior of the flow. (CFX-5 manual)

Even though the main method used in such applications is the finite volume method some times other approaches may be associated to get better results. For example, CFX-TASCflow, the software used in this study, is using the finite element approach to represent the geometry. Thus, this way of associating the finite element approach with the finite volume method maintains much of the geometric flexibility of finite element methods as well as the important conservation properties of the finite volume method. (CFX-TASCflow Theory Documentation Version 2.12)

3.3 Engineering Approaches

As it has been discussed before, the three methods available for a designer are the Experimental, Theoretical, and Computational methods. Each Method has its advantages and disadvantages (Table 3-1). If a good understanding of the problem is obtained and faster computer is used, then CFD would save more time than the experimental and theoretical methods. Saying that does not mean that computational methods will soon completely replace experimental testing to gather information for design purposes. Rather, it is believed that CFD will be used even much more in the future. In many fluid flow and heat transfer design situations experimental testing may be still be necessary. However, CFD can be used to reduce the range of conditions where testing is required.

In some fields such as turbomachinery, experiments will remain for some time in applications because of the involvement of turbulent flow and the complex geometry. This situation is destined to change in the long run, because it has become clear that the time-dependent Navier-Stokes equations can be solved numerically to give accurate details of turbulent flow. Thus, as computer hardware and algorithms improve, the limit will be pushed back continuously allowing flows of increasing practical interest to be

computed using CFD. Even though, there was a progress in simulating turbulent flow, the work still needs more development compared to the status of the models used for laminar single-phase flow over aerodynamic bodies. (Tannehill and others 1997)

Table 3-1 Comparison of approaches (adapted from Tannehill)

Approach	***Advantages***	***Disadvantages***
Experimental	1. Capable of being most realistic	1. Equipment required 2. Scaling problems 3. Tunnel corrections 4. Measurement difficulties 5. Operating costs
Theoretical	1. Clean, general information, which is usually in formula form	1. Restricted to simple geometry and physics 2. Usually restricted to linear problems
Computational (CFD)	1. No restriction to linearity 2. Complicated physics can be treated 3. Time evolution of flow can be obtained	1. Truncation errors 2. Boundary condition problems 3. Computer costs

Commercial codes are available for some time and many compressors' companies started using them more often which help the development in this area. More demand on codes that can deal with turbulence is noticeable.

3.4 CFD in Current Practice for Centrifugal Compressor Design

The emergence of Computational Fluid Dynamics (CFD) in the last twenty-five years provided a major movement to solve the Euler and Navier-Stokes equations, which also govern the flow fields in turbomachines. This has been possible mainly due to advances in, grid generation, turbulence modeling, boundary conditions, pre- and post-data processing, and computer architecture. Most of the techniques used for the solution of the Navier-Stokes equations can be classified as finite difference, finite area/volume finite element, and spectral methods. Only the first two techniques are widely used in turbomachinery.

Compressor designers and analysts require CFD software to provide accurate solutions to their applications of interest in a cost-effective and timely manner. With the widespread availability of affordable workstation class computing, the main issues are therefore accuracy and productivity. The information provided by the CFD must be of sufficient accuracy to allow the designer to make appropriate decisions based on the available information, and it must be available rapidly enough to fit within the time scales of the design cycle. For the designer, "accuracy" means providing reliable information of the following type:

- Qualitative: correctly reproduces the important flow features, such as swirl, boundary layers, shocks, wakes, separation zones, stagnation points, mixing layers, etc.

- Quantitative: efficiency, work input, pressure rise, blade profiles, component loss coefficients, flow distortion parameters, incidence, deviation or slip, etc.

While it is desirable that such features are perfectly reproduced, this expectation is unrealistic given limitations due to mesh size, turbulence modeling and other modeling assumptions such as steady state flow. To be used confidently, it is therefore of importance that CFD provide:

- A "Sufficient" level of accuracy
- Repeatability and consistency

The two factors that influence accuracy most for compressor applications are the discretization accuracy of the flow solver and the computational mesh. Only after these two are adequately treated do other issues such as the turbulence model become of primary significance. In particular, the turbulence model is the usual scapegoat for poor CFD predictions, while in reality other causes are often more significant. Hence, it is often the case that "numerical errors" exceed "model errors".

3.4.1 CFD Model

TASCflow-CFX is a general purpose, commercially available CFD code, widely used among turbomachinery industry. For the present study, TASCflow-CFX is used for steady-state compressor stage numerical simulation. TASCflow-CFX solves three-dimensional, Reynolds-stress-averaged, Navier-Stokes equations with mass-averaged velocity and time-averaged density and pressure and energy equations. The mean form of the governing equations, expressed in a finite-volume formulation that is fully conservative, include the following.

1. Conservation of mass

$$\frac{\partial \rho}{\partial t}+\frac{\partial}{\partial x_j}\left(\rho u_j\right)=0 \tag{3.1}$$

2. Conservation of momentum

$$\frac{\partial}{\partial t}\left(\rho u_i\right)+\frac{\partial}{\partial x_j}\left(\rho u_j u_i\right)=-\frac{\partial p}{\partial x_i}+\frac{\partial}{\partial x_j}\left\{\mu_{eff}\left(\frac{\partial u_i}{\partial x_j}+\frac{\partial u_j}{\partial x_i}\right)\right\}+S_{ui} \tag{3.2}$$

where $\mu_{eff}=\mu+\mu_t$. S_{ui} is the momentum source term for the impeller in the rotating frame of reference. The effect of Coriolis and Centripetal forces are modeled in the code by including

$$\vec{S}_{ui}=-2\vec{\Omega}\times\vec{U}-\vec{\Omega}\times(\vec{\Omega}\times\vec{r}) \tag{3.3}$$

3. Energy equation

$$\begin{aligned}\frac{\partial}{\partial t}(\rho H)-\frac{\partial P}{\partial t}+\frac{\partial}{\partial x_j}\left(\rho u_j H\right)&=\frac{\partial}{\partial x_j}\left(\lambda\frac{\partial T}{\partial x_j}+\frac{\mu_t}{\mathrm{Pr}_t}\frac{\partial h}{\partial x_j}\right)+S_E\\&+\frac{\partial}{\partial x_j}\left\{u_i\left[\mu_t\left(\frac{\partial u_i}{\partial x_j}+\frac{\partial u_j}{\partial x_i}\right)-\frac{2}{3}\mu_t\frac{\partial u_l}{\partial x_l}\delta_{ij}\right]\right\}\end{aligned} \tag{3.4}$$

where the total enthalpy is defined by $H=h+\frac{1}{2}u_i u_i+k$. In the rotating frame of reference, the rothalpy $I=H-\frac{\omega^2R^2}{2}$ is advected in the energy equation in place of the total enthalpy. ω is the rotation rate, and R is the local radius.

For the sliding interfaces between stationary (inlet and diffuser) and rotating (impeller) components, two models are available: one is the "frozen rotor model" and the other is the "stage model". The stage model circumferentially averages the fluxes at the interface before the interpolation of the flow variables across the different frame of reference

although the pressure distortion caused by any perturbation (for example the impeller and the diffuser leading edge) is still allowed. For an axisymmetric inlet flow condition, the stage model can be used with the advantage of modeling one or two passages having a periodic boundary condition for the tangentially-neighbored blade passages instead of modeling fully 360 degree passages, which is significantly economical for computation time and effort.

On the other hand, the frozen-rotor model achieves a frame change across the interface without a relative position change over time as well as without any interface averaging of flow variables. This model is an exact representation of the case when the Strouhal number is zero; in which case, either the sound speed is infinite or the impeller rotating speed is zero. Therefore, when the Strouhal number is small enough such as the compressor stage simulation presented here (*St* is between 0.1423 and 0.1431, depending each inlet models), the predicted simulation result is an approximation of the real situation. In the case of the frozen rotor model, all of the passages have to be modeled and this model is adequate to investigate the influence of the distorted flow caused by the bend inlet along the compressor stage flow passages since local flow features are allowed to transport across the interface; and thus, the non-uniformities of flow variables among the passages can be predicted, which results in different flow conditions at the compressor stage exit

3.4.2 CFD Process Components

Performing a single CFD simulation is a process that involves many steps. These steps can be grouped into three major components: pre-processing, solving, and post-processing. Each one of these components involves many steps. The following

paragraphs will go over them in more detail and give the specific subprograms for each one under the CFX-TASCflow.

3.4.2.1 The Pre-processor:

The pre-processor, as it appears from its name, is the first component in the CFD process. It is used to generate the input for the solver. Pre-processing involves the following steps:

- Defining the geometry of the region of interest where the flow simulation will take place. This step may also be called the grid generation
- Choosing the physical models that are needed to be integrated in the simulation
- Stating the fluid properties
- Stating the boundary conditions
- Stating the initial condition
- Generating a mesh of control volumes

In most commercial codes it is now common to have automated Pre-processing operations. The original geometry may be imported from major CAD packages using native format or the CFD code may have its own package. A mesh of control volumes is then generated automatically. (CFX-5)

3.4.2.2 The Solver:

The solver is the second component in the CFD process. It is the heart of the CFD process because it solves the CFD problem, generating the required results. This is done through the following steps:

- Integrating the partial differential equations over all the control volumes in the simulation region. In other words, applying a basic conservation law (e.g. for mass or momentum) to each control volume in the region of interest.
- Transferring these integral equations into a system of algebraic equations. This can be done by producing a set of approximations for the terms in the integral equations.
- Solving iteratively the non-linearity of these algebraic equations.
- The solution is said to converge when it approaches the exact solution. As a measure of the overall conservation of the flow properties, an error (or residual) is reported for each step. There are number of factors that affect how close the final solution is to the exact solution. These factors include the size and shape of the control volumes and the size of the final residuals. Combustion and turbulence are often modeled using empirical relationships because of their complexity. This includes more approximations that contribute to the difference between the solution obtained by CFD and the real flow. This component of the CFD process (the solver) does not require user interaction and is therefore usually carried out as a batch process. Finally, the solver creates a complete file of results that will be passed to the post-processor. (CFX-5)

3.4.2.3 The Post-processor:

The post-processor is the last component of the CFD process or may be called the end result of the whole process. It helps the user to get and analyze the results. Post-processing could include anything from obtaining values at certain points to some

complex animated sequences. Some important features of post-processors that the user needs to get are:

- Visualizing the geometry as well as the control volumes.
- Plotting the direction and magnitude of the flow field.
- Visualizing of the variation of scalar variables (such as temperature) through the domain.
- Calculating quantities that are not available if needed.
- Animating of the flow field.
- Plotting charts that shows graphical plots of variables
- Printing to file as well as hardcopy output.

As it may be noticed that pre-processing as well as post-processing are interactive processes while the solver in a non-interactive one. (CFX-5)

3.5 The Simulation Process

The following flow chart (Figure 3-1) explains the process of the CFD simulation that was followed for this work and includes the CFX-TASC flow subprograms.

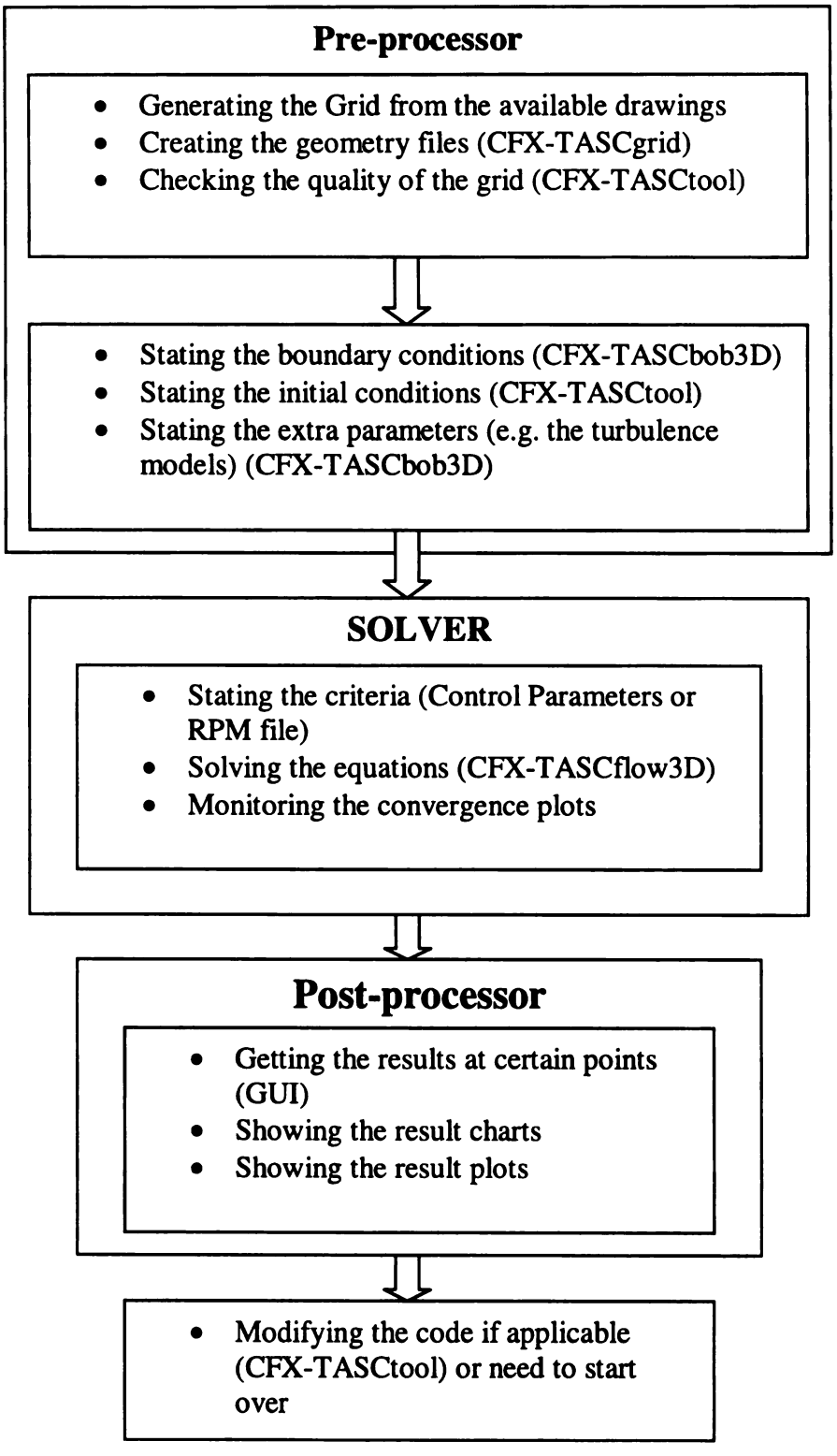

Figure 3-1 Flow chart - Process of the CFD Simulation

3.5.1 Grid Generation

Grid generation is the first essential part in the CFD process. Since CFD works numerically to solve the needed flow and heat equations, so it needs to discretiz the domain into small volumes to be able to perform the calculations. In other words grid generation is the process of breaking the solution domain up into discrete sub-domains. Many methods and software were developed to do this for simple objects. Grid generation becomes more difficult when the domain of interest is complex. Since a centrifugal compressor already has a very complicated shape, it involves more attention to develop the grid.

In many cases having the grid is not enough because during the simulation process it may be needed to refine the mesh, which also needs some time if the object is complicated. When the object is complicated, many steps are then required to generate the grid. Some CFD solvers do not have a grid generator combined with them and they require the user to build macros to import the grid. Grid generator software vary in difficulties.

3.5.1.1 Geometry from Drawing:

The first step in the grid generation process is to transfer the data from the hardware to the software. This is a non-automated step that needs to be done manually. It is the most time consuming step that needs to be done before any computational work. For this step to be done the geometry was transformed from a non-standard coordinate system to a standard one. There were 20 points given in the drawing for each edge of the impeller's blade. The edges of the blade are at the hub-pressure side, the hub-suction side, the shroud-pressure side, and at the shroud-suction side.

The standard X, Y, Z system was chosen because of it is easiness to visualize and for compatibility issue. Since the blades of the impeller are identical, getting the data for one of them is enough to create the geometry of the whole impeller. It is also wise to do the simulation for one blade to reduce the simulation time. After having the X, Y, and Z coordinates for each point in the drawing, the blade geometry should be visualized using one of the CAD software to check its smoothness and accuracy. AUTOCAD was used for this purpose.

After making sure the blade shape looks right, Excel spread sheets were created to manipulate the data and find the angles and transfer the data to the cylindrical coordinate. Then, the data were tabulated in a certain format in two files. Those files are imp.mnl, which include the mean line data and imp.srf, which include the surface data. A third file was created (impup.mnl) to represent the up stream segment (e.g. the inlet section of the impeller). The Fourth file needs to be created is a data file that includes some input parameters such as the general dimensions and number of blades. This file is named in.dat A FORTRAN code, which was made originally by SOLAR TURBINES named, was then used to create the geometry files that will be read by CFX-TASCflow.

The FORTRAN code generates six data files (named bld_sb.dat, bld_st.dat, bld_nb.dat, bld_nt.dat, interpst.dat, and interpsb.dat). These files are used as an input files to CFX-TASCflow.

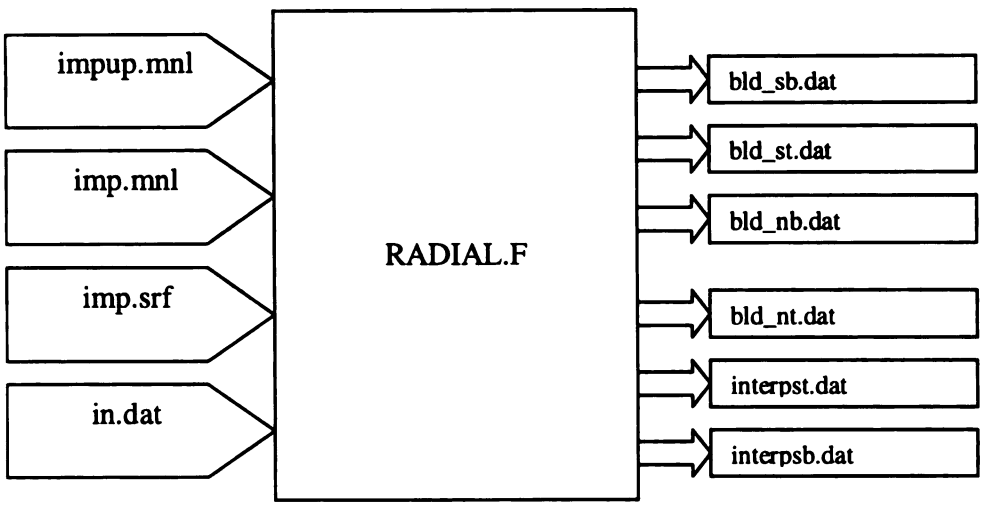

Figure 3-2 Flow chart for initial geometry files generated by FORTRAN code

3.5.1.2 CFX GRID:

Since Grid generation is the process of dividing the solution domain into discrete sub-domains, TASCflow like other CFD package need a grid to work with. CFX-TASCflow accepts grids that are boundary-fitted, generally non-orthogonal and curvilinear.

CFX-TASCgrid is the grid generator in TASCflow, and it generates three-dimensional structured computational grids that are suitable for use with the rest of the CFX-TASCflow software in the numerical solution of fluid flow and heat transfer problems.

The computational domain is defined as a three-dimensional (for 3-D problems) volume completely enclosed by a three-dimensional surface which is called the exterior boundary surface. Within the fully enclosed domain, there may be one region or more that are to be excluded from the computational domain. Each of these excluded regions are called internal objects. These objects must be enclosed fully by a single two-or three

dimensional interior boundary surface. A grid normally given in terms of the x, y and z location of grid nodes distributed throughout the computational domain. At each node in the domain, the code should be able to determine values for all dependent variables including pressure, velocity components, the turbulence quantities, temperature and others. The nodes should be distributed throughout the volume enclosed by the exterior boundary surface of the domain such that they form a complete three-dimensional matrix of nodes. Each node in the matrix will have an index (i; j; k) with the range of i, j and k given by:

$$1 \leq i \leq ID$$
$$1 \leq j \leq JD$$
$$1 \leq k \leq KD$$

where *ID, JD*, and *KD* are the dimensions of the grid in the *I, J* and *K* respectively.

This type of node layout is often named structured or logically Cartesian.

It is useful to introduce the concept of a flux element, in order to completely describe the distribution of nodes in the computational domain. A flux element, used in this work, is a linear, hexahedral element defined by eight nodes as shown in Figure 3-3.

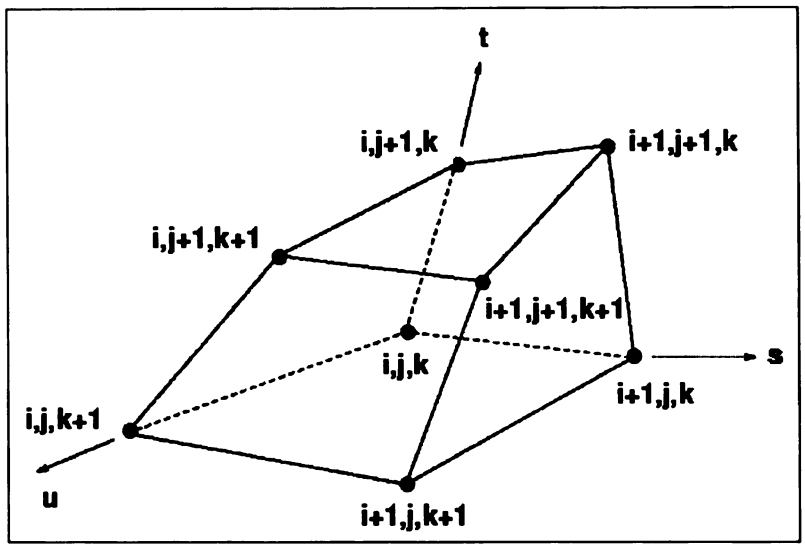

Figure 3-3 Eight-noded hexahedral flux element. (Adapted from CFX- TASC flow)

As was mentioned earlier, TASCflow code adopts a strongly controlled volume approach. To define a control volume within the node plan and flux element definition, already mentioned, the concept of an octant is introduced. An octant is defined such that eight octants forms a flux element with an octant associated with each of the eight nodes (Figure 3.3)

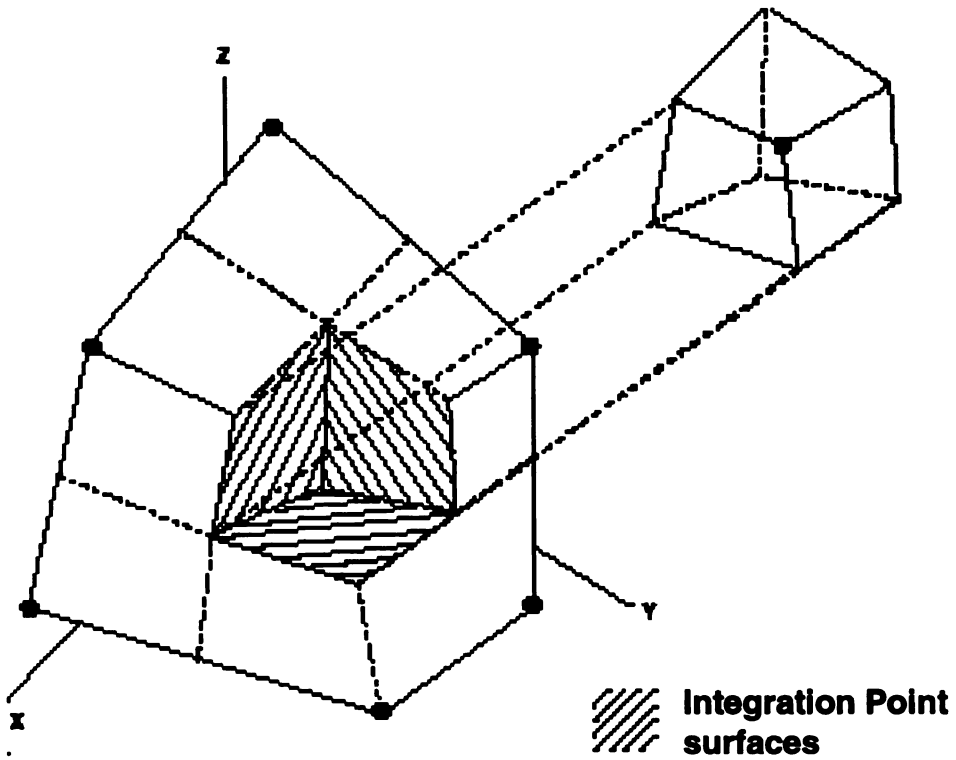

Figure 3-4 A Flux Element Divided into Octants (Adapted from CFX Manual)

Figure 3-4shows a flux element divided into octants and one octant removed. The six sides of each octant are divided into two groups. Some are coincident with the flux element sides and others are in the interior of the flux element. These will form the surfaces of the control volume over which surface integrals will be evaluated; they are referred to as integration point surfaces.

Furthermore, the control volume over which mass, momentum, energy, etc. will be conserved is defined by all octants. The following notes give more understanding for the interaction between the nodes and control volume.

- Interior nodes are completely surrounded by control volumes (8 octants).

- Nodes that lie on a control volume side, edge or corner are called boundary and they are not completely surrounded by the control volumes.
- Control volumes, which are on exterior boundary surfaces, do not include more than four octants.
- Control volumes, which are on exterior boundary edges, do not include more than two octants.
- Control volumes, which are on exterior boundary corners, include only one octant.

3.5.1.3 CFX creates its Grid:

After creating the initial geometry files, the work will be carried out through many stages. TASCflow has CFX-TASCgrid as its grid generator. It generates three-dimensional structured computational grids that are suitable to be with the other CFX-TASCflow software in the numerical solution of fluid flow and heat transfer problems. Figure 3-5is a flow chart shows that the goal of the CFX-TASCgrid is to create the GRD (Grid) file, which contains the coordinates of the finished grid. For this to be done a series of steps must be followed. The CFX-TASCgrid had four subprograms which need to be compiled in a certain order. Each subprogram corresponds to a phase in the grid generation process.

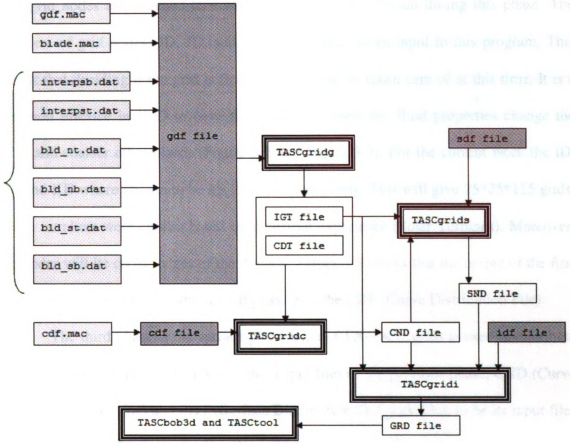

Figure 3-5 CFX-TASCgrid Data Flow Diagram

The first phase is the Geometry Phase, which defines the geometry using a subprogram called CFX-TASCgridg. It gives a means to describe the physical domain. As can be seen from Figure 3-5, CFX-TASCgridg requires a file named GDF (Geometry Definition File) to be its input. The GDF file itself needs other files to supply CFX-TASCgridg the needed data. These files are the ones created by RADIAL.F plus two macro files that will supply enough data for CFX-TASCgridg to create two files IGT (Internal GeomeTry file) and CDT (Curve Distribution Template file).

After doing the first phase, the second one may be done. The second phase is the Curve Phase in which the nodes are distributed on curves using CFX-TASCgridc. The

first grid nodes are attached to corners of the physical domain during this phase. The numbers of grid nodes (ID, JD, and KD) are defined as an input to this program. This means that deciding if the grid is fine or coarse is to be taken care of at this time. It is a common practice in CFD to have the grid finer where the fluid properties change the most and coarser other places (Figure 3-6 and Figure 3-7). For the current work the ID, JD, and KD where chosen to be 25, 25, 115 respectively. This will give 25*25*115 grids. These numbers were chosen based on industrial experience (Solar Turbines). Moreover, the nodes will lie on the edges of the domain. Figure 3-5 shows that the output of the first phase was used as inputs to the second phase plus the CDF (Curve Distribution File).

The third phase is the surface phase where CFX-TASCgrids is used to distribute nodes on surfaces. This program uses the output files of the pervious phase, CND (Curve Node Distribution file) and SDT (Surface Distribution Template file), to be its input files in addition to one file from the first phase (IGT).

The fourth phase is the interior phase in which the CFX-TASCgridi program is used to distribute nodes in the interiors of regions. This program also uses an output file of the pervious phase, SND (Surface Node Distribution file), to be its input file in addition to one file from the first phase (IGT) and IDF (Interior Distribution File). The output of this phase is the final output of CFX-TASCgrid which is GRD file (GRID coordinates file).

3.5.1.4 Grid Quality:

At this stage the grid is ready for CFX-TASCflow, but its quality needs to be tested before going any farther. This can be done using CFX-TASCtool to do three major checks for the grid. The first check is for the volumes to know if all the volumes (and

Octants) are positive if there will be even one negative the code will not start. The second check is for the skew to know the maximum and minimum angles in the grid. The angles should be above 20 to have no warnings but still the code may give good results even if there are some angels above 15. The third check that needs to be performed is the aspect to be between 1 and 100 in value. If there is a problem with the grid, the original input geometry files need to be reviewed and it may require some adjustments for files such as CDF. If the quality check did not turn the way it should be, then trying to fix it may consume a lot of time.

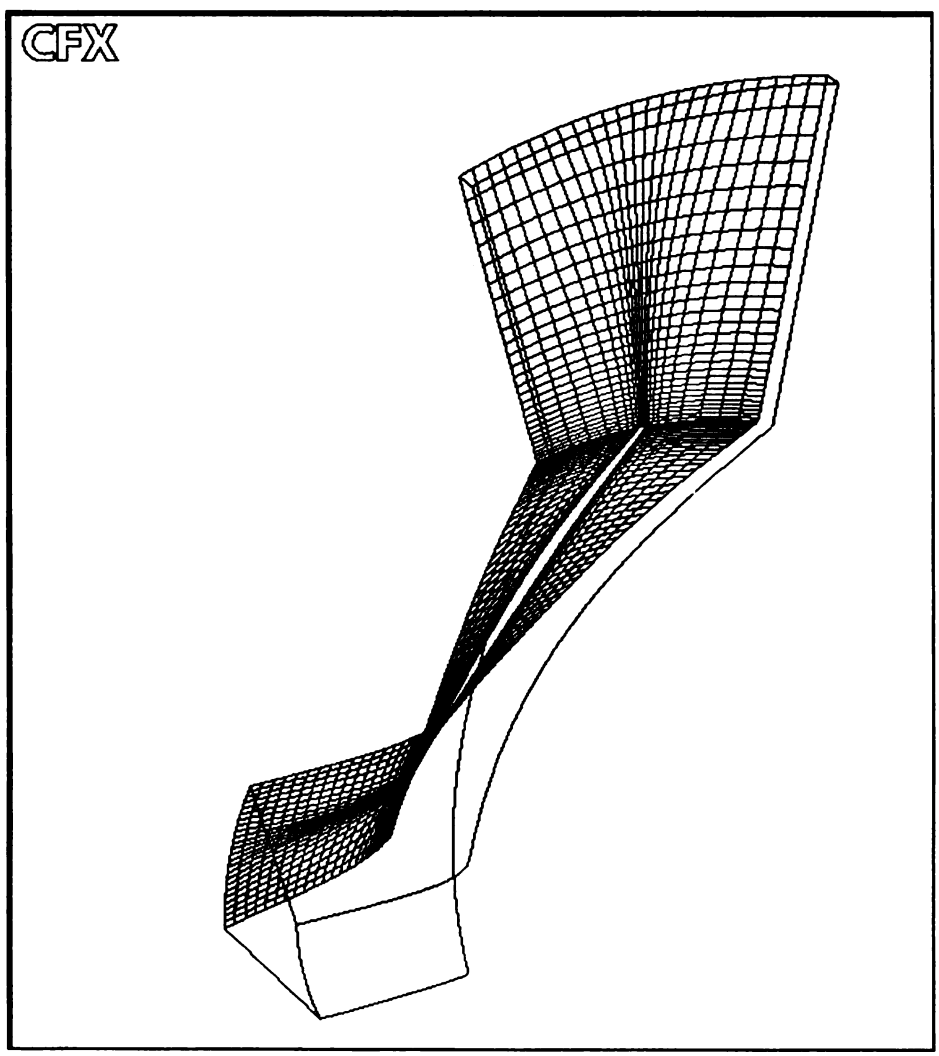

Figure 3-6 Blade to Blade grid that is used in the simulation

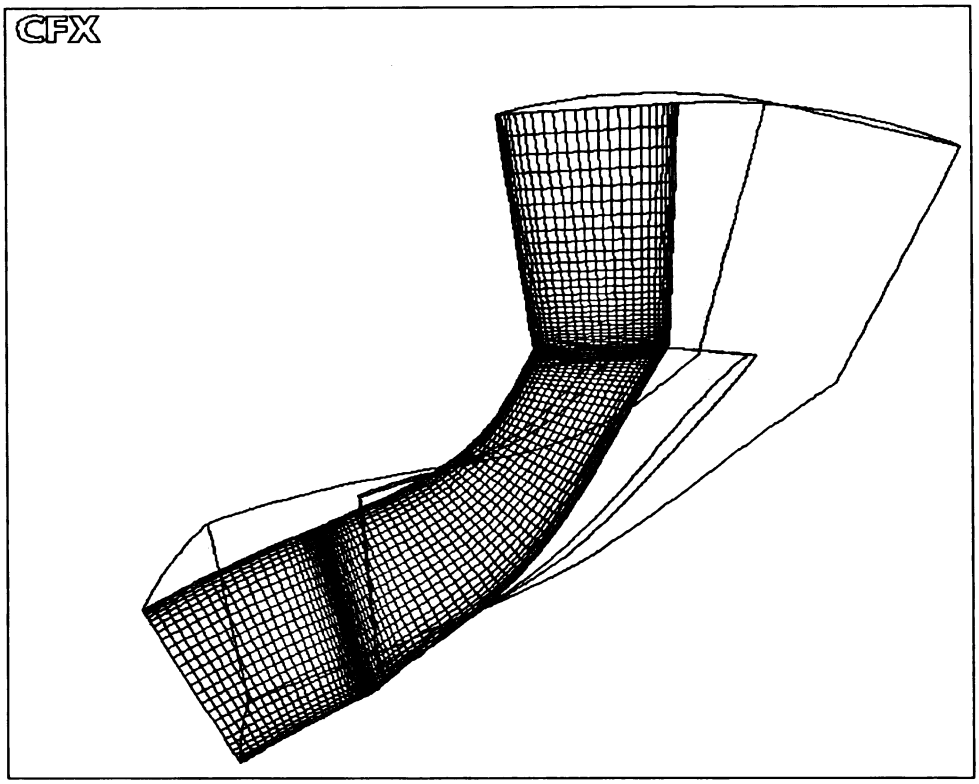

Figure 3-7 Inlet to Exit Grid that is Used in the Simulation

3.5.2 Turbulence Modeling

Modeling the turbulences in the flow is what makes modeling the flow in the impeller very difficult. This is because of the high rotation of the impeller and high velocities of the fluid and the compressibility affects. Up to this date, no one turbulence modeling can handle all the fluid flows. Some of them are preferred in some cases others are better in other cases. Experienced people suggest that for flow in a centrifugal impeller Ronald's Stress Model works the best because it takes care of the centrifugal motion.

In theory, the Navier-Stokes equations describe both laminar and turbulent flows without the need for additional information. But turbulent flows at high Reynolds

numbers experience a large range of turbulent length- and time scales. The direct numerical simulation (DNS) of these flows would require a very high computing power. This power is many orders of magnitude higher than what could be available in the foreseeable future. It is therefore necessary to reduce the complexity of the simulations by the introduction of the Reynolds averaged equations, which describe the mean flow, without a need for the resolution of the turbulence. The averaging procedure introduces additional terms into the equations that need to be modeled in order to achieve what is called closure, to have a sufficient number of equations for all the unknowns, including the Reynolds-Stress tensor resulting from the averaging procedure.

The Reynolds-averaged Navier-Stokes (RANS) equations correspond to the transport equations for the mean flow quantities only. This approach greatly reduces the time required for computational when compared with a direct numerical simulation and is generally adopted for practical engineering calculations. Closure of the equations is achieved by the introduction of additional equations to model turbulent correlations, like the turbulent kinetic energy. The Reynolds-Stress tensor can be related to the mean flow variables by the mean of these variables.

The following (RANS) turbulence models are available in CFX-TASCflow:

- Two-Equation Models
    - Standard k- ε model
    - k- ε RNG model
    - Standard k-ω model
    - BSL and SST zonal k-ω based models
- Algebraic-Stress Models (ASM)

- o k- ε based ASM model
- o k-ω based ASM model
- o Zonal k-ω based ASM model

- Reynolds-Stress Models (RSM)
  - o Launder, Reece and Rodi model (LRR)
  - o Speziale, Sarkar and Gatski (SSG)

This gave a variety of choices for TASCflow to choose the most suitable one depending on the time, grid, and flow type. (TASCflow User Documentation).

3.5.3 Boundary Conditions Used in Simulation

Boundary conditions specification is an essential part in using CFD. They vary from symmetric to periodic, from wall to another, and from inlet to outlet. As was mentioned earlier specifying the boundary conditions is a pre-processing process. CFX-TASCbob3D is a subprogram in CFX-TASCflow that was used to specify the boundary conditions. BCF (**B**oundary **C**onditions **F**ile) is the file where the boundary conditions are stored. When specifying the boundary conditions, the location must be given with respect to the nodes.

The boundary conditions used in this work are as follows

- Inlet: the pressure and Temperature is given.

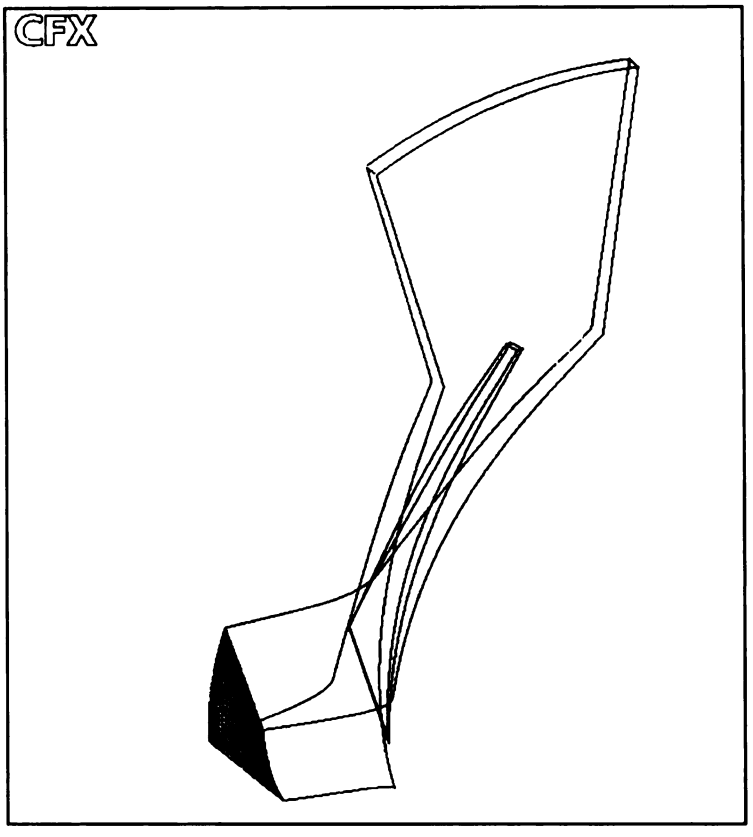

Figure 3-8 Inlet Boundary Condition

- Outlet: the mass flow rate is given.

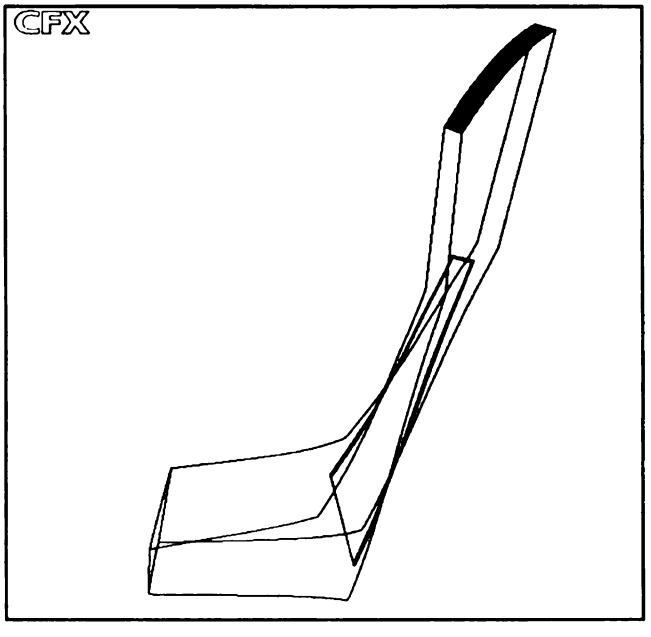

Figure 3-9 Outlet Boundary Condition

- Wall (stationary) which is the none moving boundary.

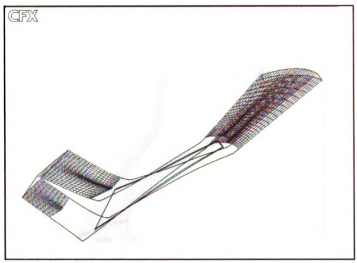

Figure 3-10 Wall (stationary) Boundary Condition

- Wall (moving) which is either the hub or shroud.

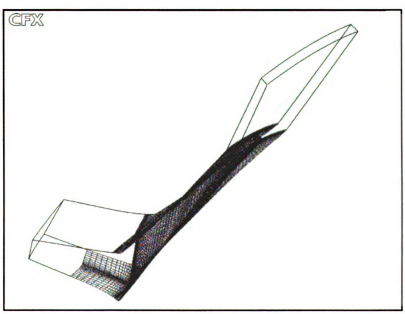

Figure 3-11 Wall (moving) Boundary Condition

- Periodic: this boundary is making the problem easer to solve because the number of nodes is small compared to the whole impeller.

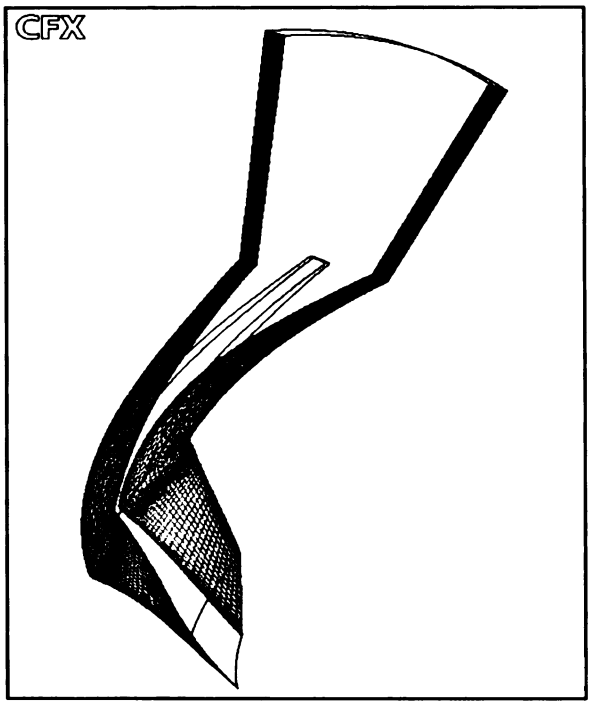

Figure 3-12 Periodic Boundary Condition

- Symmetric: this boundary condition is some times wanted to take care of the slip.

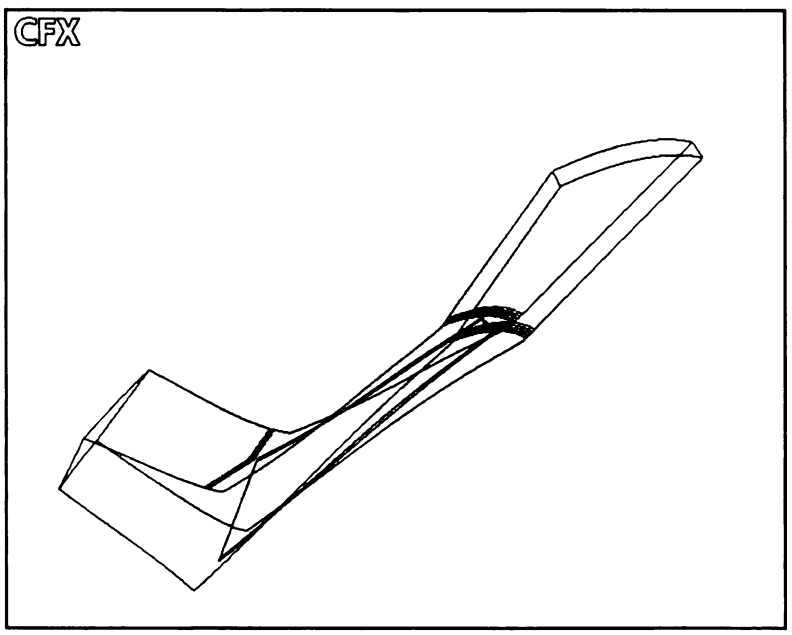

Figure 3-13 Symmetric Boundary Condition

3.5.4 Use of Initial Conditions

The initial flow conditions need to be set using CFX-TASCtool before starting the solver. These initial conditions are stored in GCI (General Command Initialization). For this study the initial conditions were Pressure, Temperature, and turbulence model parameters.

3.5.5 Control Parameters

Before running the solver, a file containing parameters that control the solution of the fluid flow problem should be created (Parameter file containing job control parameters). These parameters include the rotational speed, the memory needed.

3.5.6 Solver

The fluid flow solver that was used is CFX-TASCflow3D or "flow code" of CFX-TASCflow. The governing equations of fluid flow are coupled, non-linear, and partial differential equations.

When it starts running, CFX-TASCflow3D requires no interactive input from the user because it is a batch-oriented program. Selecting input parameters enables the code to produce a converged solution for a certain problem. The convergence criterion was to have the maximum residual to be 0.00005. The user is able to see the convergence of his problem while the simulation is running and some times it will save some time.

After completing the simulation, the user will be able to look at the results in many forms some of them will be shown and discussed in chapter 5.

Chapter 4 EXPERIMENTAL DATA ANALYSIS

4.1 Background

A series of compressor rig tests were done between 1976 and 1977 at Solar Turbine Laboratories. Four different impellers with two configurations each were tested. The wide term was used refer to the original impeller tip width, while the narrow is used to refer to the impellers after the trim. The impeller exit tip widths were reduced by 25% each. The tested stages' specific speed ranged from 59 to 135. The four impellers were named B, C, D, and E starting from lower to higher specific speeds (Figure 4-1).

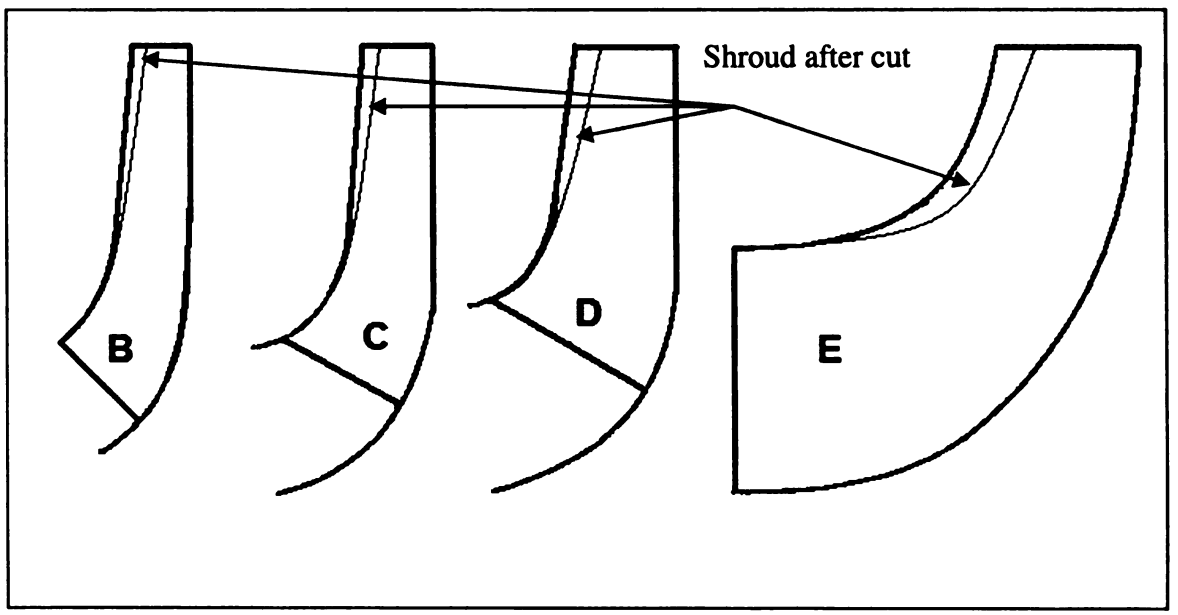

Figure 4-1 The Tested Impellers Before and After the Modification

A turbocharger with shop air was used to drive the compressor rig. The test gas used was the ambient air in an open loop. The total (stagnation) pressures and the static pressures instrumented from the compressor inlet to the exit scroll. The diffusers were

unpinched in all cases. Table 4-1 shows all major dimensions with respect to a reference dimension (Rref) for the eight impellers and their vaneless diffusers. All the tested impellers were open-faced (unshrouded) impellers.

Table 4-1 Major stages dimensions in dimensionless form

	B(Orig)	B(Trim)	C(Orig)	C(Trim)	D(Orig)	D(Trim)	E(Orig)	E(Trim)
Impeller								
Inlet Shroud Radius (R1s/Rref)	6.818	6.818	7.182	7.182	8.000	8.000	9.091	9.091
Inlet Hub Radius (R1h/Rref)	4.545	4.545	4.545	4.545	4.545	4.545	4.545	4.545
Exit Tip Radius (R2/Rref)	12.727	12.727	12.727	12.727	12.727	12.727	12.727	12.727
Exit blade width (B2/Rref)	1.000	0.749	1.273	0.956	1.716	1.356	2.545	1.909
Vaneless diffuser								
Inlet Radius (R3/Rref)	14.182	14.182	14.182	14.182	14.182	14.182	14.182	14.182
Inlet width (B3/Rref)	0.909	0.909	1.164	1.164	1.636	1.636	2.364	2.364
Exit Radius (R4/Rref)	19.091	19.091	19.091	19.091	19.091	19.091	19.091	19.091
Exit width (B4/Rref)	0.909	0.909	1.164	1.164	1.636	1.636	2.364	2.364

4.2 Effect of Specific Speed on Impeller Characteristics

The specific speeds for the original B, C, D, and E impellers are 58, 82, 115, and 126 respectively; while the specific speeds for the trimmed B, C, D, and E impellers are 68, 84, 117, and 133 respectively. So, for both configurations the specific speed increases from the B through C then D to E. Having two sets of impellers gives a great understanding of the effect of changing the specific speed on the impeller characteristics. Looking carefully at the general trend of figure 4.2 and 4.3, a simple conclusion such as stages with higher impeller specific speed gives higher stage efficiency can be made. This can be said about the wide impellers as well as the narrow ones.

Figure 4.4 and 4.5 shows how the operation range changes from a narrow one for the lower specific speed impeller to wider operation range as the specific speed increases. An additional factor needs to be considered in this case which, is that each impeller of these impellers has its own range of flow coefficients.

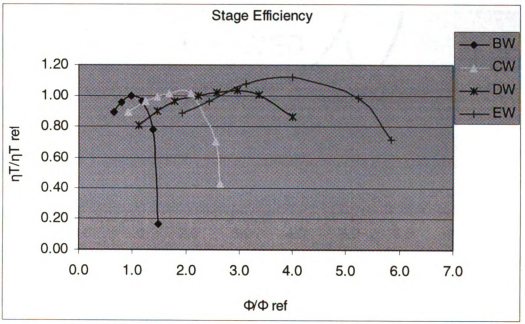

Figure 4-2 Variation Of The Stage Efficiency For The Wide Impellers

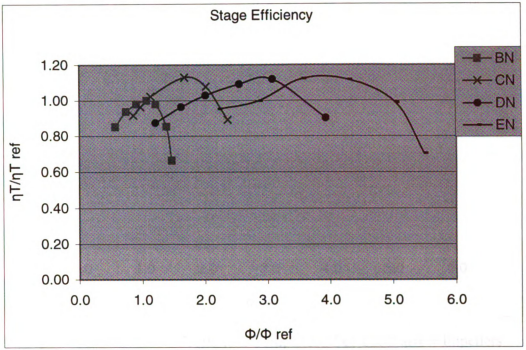

Figure 4-3 Variation Of The Stage Efficiency For The Narrow Impellers

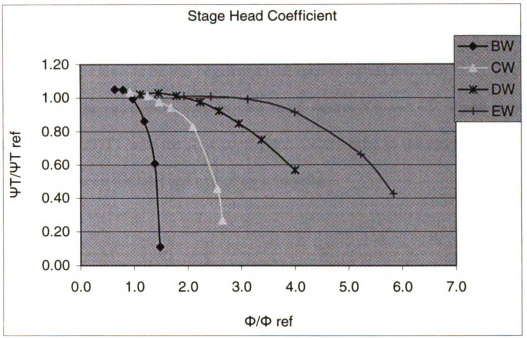

Figure 4-4 Stage Head Coefficient Comparison For The Wide Impellers

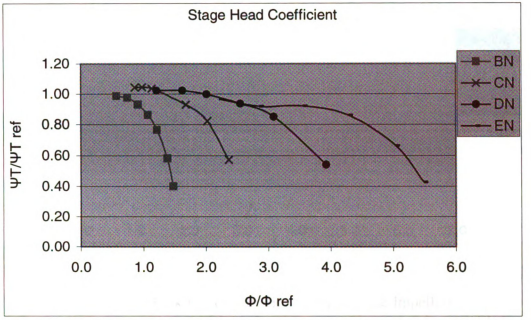

Figure 4-5 Stage Head Coefficient Comparison For The Narrow Impellers

The variation of the work factor is shown in figures 4.6 and 4.7. Looking at each series alone, one may notice that the change is almost liner. Another valid notice is that the slopes of these lines are all negative. If the four lines in each figure are compared, it is clear that the slope tents to be less negative as the specific speed increases.

Almost exactly the same thing may be said about figures 4.8 and 4.9, which show the variation of DeltaT/T1 with the flow coefficient. DeltaT refer to the change of the total temperature between the inlet and exit of each impeller.

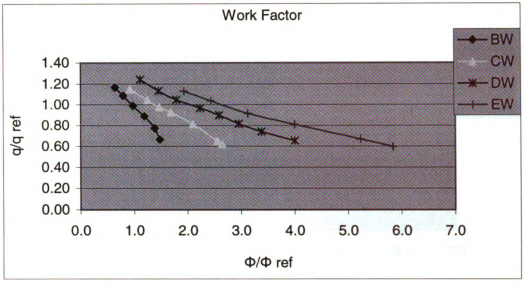

Figure 4-6 Work Factor Variations for The Wide Impellers

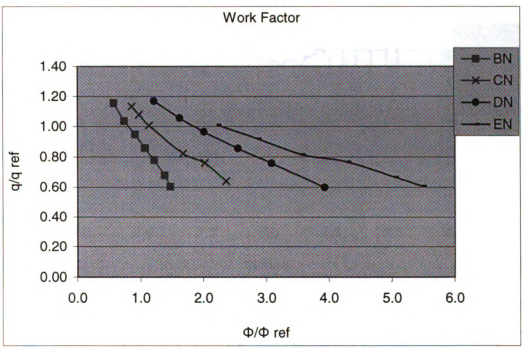

Figure 4-7 Work factor variations for the narrow impellers

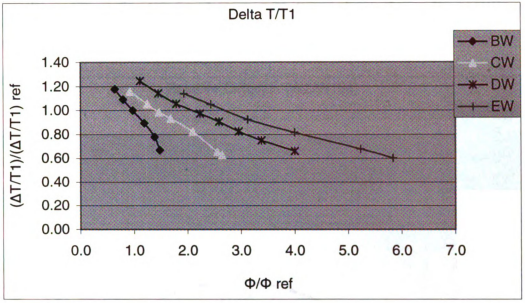

Figure 4-8 DeltaT/T1 variations for the wide impellers

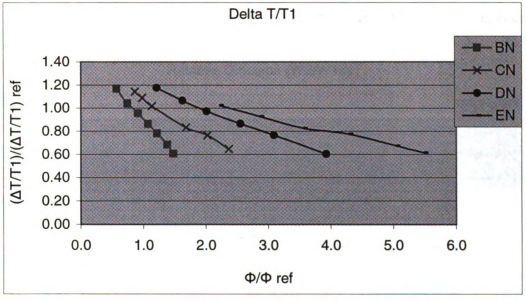

Figure 4-9 DeltaT/T1 variations for the narrow impellers

The change of the relative diffusion (W2/W1tip) with respect to the flow coefficient is shown in figures 4.10 and 4.11. Looking at the individual impeller, one may notice that all the variations are almost linear. The positive slope is another characteristic

of these lines. Comparing the four lines in each figure shows that as the specific speed increases the slope tends to be less.

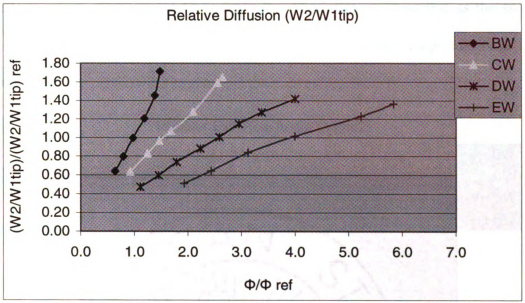

Figure 4-10 The change of the relative diffusion (W2/W1tip) for the wide impellers

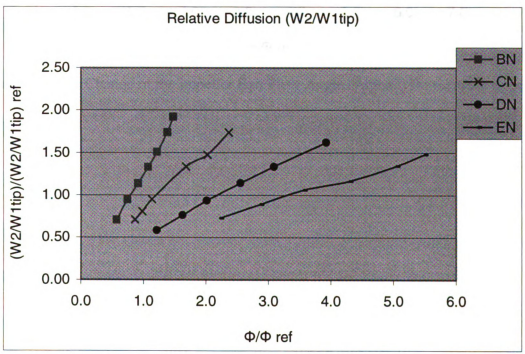

Figure 4-11 The Change of the Relative Diffusion (W2/W1tip) For the Narrow Impellers

Another important characteristic of any impeller flow is the impeller exit flow angle (Alpha2). The normalized angles are given for both the wide and the narrow impellers in figure 4.12 and 4.13 respectively. These figures show that as the specific speed gets higher, the curve tends to flatten over the operating range and have more negative slope.

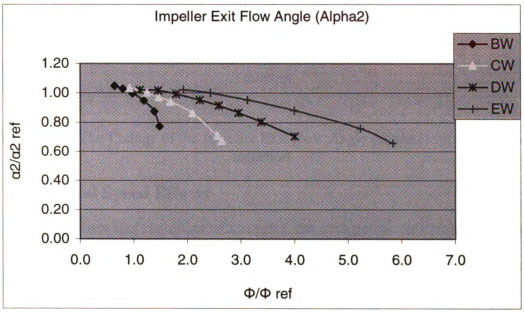

Figure 4-12 The Change of the Impeller Exit Flow Angle (Alpha2) for the wide impellers

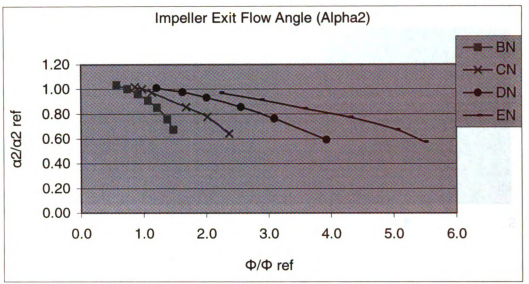

Figure 4-13 The Change of the Impeller Exit Flow Angle (Alpha2) for the narrow impellers

4.3 Rotational Speed Effects

This part discusses the effect of changing the compressor rotational speed on the performance of the four impellers. These impellers are B and E with both configurations wide and narrow. These four were chosen from the eight impellers specifically because they are the extreme ones in their specific speed and operation range. These experimental results refer to four different rotational speeds 22000, 28000, 34000, and 40000 rpm for the four impellers.

Figures 4.14 to 4.17 shows that stage efficiency stays almost constant at the design point in all rotational speeds for the low specific speed impellers (B wide and narrow), while it clearly decreases with increasing the rotational speed for the high specific speed impellers (E wide and narrow). The same thing can be said about the impeller efficiency for the high specific speed impellers (Figure 4.20 and 4.21). For the low specific speed impellers (spatially the narrow one), the impeller efficiency is clearly more for the higher rotational speed (Figure 4.19).

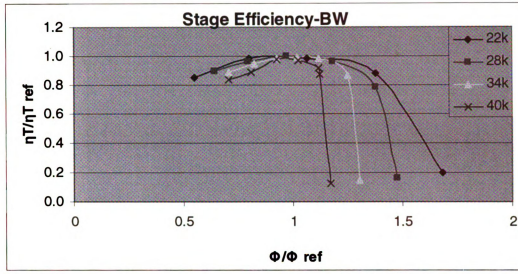

Figure 4-14 Variation of the Stage Efficiency for B Wide at Variable Rotational Speeds

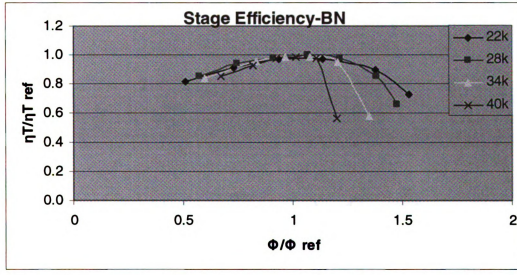

Figure 4-15 Variation of the Stage Efficiency for B Narrow at Variable Rotational Speeds

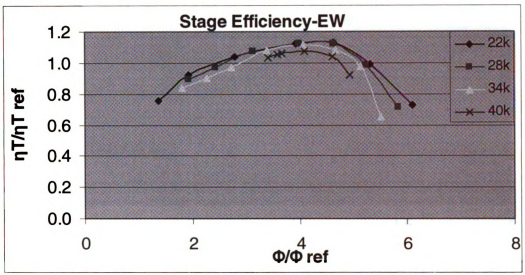

Figure 4-16 Variation of the Stage Efficiency for E Wide at Variable Rotational Speeds

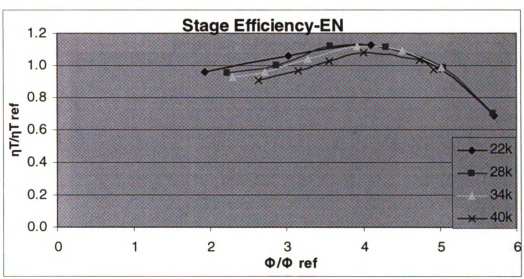

Figure 4-17 Variation of the Stage Efficiency for E Narrow at Variable Rotational Speeds

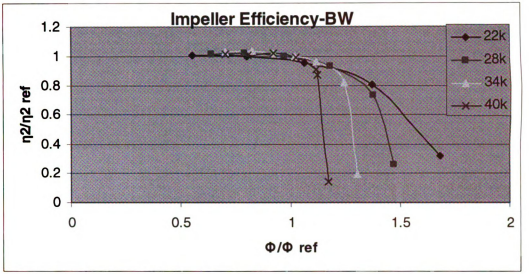

Figure 4-18 Variation of the Impeller Efficiency for B Wide at Variable Rotational Speeds

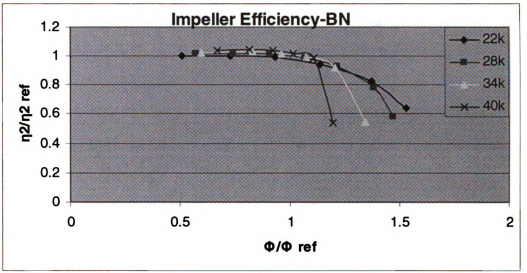

Figure 4-19 Variation of the Impeller Efficiency for B Narrow at Variable Rotational Speeds

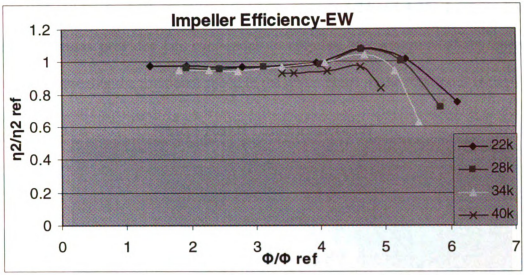

Figure 4-20 Variation of the Impeller Efficiency for N Wide at Variable Rotational Speeds

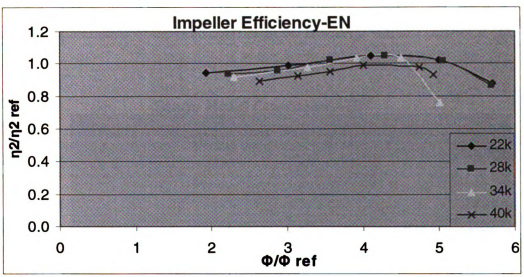

Figure 4-21 Variation of the Impeller Efficiency for N Narrow at Variable Rotational Speeds

Another interesting point worth mentioning is that the referenced head coefficient increases at the design point with the increase of the rotational speed for the low specific speed impellers (figures 4.22 and 4.23) while it clearly increases with decreasing the

rotational speed for the high specific speed ones (figures 4.24 and 4.25). Looking back to these four figures provides fair confidence to correlate the wideness of the operating range to the lowering the rotational speed in the given range of the rotational speeds.

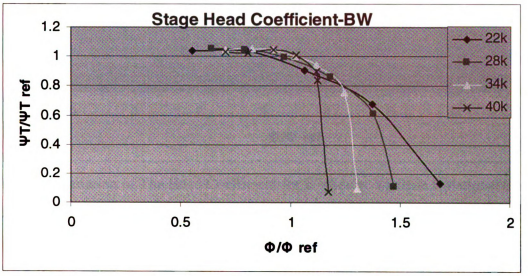

Figure 4-22 Variation of the head coefficient for B wide at variable rotational speeds

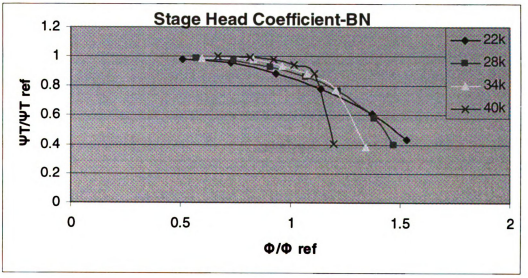

Figure 4-23 Variation Of The Head Coefficient For B Narrow At Variable Rotational Speeds

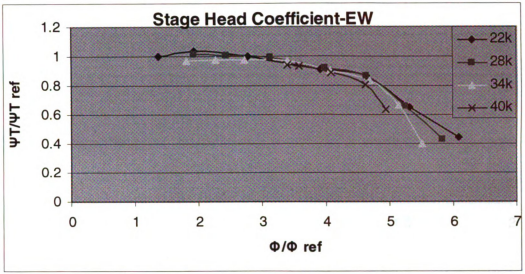

Figure 4-24 Variation of The Head Coefficient for E Wide at Variable Rotational Speeds

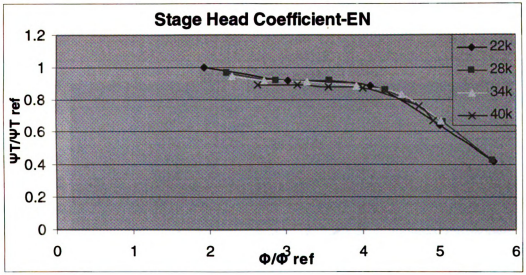

Figure 4-25 Variation Of The Head Coefficient For E Narrow At Variable Rotational Speeds

Figures 4.26-4.29 show that the work factor is higher for the higher rotational speed, it then goes down when the rotational speed decreases. This is true for most of the operation range except for a relatively high flow coefficient where the work factor decreases more rapidly for higher rotational speed.

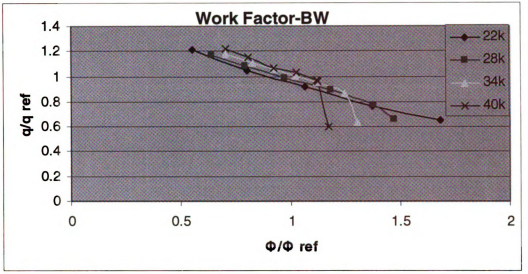

Figure 4-26 Variation of the Work Factor for B Wide at Variable Rotational Speeds

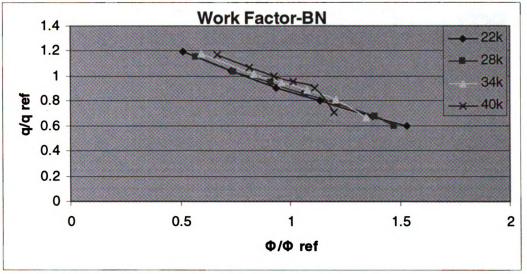

Figure 4-27 Variation Of The Work Factor For B Narrow At Variable Rotational Speeds

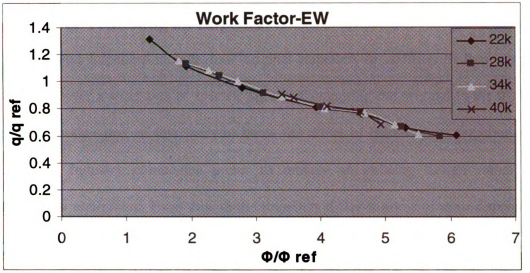

Figure 4-28 Variation of the work factor for E wide at Variable Rotational Speeds

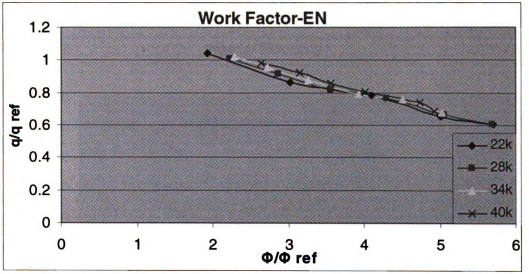

Figure 4-29 Variation of the work factor for E narrow at Variable Rotational Speeds

4.4 Effect of Trimming an Impeller

The tested impellers include four original impellers in addition to four trimmed ones, which cover a wide area of specific speeds. Comparing the original to the trimmed impeller is another task of this study to know the effect of trimming an impeller on its performance. Industry companies prefer to modify an existing design rather than designing new equipment. Even though the impellers differ in some of their dimensions, all the original ones were smoothly cut 25% at their impeller exit width from the shroud side.

Trimming all four impellers showed better impeller efficiency (Figure 4.30). Looking at figure (4.31) shows also an increase in the stage efficiency after trimming the impellers.

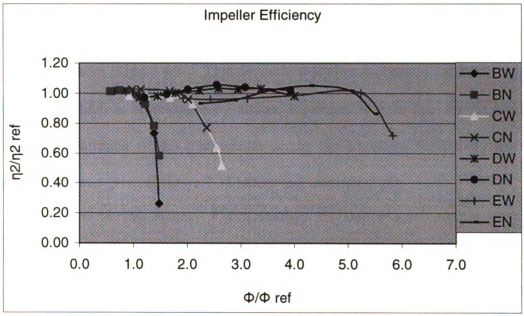

Figure 4-30 Impellers Efficiencies Before and After Trimming

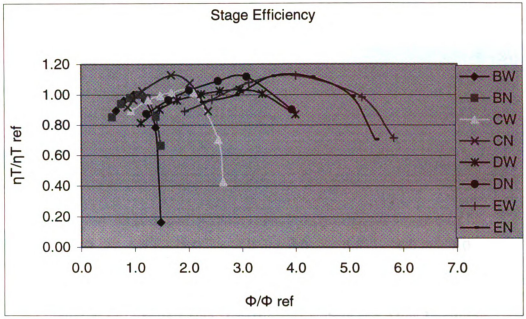

Figure 4-31 Stage Efficiencies for All Impellers before and After Trimming

Impellers' head coefficients (Figure 4.32) had decreased for all four impellers after trimming them. Stage head coefficients (Figure 4.33) also experienced a slit increase after the modification. Work factors at all points for all impellers were clearly decreased after trimming them (Figure 4.34). That decrease was almost constant for every impeller after the cut, which is represented by almost a parallel straight line for the trimmed impeller. The variation of the temperature across the impellers divided by the inlet temperature for was given in figure 3.35 before and after trimming.

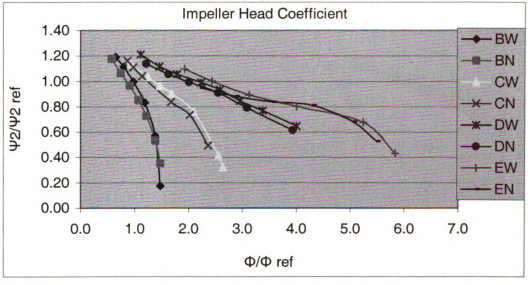

Figure 4-32 Impellers Head Coefficients Before and After Trimming

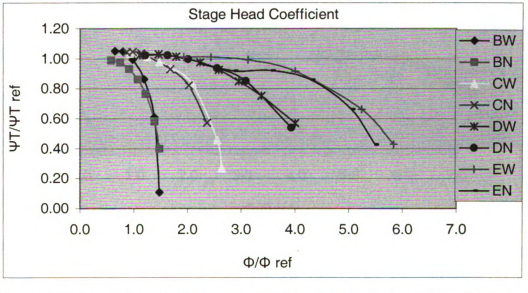

Figure 4-33 Stage Head Coefficients for All Impellers Before and After Trimming

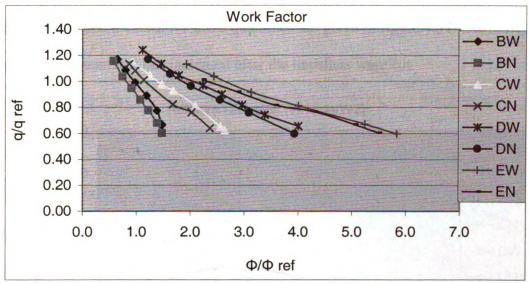

Figure 4-34 Work Factors for All Impellers Before and After Trimming

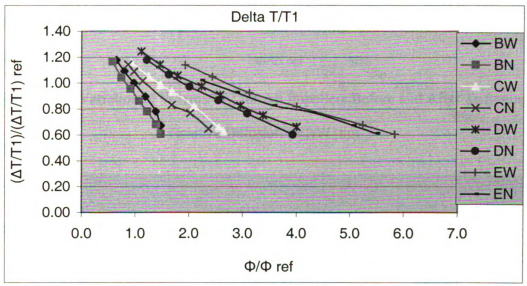

Figure 4-35 Variation of Deltat/T1 For All Impellers Before and After Trimming

The relative diffusion, W1rms/W2, is one of the considerations in determining the tip width of an impeller design. This relative diffusion for all impellers was clearly reduced as shown in figure 4.36 because of the 25% reduction in the tip width.

Another non-dimensional quantity of interest to the designer is the W2/W1tip relative diffusion. Normalized values for these quantities are given in figure 4.37. Obviously, the values of these quantities had increased after the impellers were cut.

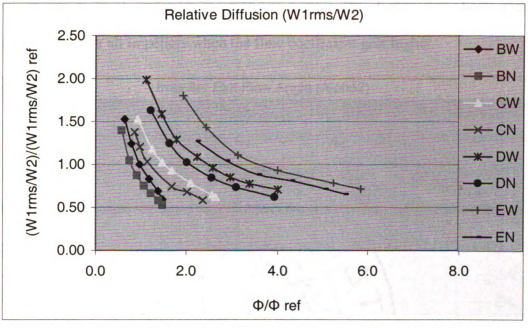

Figure 4-36 Variation of W1rms/W2 for All Impellers Before and After Trimming

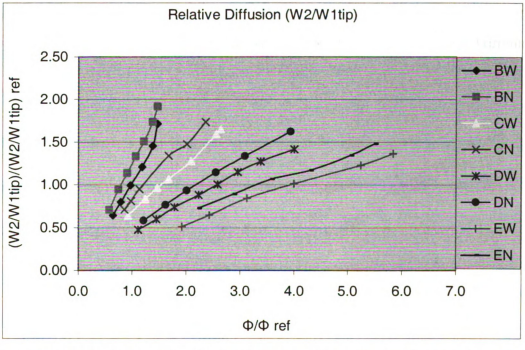

Figure 4-37 Variation of W2/W1tip for All Impellers Before and After Trimming

The variation of the impellers' exit flow angles are given in the following figure. Looking at this figure, provides great confidence that trimming such impellers will reduce the impeller exit flow angle. This is sometimes desired to satisfy some design considerations, such as matching the diffuser design. This figure also shows that the decrease is more for all impellers when the flow coefficient gets higher.

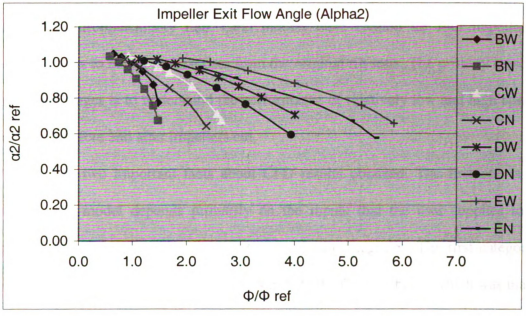

Figure 4-38 Variation of The Impellers Exit Flow Angles Before and After Trimming

Chapter 5 CFD RESULTS AND VALIDATION

5.1 Background

This chapter deals mainly with the results of the CFD model. Experimental and 1-D code results are available for validation. The Experimental results were provided by Solar Turbines Company while the 1-D results were obtained from a code that was developed by the MSU Turbomachinery Lab. CFD models were created for four impellers to simulate the flow to match the test data from the original rig tests. The primary reason to analyze these stages is to understand the performance of relatively low and high specific speeds stages before and after impellers cut.

There are two important facts about CFD results obtained. The first one is that output of CFD model depends primarily on the inputs that the user supplies to the computer. These inputs may be divided into two main categories. The first category is supplying the equations and models used to simulate the flow problem, which was mainly taking care of by CFX TASCflow that is a known CFD package in turbomachinery simulation. The other category is supplying the parameters and values, like the grid generation and boundary condition, used to run the model. The second important fact about the CFD results is that it gives much more information about the flow than what can be obtained from the test data or the 1-D results. More specifically, the data needed may be obtained at locations where the experimental setup or 1-D analysis would not help because of the some difficulties.

5.2 Primary Check

The CFD simulation that was done for this study includes running about 50 cases. Running these cases took variable times using a Pentium 4 computer with 526 Ram. Some took about 2; hours others took tens of hours to be done. The convergence criterion was chosen to be that the maximum residual is less than $5*10^{-5}$. The major sets of these cases refer to the wide B, narrow B, wide E, and narrow E impeller. After doing the required preprocessing and running the code, the results were obtained. Being able to get the results doesn't necessarily mean that they are correct. So, it is required to check the output of the code. This may be primarily done by checking the output with common behavior of such flow. The results then need to be validated with the other methods of getting the result.

For this study the CFD results, obtained from CFX TASCflow, were primarily compared with the common behavior of the fluid flow in centrifugal compressor. Figure 2-7 and Figure 2-8 show that the pressure and temperature trend in centrifugal compressors. The variation of the total pressure, static pressure, total temperature, and static temperature matched what was expected as in Figure 2-7 and Figure 2-8. Other parameters like the density were also check and the CFD output where matching what was expected .

5.3 CFD Validation

In general, the CFD results give a good trend match compared with the test and 1-D results. A more in-depth look at these results shows some carves with almost exact matching; other show some differences in the values obtained for some of the dimensionless parameters.

Figures 5.5 and 5.6 show the stage efficiency curves for the low, specific-speed impellers (B wide and narrow), while figures 5.7 and 5.8 show it for the high specific speeds impellers (E wide and narrow). In all cases, CFD over predicts the stage efficiency. For the low specific speeds impellers the over prediction is constant with a value about 20% from the design point to surge point (the lowest flow coefficient) while it is more above the design point. For the same impellers, the stage efficiency was well predicted using the 1-D code above the design point (higher flow coefficient) but almost as good as the CFD for low flow coefficient. For the high specific-speeds impellers (E wide and narrow) the over prediction is minimum at the design point (less than 10%), but it increases as the flow coefficient gets higher or lower.

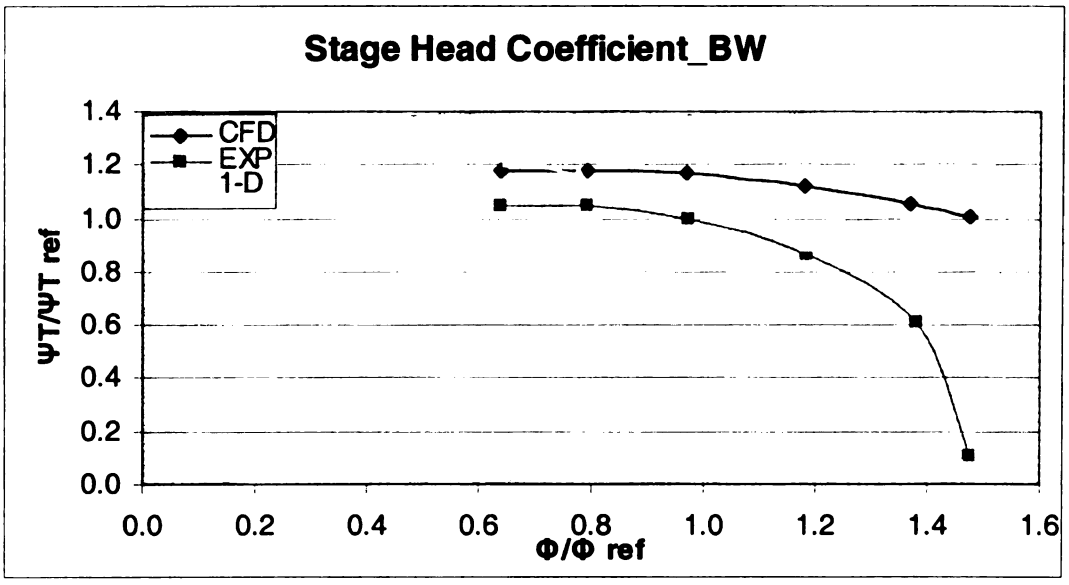

Figure 5-1 Experimental, CFD, and 1-D Stage Efficiency for B Wide

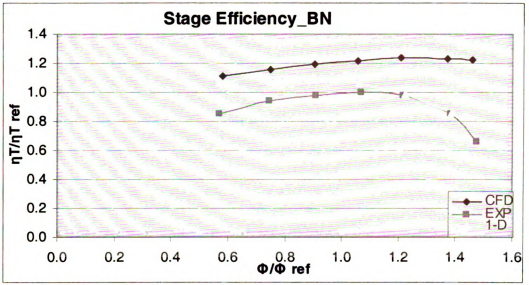

Figure 5-2 Experimental, CFD, and 1-D Stage Efficiency for B Narrow

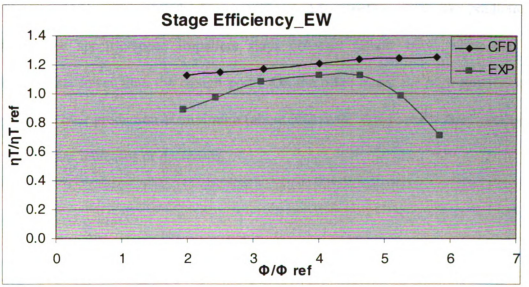

Figure 5-3 Experimental and CFD Stage Efficiency for E Wide

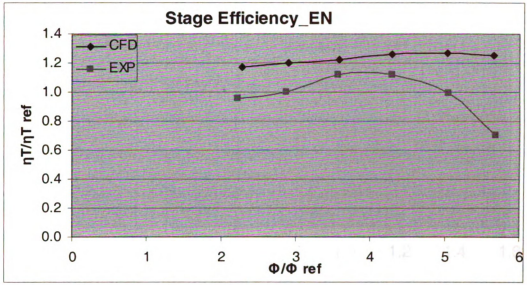

Figure 5-4 Experimental and CFD stage efficiency for E narrow

The following four figures (5.9-5.12) show the impeller efficiency for the four impellers. For all of them, CFD also over predicts the impeller efficiency while the 1-D code gave accurate values for the low specific-speeds impellers. The over prediction of CFD for low specific-speed impellers stays constant (about 10%) when the flow coefficient gets lower than the design point. On the other hand, for high specific-speed impellers the over prediction is minimum (about 5%) at the design point then increases as flow coefficient increases or decreases.

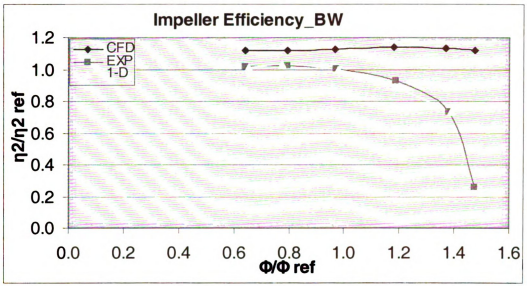

Figure 5-5 Experimental, CFD, and 1-D Impeller Efficiency for B Wide

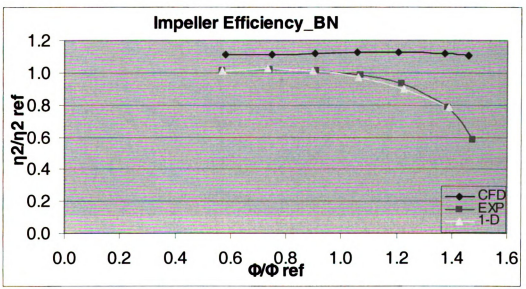

Figure 5-6 Experimental, CFD, and 1-D impeller efficiency for B narrow

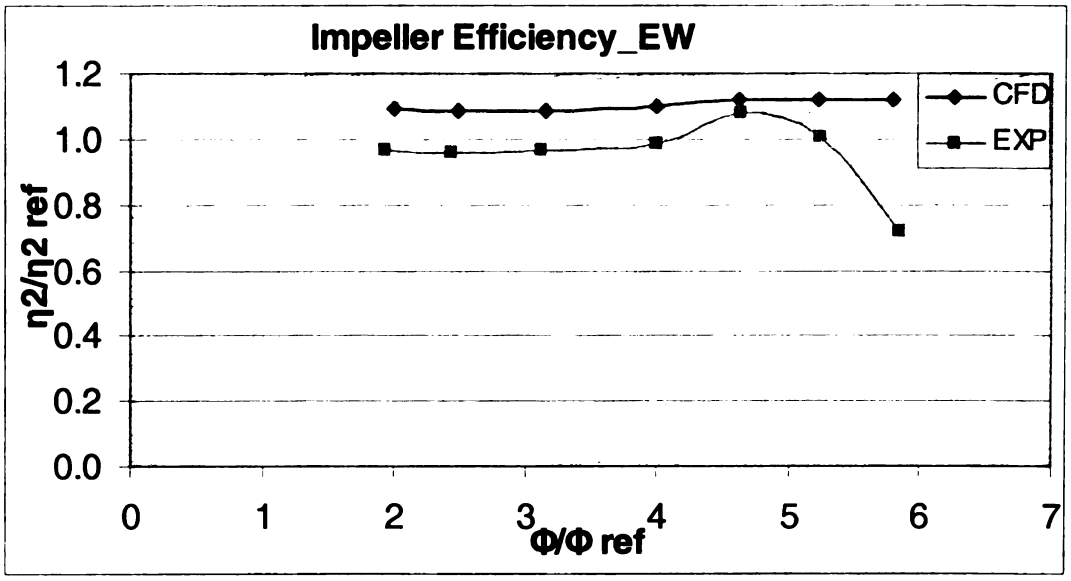

Figure 5-7 Experimental and CFD Impeller Efficiency for E Wide

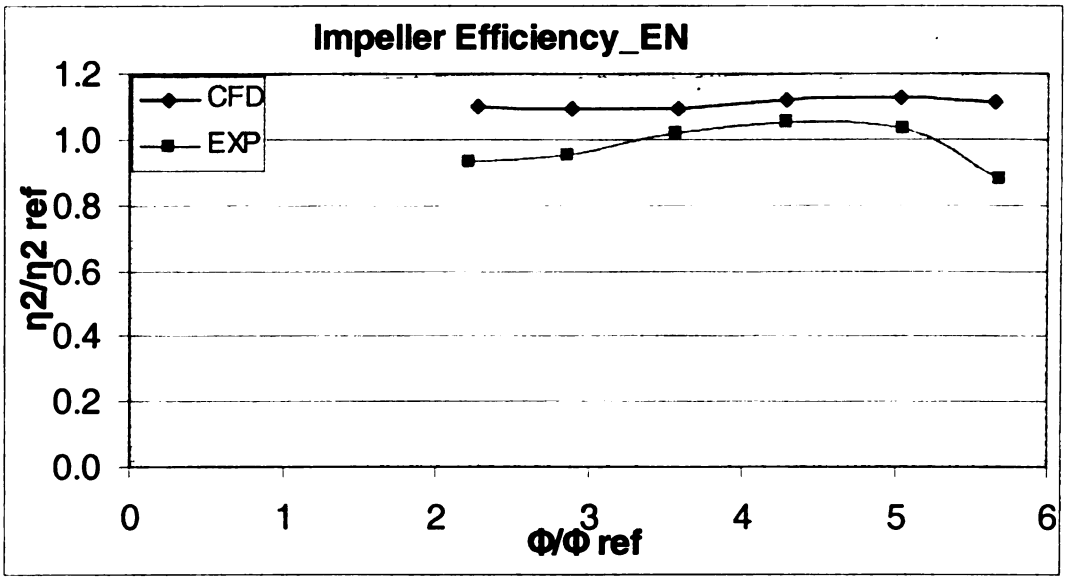

Figure 5-8 Experimental and CFD impeller efficiency for E narrow

Another important characteristic of any stage is the head coefficient. It gives good indication of the surge and choke limes of the flow. Figures 5.13 to 5.16 shows that CFD over predict the head coefficient. For the low specific-speeds impellers (Figure 5.13 and 5.14), the over prediction is constant from the lowest flow coefficient to the design point

then it increases as the flow coefficient increases. For the same impellers the 1-D code predicts the head coefficient well at the higher flow coefficient but over predict it at lower flow coefficient.

For the high specific-speeds impellers (Figure 5.15 and 5.16) the best CFD prediction was at the design point (less than 20%), but it increases as the flow coefficient increases or decreases.

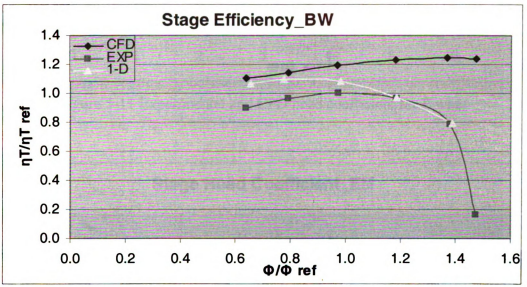

Figure 5-9 Experimental, CFD, and 1-D head coefficient for B wide

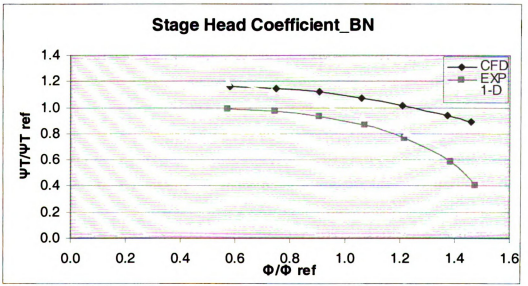

Figure 5-10 Experimental, CFD, and 1-D head coefficient for B narrow

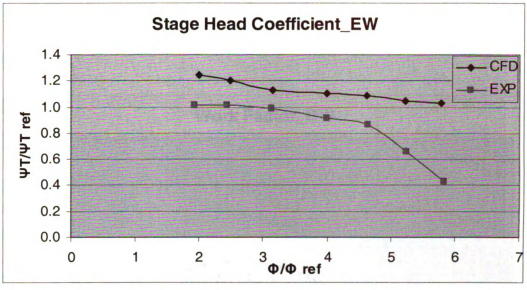

Figure 5-11 Experimental and CFD head coefficient for E wide

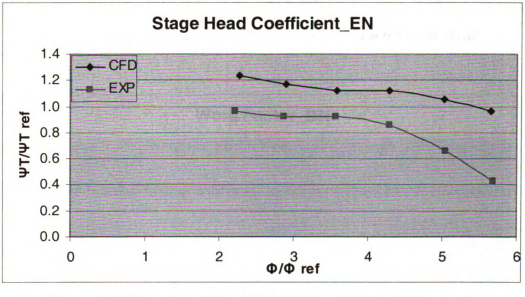

Figure 5-12 Experimental and CFD head coefficient for E narrow

Figure 5-13 to Figure 5-16 show comparison of the work factor curves. In general, the first two figures show excellent match, between all three methods for the low specific speed impellers. In addition, the match is exact at the design point. For the high specific speed impellers (figures 5.19 and 5.20), there is a good match between the

experimental and CFD results at the lowest flow coefficient; but as it increases, the CFD over predicts the values.

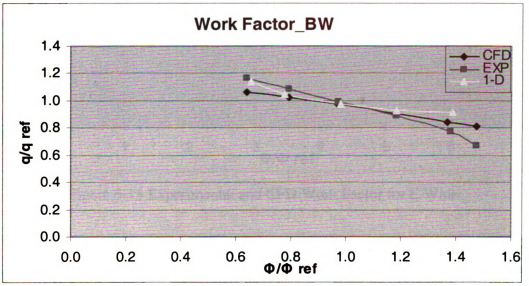

Figure 5-13 Experimental, CFD, and 1-D Work Factor for B Wide

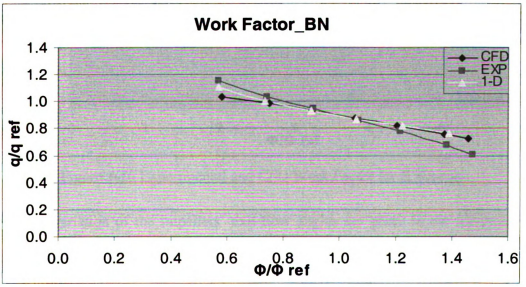

Figure 5-14 Experimental, CFD, and 1-D Work Factor for B Narrow

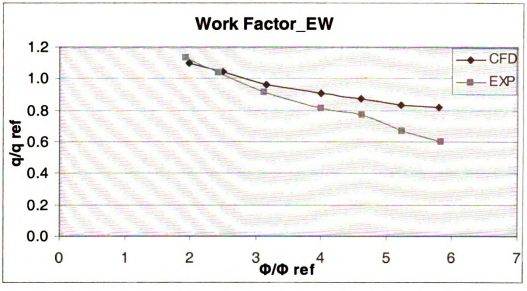

Figure 5-15 Experimental and CFD Work Factor for E Wide

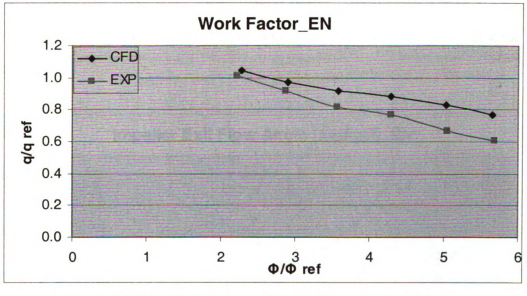

Figure 5-16 Experimental and CFD Work Factor for E Narrow

The variation of the impellers' exit-flow angles are given in the following four Figure 5-17 to Figure 5-20. Comparing these curves, the first two figures show excellent match, between all three methods for the low specific speed impellers. Moreover, the match is exact at the design point. For the high specific speed impellers (figures 5.23 and

5.24), there is a good match between the experimental and CFD results near the design point, but clearly the values get off for higher and lower flow coefficients.

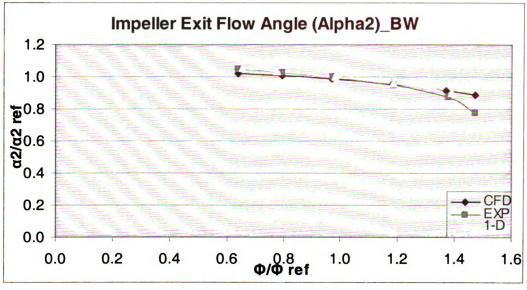

Figure 5-17 Experimental, CFD, and 1-D Impeller Exit Flow Angle for B Wide

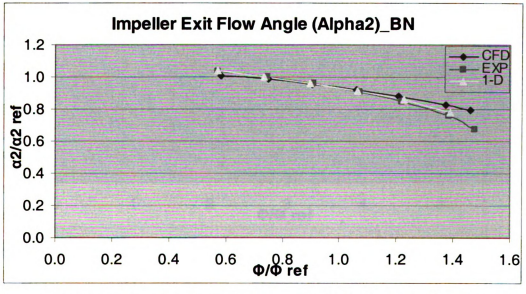

Figure 5-18 Experimental, CFD, and 1-D Impeller Exit Flow Angle for B Narrow

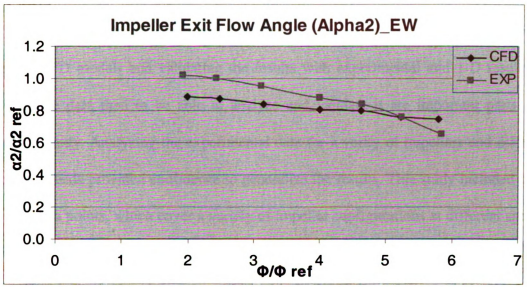

Figure 5-19 Experimental and CFD Prediction of Impeller Exit Flow Angle for E Wide

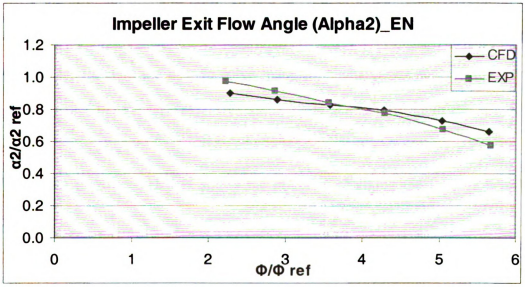

Figure 5-20 Experimental and CFD Prediction of Impeller Exit Flow Angle for E Narrow

Chapter 6 CONCLUSIONS

This study mainly consisted of analyzing experimental data as well as creating a complete CFD models and validating the results with experimental and 1-D results. to have reliable data then to be able to analyze and validate it are important parts of a successful study. Analyzing the experimental data for a verity of impellers and different rotational speeds provided confidence to generalize the results. This study included more than 200 data points, which cover a variety of impeller configurations at different speeds, which provide more convenience to generalize the results.

CFD is another tool that was used in this study. CFD analysis could be the future of design in turbomachinery world. With the development of computers and CFD packages, the designer needs to do much less work to design and analyze compressors. CFD models give a much deeper understanding of the flow inside centrifugal compressors and enable the user to solve many problems easier and much faster. To ensure accurate CFD models, extensive simulations and validation of the results was done.

Analyzing the experimental data shows the effect of changing the specific speed, the rotational speed, and 25% impeller trimming on the stage and impeller dimensionless parameters.

Four CFD models were created for impellers with variable specific speeds. These impellers are two original impellers with two extreme specific speeds (58 and 125) in addition to the two modified (trimmed) impellers.

Overall the analysis shows logical results, a reasonable agreement, and an agreement in the trend with most of the 1-D and CFD results.

More CFD analysis for the other four impellers (C original, C trimmed, D original, and D trimmed) will give more convincing results. Having more experimental data about different impellers' outer diameters (before and after cut) will be a great help to generalize the results even more.

APPENDIX

Table A: The experimental referenced values of all the pointes for both the wide and narrow impellers. The shaded values are the design point for each impeller.

B-Original										
Phi	*Eff1-2*	*Eff1-etot*	*Psi2*	*Psi1-eq*	*(Work)*	*Del T/T1*	*W2/W1tip*	*W1rms/W2*	*Alpha2*	Ns
0.641	1.015	0.895	1.191	1.050	1.167	1.179	0.644	1.527	1.047	46
0.792	1.020	0.960	1.114	1.048	1.086	1.091	0.798	1.242	1.030	51
0.971	1.000	1.000	0.996	0.995	0.990	1.000	0.993	1.002	0.999	58
1.184	0.932	0.966	0.833	0.862	0.889	0.897	1.208	0.828	0.949	72
1.380	0.734	0.784	0.571	0.609	0.774	0.781	1.455	0.692	0.875	101
B-Trimmed										
Phi	*Eff1-2*	*Eff1-etot*	*Psi2*	*Psi1-eq*	*(Work)*	*Del T/T1*	*W2/W1tip*	*W1rms/W2*	*Alpha2*	Ns
0.571	1.013	0.852	1.176	0.987	1.155	1.168	0.707	1.397	1.033	45
0.743	1.019	0.937	1.061	0.975	1.036	1.042	0.946	1.047	1.000	52
0.910	1.013	0.979	0.964	0.930	0.947	0.956	1.137	0.873	0.959	60
1.069	0.987	1.000	0.851	0.861	0.858	0.863	1.330	0.750	0.908	68
1.216	0.929	0.978	0.727	0.765	0.778	0.783	1.507	0.664	0.850	80
1.384	0.782	0.854	0.533	0.581	0.678	0.682	1.736	0.580	0.757	104
1.473	0.582	0.662	0.352	0.400	0.601	0.606	1.916	0.527	0.673	143
C-Original										
Phi	*Eff1-2*	*Eff1-etot*	*Psi2*	*Psi1-eq*	*(Work)*	*Del T/T1*	*W2/W1tip*	*W1rms/W2*	*Alpha2*	Ns
0.922	0.984	0.895	1.137	1.033	1.149	1.159	0.638	1.528	1.035	55
1.241	0.983	0.965	1.033	1.013	1.045	1.053	0.831	1.180	1.002	65
1.465	0.979	0.995	0.962	0.977	0.978	0.987	0.964	1.023	0.972	73
1.682	0.970	1.014	0.903	0.942	0.926	0.934	1.067	0.930	0.941	80
1.785		1.045		0.943	0.898					82
2.094	0.929	1.012	0.761	0.828	0.815	0.823	1.278	0.786	0.864	98
2.555	0.638	0.702	0.416	0.458	0.649	0.656	1.594	0.641	0.711	170
2.641	0.515	0.428	0.322	0.267	0.622	0.628	1.652	0.620	0.673	258
C-Trimmed										
Phi	*Eff1-2*	*Eff1-etot*	*Psi2*	*Psi1-eq*	*(Work)*	*Del T/T1*	*W2/W1tip*	*W1rms/W2*	*Alpha2*	Ns
0.861	1.020	0.917	1.161	1.043	1.133	1.143	0.708	1.376	1.017	53
0.976	1.023	0.965	1.111	1.045	1.079	1.090	0.809	1.206	1.001	56
1.135	1.027	1.024	1.040	1.036	1.008	1.018	0.950	1.030	0.973	61
1.678	1.016	1.129	0.839	0.931	0.822	0.832	1.338	0.741	0.854	81
1.763		1.130		0.916	0.807					84
2.020	0.961	1.077	0.735	0.822	0.760	0.767	1.476	0.679	0.776	97
2.363	0.770	0.892	0.495	0.573	0.640	0.647	1.736	0.584	0.642	138

Table A contd.

D-Original										
Phi	*Eff1-2*	*Eff1-etot*	*Psi2*	*Psi1-e*	*q (Work)*	*Del T/T1*	*W2/W1tip*	*W1rms/W2*	*Alpha2*	**Ns**
1.110	0.972	0.813	1.212	1.022	1.241	1.246	0.475	1.989	1.019	61
1.453	0.980	0.905	1.116	1.029	1.133	1.143	0.597	1.589	1.017	70
1.784	1.003	0.964	1.055	1.014	1.047	1.057	0.739	1.290	0.994	78
2.233	1.019	1.004	0.992	0.976	0.968	0.974	0.883	1.088	0.954	90
2.584	1.034	1.024	0.934	0.925	0.899	0.907	1.006	0.962	0.916	101
2.955	1.028	1.034	0.845	0.850	0.818	0.826	1.147	0.851	0.865	115
3.376	1.031	1.008	0.770	0.751	0.742	0.751	1.274	0.775	0.803	135
4.000	0.983	0.869	0.646	0.570	0.653	0.661	1.417	0.708	0.704	180
D-Trimmed										
Phi	*Eff1-2*	*Eff1-etot*	*Psi2*	*Psi1-e*	*q (Work)*	*Del T/T1*	*W2/W1tip*	*W1rms/W2*	*Alpha2*	**Ns**
1.212	0.971	0.873	1.139	1.023	1.167	1.177	0.580	1.630	1.008	64
1.624	0.995	0.965	1.056	1.022	1.056	1.066	0.764	1.244	0.975	74
2.012	1.026	1.029	0.995	0.997	0.964	0.973	0.934	1.024	0.930	84
2.551	1.055	1.090	0.908	0.937	0.856	0.867	1.143	0.846	0.855	99
3.086	1.041	1.118	0.793	0.851	0.758	0.766	1.334	0.734	0.764	117
3.931	1.022	0.901	0.614	0.540	0.597	0.603	1.621	0.618	0.591	186
E-Original										
Phi	*Eff1-2*	*Eff1-etot*	*Psi2*	*Psi1-e*	*q (Work)*	*Del T/T1*	*W2/W1tip*	*W1rms/W2*	*Alpha2*	**Ns**
1.927	0.966	0.891	1.097	1.012	1.130	1.140	0.511	1.802	1.023	81
2.433	0.959	0.968	1.001	1.010	1.038	1.050	0.645	1.433	1.001	91
3.122	0.968	1.079	0.891	0.992	0.916	0.926	0.840	1.108	0.953	105
3.996	0.985	1.124	0.803	0.915	0.811	0.818	1.013	0.930	0.882	126
5.237	1.004	0.984	0.676	0.661	0.670	0.678	1.230	0.783	0.758	184
5.837	0.717	0.714	0.431	0.428	0.597	0.604	1.363	0.715	0.657	270
E-Trimmed										
Phi	*Eff1-2*	*Eff1-etot*	*Psi2*	*Psi1-e*	*q (Work)*	*Del T/T1*	*W2/W1tip*	*W1rms/W2*	*Alpha2*	**Ns**
2.220	0.933	0.952	0.949	0.966	1.011	1.023	0.725	1.272	0.971	90
2.869	0.956	0.997	0.882	0.919	0.918	0.929	0.889	1.043	0.913	107
3.563	1.021	1.122	0.838	0.920	0.816	0.827	1.063	0.880	0.843	119
4.148		1.125		0.878	0.777					133
4.294	1.050	1.116	0.810	0.860	0.767	0.775	1.168	0.811	0.775	137
5.045	1.017	0.989	0.682	0.662	0.667	0.675	1.343	0.714	0.672	181
5.490	0.865	0.703	0.526	0.427	0.605	0.614	1.480	0.656	0.576	262

BIBLIOGRAPHY

Aungier, Ronald, H . "Centrifugal Compressors A Strategy for Aerodynamic Design and Analysis" .2000.

Balje, O. E. "Turbomachines A Guide to Design, Selection, and Theory". 1981.

Casey, M. and Marty, F., , "Centrifugal Compressors - Performance at Design and Off-Design", Proc. of the Institute of Refrigeration, London, pp.71-80, 1986

CFX-TASCFlow Computational Fluid Dynamics Software, Version 2.12, Theory Documentation, AEA Technology Engineering Software Ltd. Waterloo, Ontario, Canada, 2002

CFX-TASCFlow Computational Fluid Dynamics Software, Version 2.12, Tutorial Documentation, AEA Technology Engineering Software Ltd. Waterloo, Ontario, Canada, 2002

CFX-TASCFlow Computational Fluid Dynamics Software, Version 2.12, User Documentation, AEA Technology Engineering Software Ltd. Waterloo, Ontario, Canada, 2002

Dixon, S.L. "Fluid Mechanics and Thermodynamics of Turbomachinery" fourth edn, Pergram Press.(1998),

Engeda, A. ME 442 " Introduction to Turbomachinery" Class notes and class discussion, spring, 2002.

Engeda, A. ME 842 " Advanced Turbomachinery" Class notes and class discussion, spring, 2002 .

Engeda, A. ME 842 " Advanced Turbomachinery" Class notes and class discussion, spring, 2004 .

Gibbs, Charles W. (editor) " Compressed Air and Gas Data". 1971

Japikse, D. "Acritical Evaluation of Three Centrifugal Compressors With Pedigree Data Sets : Part5-Studies in Component performance". journal of Turbomachinery JANURY 1987, Vol .109.

Japikse D, Baines NC: Introduction to Turbomachinery. Oxford, Oxford University Press, 1994

Jansen, W . "A Method For Calculating the Flow in a centrifugal Impeller when Entropy Gradients are Present "Instn Mech Engrs . 1990

Lakshminarayana, B., 1995, "Fluid Dynamics and Heat Transfer of Turbomachinery", Wiley-Interscience Publication.

Lenke , L .J . and H . Simon . " Aerodynamic Analysis of Return Channels of Multi-Stage Centrifugal compressors."

Lenke , L .J . and H . Simon . "Numerical Investigations on the Optimum Design of return Channels of multi-Stage Centrifugal Compressors" . Presented at The international Gas Turbine & Aeroengine Congress &exhibition Indianapolis, Indiana – June 7-june 10 .1999

Liu, Z. and D. Lee Hill "Issues Surrounding Multiple Frames Of Reference Models For Turbo Compressor Applications" Dresser-Rand, Olean, NY USA

Moffat R., "Putting Industrial Vaccum to Work", Hydraulics & Pneumatics, 1987. pp58-63

McKee, R. J. and Danny M. Deffenbaugh, "FACTORS THAT AFFECT SURGE PRECURSORS IN CENTRIFUGAL COMPRESSORS" GMRC Gas Machinery Conference – October 6-8, 2003

McKee, R. J., C. E. Edlund and P. J. Pantermuehl "Development on an Active Surge Control System", Report, Mechanical and Materials Engineering Division, Southwest Research Institute December 2000

NASA web site "http://www.grc.nasa.gov/WWW/K-12/airplane/compress.html" April, 2004

Pampreen, R . C . "A Blockage Model for Centrifugal Compressor Impellers". Journal of Engineering for power . ASME

Patankar, S.V.Numerical Heat Transfer and Fluid Flow, Hemisphere (McGraw-Hill), New York, 1980.

Private discussion with Dr. Wang Z. at ME , MSU, about grid generation and turbulence modeling on rotating equipments, Sep, 2003 and April, 2004

Private discussion with Dr. Jabery, at ME , MSU, about grid generation and turbulence modeling on rotating equipments, April, 2004.

Sapiro, L. "Effect of Impeller-Extended Shrouds on Centrifugal Compressor Performance as a Function of Specific Speed "journal of Engineering for power . JULY 1983, Vol .105

Senoo, Y. and Kinoshita, Y., 1978, "Limits of Rotating Stall and Stall in Vaneless Diffuser of Centrifugal Compressors", ASME Paper 78-GT-19.

Shaw, C. T. "Using Computational Fluid Dynamics" Prentice Hall in 1992

Smith, D.G. – "ERCOFTAC Seminar and Workshop on 3D TURBOMACHINERY FLOW PREDICTION VI", REPORT, France, 5-8th January 1998

Smith, D. J. and H. MERRYWEATHER, "THE USE OF ANALYTIC SURFACES FOR THE DESIGN OF CENTRIFUGAL IMPELLERS BY COMPUTER GRAPHICS" 1973

Smith, G.D. Numerical Solution of Partial Differential Equations: Finite Difference Methods, Third Edition, Oxford University Press, Oxford, 1985.

Sorokes J. M. "Rotating Stall - An Overview of Dresser-Rand Experience" Dresser-Rand, Olean, NY, USA

Stodola, A., 1927, "Steam and Gas Turbines. McGraw-Hill Inc.

Tannehill, J. C., D. A. Anderson and R. H. Pletcher "Computational Fluid Mechanics And Heat Transfer" Taylor & Francis, Inc, 1997

U.S. Department of Energy "Improving Compressed Air System Performance", a sourcebook for industry, 2003

Van den Braembussche, R., 1984, "Surge and Stall in Centrifugal Compressors" VKI Preprint 1984-15.

Van den Braembussche, R. "Flow in Volutes of Centrifugal Compressors" Elliot Turbomachinery Company, Inc., Jeannette, PA, USA, April 1998.

Wiesner, F., 1967, "A Review of Slip Factors for Centrifugal Compressors", ASME Journal of Engineering for Power, pp.558-572.

Wilson, D.G. "The Design of High-Efficiency Turbomachinery and Gas Turbines", Second edition

Whitefield, A., "Preliminary design and performance prediction techniques for centrifugal compressors", Developments in industrial compressors, London, 3-4 Oct 1989.

Wilson D. G. and Theodosios K. "The Design of High-Efficiency Turbomachinery and Gas Turbines", Second Edition, 1998

Zienkiewicz, O.C. and R.L. Taylor, the Finite Element Method, Fourth Edition, Volume 1: Basic Formulation and Linear Problems, McGraw-Hill, New York, 1989.